

UNIVERSIDADE DE SÃO PAULO
INSTITUTO DE GEOCIÊNCIAS

**EXTENSÃO SUL DO SISTEMA OROGÊNICO
TOCANTINS NO CONTEXTO GEODINÂMICO DA
AGLUTINAÇÃO DO GONDWANA: EXERCÍCIO DE
TECTÔNICA**

Mario da Costa Campos Neto

Tese apresentada para o Concurso de
Livre-Docência junto ao Departamento de
Mineralogia e Geotectônica do Instituto
de Geociências da Universidade de
São Paulo. Área de Conhecimento:
de Geologia Estrutural/Geotectônica.

SÃO PAULO

1999

**UNIVERSIDADE DE SÃO PAULO
INSTITUTO DE GEOCIÊNCIAS**

**EXTENSÃO SUL DO SISTEMA OROGÊNICO TOCANTINS NO
CONTEXTO GEODINÂMICO DA AGLUTINAÇÃO DO
GONDWANA: EXERCÍCIO DE TECTÔNICA**

Mario da Costa Campos Neto



Tese apresentada para o Concurso de Livre-Docência junto ao Departamento de Mineralogia e Geotectônica do Instituto de Geociências da Universidade de São Paulo. Área de conhecimento de Geologia Estrutural/Geotectônica.

**SÃO PAULO
1999**

DEDALUS - Acervo - IGC



30900006692

ÍNDICE

CAPÍTULO 1 – BREVE APRESENTAÇÃO 1

CAPÍTULO 2 – NEOPROTEROZOIC HIGH-PRESSURE METAMORPHISM AND TECTONIC CONSTRAINT FROM THE NAPPE SYSTEM SOUTH OF THE SÃO FRANCISCO CRATON, SOUTHEAST BRAZIL

Abstract

| | |
|--|----|
| 2-1. Introduction | 3 |
| 2-2. Geological setting | 4 |
| 2-2.1. The Socorro-Guaxupé nappe | 5 |
| 2-3. The kyanite-granulite nappe | 6 |
| 2-3.1. Lithology | 6 |
| 2-3.2. Kinematics | 8 |
| 2-3.3. Microstructures and mineral assemblages | 9 |
| 2-3.4. Mineral chemistry and P/T estimation | 10 |
| 2-4. The metapelite nappe complex | 16 |
| 2-4.1 Petrology of eclogitic rocks and kyanite metapelites | 17 |
| 2-4.2. P-t estimates | 18 |
| 2-5. The quartzite nappe complex | 20 |
| 2-6. The parautochthonous unit | 22 |
| 2-7. Discussion | 22 |
| 2-8. Conclusion | 23 |
| Acknowledgements | 24 |

CAPÍTULO 3 – TERRANE ACCRETION AND UPWARD EXTRUSION OF HIGH-PRESSURE GRANULITES IN THE NEOPROTEROZOIC NAPPES OF SOUTHEAST BRAZIL: PETROLOGIC AND STRUCTURAL CONSTRAINTS

Abstract

| | |
|-------------------------|----|
| 3-1. Introduction | 25 |
| 3-2. Geological setting | 26 |

| | |
|---|----|
| 3-3. Tectonic units | 27 |
| 3-3.1. The Socorro-Guaxupé nappe (SGN) | 27 |
| 3-3.1.1 The Basal Granulitic Unit | 27 |
| 3-3.1.2. The Middle Diatectic Unit | 28 |
| 3-3.1.3. The Upper Migmatitic Unit | 28 |
| 3-3.1.4. The syn-kinematic plutonic intrusives | 28 |
| 3-3.2. The Três Pontas-Varginha nappe | 29 |
| 3-4. Nappe geometry, kinematics and metamorphic evolution | 30 |
| 3-4.1. The Socorro-Guaxupé nappe (SGN) | 31 |
| 3-4.1.1. Basal sole thrust | 32 |
| 3-4.1.2. Syn-metamorphic normal shearing and late-metamorphic NE-direct thrusting | 33 |
| 3-4.1.3. P/T estimation for SGN | 34 |
| 3-4.2. The Três Pontas-Varginha nappe (TPVN) | 34 |
| 3-4.2.1. Microstructures of kyanite-granulites | 35 |
| 3-4.2.2. Successive mineral assemblages and P/T estimates of Kyanite and sillimanite granulites | 35 |
| 3-4.3. The southern shear-belt | 40 |
| 3-5. Age constraints on high-grade metamorphism and nappe emplacement | 41 |
| 3-6. Summary of data and discussion | 42 |
| 3-7. Conclusion | 44 |
| Acknowledgement | 45 |

CAPÍTULO 4 – OROGENIC SYSTEM FROM SW-GONDWANA: AN APPROACH TO BRASILIANO-PAN AFRICAN CYCLE AND OROGENIC COLLAGE IN SE-BRAZIL

Abstract

| | |
|---|----|
| 4-1. Introduction | 46 |
| 4-2. Major continental plates framework | 47 |
| 4-2.1. Statherian taphrogeny: attempts to break-up of the São Francisco plate | 48 |
| 4-3. Fragments of Rodinia history | 49 |
| 4-3.1. The Central Goiás terrane | 49 |
| 4-3.2. The Apiaí terrane | 52 |
| 4-4. The São Francisco plate margins: paleotectonic approach | 55 |
| 4-5. The Tocantins orogenic system | 58 |

| | |
|---|-----------|
| 4-5.1. Orogen's outline | 58 |
| 4-5.2. The southern Tocantins orogenic system | 62 |
| 4-5.2.1. The upper high-temperature Socorro-Guaxupé nappe | 62 |
| 4-5.2.2. The high-pressure nappes | 65 |
| 4-5.2.3. The medium-pressure lower nappes and foreland orogen propagation | 66 |
| 4-5.3. Tectonic evolution of the Southern Tocantins orogenic system | 67 |
| 4-6. Paleotectonic approach for the Mantiqueira orogenic system | 68 |
| 4-7. The Mantiqueira orogenic system | 72 |
| 4-7.1. Regional view on plate convergence in the Southern Mantiqueira orogenic system | 72 |
| 4-7.2. The Central and Northern segments of the Mantiqueira orogenic system | 73 |
| 4-7.2.1. Late-orogenic basins | 78 |
| 4-7.2.2. Post-orogenic transition from compressive to extensional collapse | 78 |
| 4-7.3. General framework: the Ribeira belt | 79 |
| 4-8. From Rodinia to Gondwana: SE-Brazil geodynamic evolution | 80 |
| REFERENCIAS BIBLIOGRÁFICAS | 83 |

CAPÍTULO 1

BREVE APRESENTAÇÃO

Essa tese de Livre Docência resulta da sistematização científica empreendida nos anos de 1998 e de 1999. Alicerçada em trabalhos de campo sistemáticos, na análise estrutural e na petrologia metamórfica como ferramentas básicas, aliadas ao manuseio do acervo isotópico e geocronológico, ela possui na análise tectônica seu principal vetor de direção.

No entanto, pressionado pela Reitoria da Universidade de São Paulo através da Comissão Especial de Regimes de Trabalho (CERT) e pelas principais agências nacionais e estadual de fomento à pesquisa, deu-se prioridade à preparação de artigos endereçados à comunidade científica internacional, antecedendo a formulação integrada em uma tese. Assim, quatro trabalhos foram preparados, três para as revistas *Precambrian Research*, *Tectonics* e *Episodes* (ver referências bibliográficas) e um para o livro *Tectonic Evolution of South America*, a ser editado pelo 31º Congresso Geológico Internacional. Destes, os dois primeiros (preparados com a colaboração do Dr. Renaud Caby, Diretor de Pesquisas do CNRS, França) e o ultimo constituem o corpo desta tese. São eles:

Campos Neto, M.C. e Caby, R., 1999. Neoproterozoic high-pressure metamorphism and tectonic constraint from the nappe system south of the São Francisco Craton, southeast Brazil. *Precambrian Research*, 97, 3-26.

Campos Neto, M.C. e Caby, R. (inédito). Terrane accretion and upward extrusion of high-pressure granulites in the Neoproterozoic nappes of southeast Brazil: Petrologic and structural constraints. *Tectonics* (aceito para publicação).

Campos Neto, M.C. (inédito). Orogenic systems from SW-Gondwana: an approach to Brasiliano-Pan African cycle and orogenic collage in SE-Brazil. E.J. Milani e A. Thomaz Filho (eds.) *Tectonic Evolution of South America, International Union of Geological Science-31th International Geological Congress* (submetido).

O tempo, constrangido a prazos rígidos, não permitiu que esses trabalhos fossem reescritos em português e integrados no contexto da tese. Por este motivo ela está sendo apresentada em inglês. Cada trabalho corresponde a um capítulo, respeitada a sua integridade, do título aos agradecimentos. As referências bibliográficas foram unificadas e as figuras renumeradas de acordo com os capítulos.

Como são artigos que se complementam, a ordenação dos capítulos permite, sem quebras maiores no encadeamento do texto, uma visão geral, dos objetos (ou dados obtidos) aos processos e a integração destes na dinâmica global. Essa relação entre os artigos, aliada ao fato de dois deles ainda não terem sido publicados, garante o caráter inédito desta tese.

O Capítulo 2 trata do sistema de nappes que se empilham lateralmente à borda sul do cráton do São Francisco. Distingue nessas estruturas, padrões cinemáticos diferenciados e trajetórias metamórficas conflitantes. A enfase está nos alóctones inferiores, onde o metamorfismo de alta pressão, caracterizado pioneiramente por Trouw (1992), situa parte

do orógeno como resultante da extrusão forçada e de baixo ângulo, de um prisma de subducção continental, grosseiramente orientado para oeste.

A ênfase do Capítulo 3 está nas nappes superiores, de alta temperatura, colocadas em evidência, inicialmente, por Campos Neto et al. (1984). São terrenos identificados com um ambiente de raiz de arco magmático, cujo registro metamórfico e estrutural assemelha-se a um orógeno colisional himalaiano. O registro químico e isotópico apresentado, reforçado no trabalho de Janasi (1999), alia-se aos distintos ambientes tectônicos deduzidos pelas incompatibilidades e diferenças nas trajetórias metamórficas, permitindo um avanço no reconhecimento de terrenos, ou de ambientes tectônicos exóticos em relação a placa do São Francisco.

A evolução geodinâmica apresentada no Capítulo 4 discute o processo de aglutinação do sudeste do continente brasileiro dentro do contexto da colagem orogênica do sudoeste do Gondwana. Parte-se dos registros, na região, dos processos de quebra e dispersão de Rodínia, de interação de placas oceânicas e do diacronismo dos regimes tectônicos.

CAPÍTULO 2

NEOPROTEROZOIC HIGH-PRESSURE METAMORPHISM AND TECTONIC CONSTRAINT FROM NAPPE SYSTEM SOUTH OF THE SÃO FRANCISCO CRATON, SOUTHEAST BRAZIL

Abstract

The Neoproterozoic giant nappe system exposed south of the São Francisco craton underwent a minimum of 150 km of near-horizontal northeastward displacement. This nappe system comprises an uppermost unit derived from a plutonic magmatic arc terrane with high-pressure, high-temperature intermediate to mafic granulites at its base (Socorro-Guaxupé nappe), underlain in sequence by a high-pressure kyanite granulite nappe, an amphibolite facies metapelite nappe, and finally by a quartzite nappe which forms the lowest part of the pile and rests on a parautochthonous unit related to the passive margin of the craton. The kyanite granulites crystallised around 13 kbar, 750°C and have only at their top sillimanite related to T-increase overprinting ($T=890^{\circ}\text{C}$), a consequence of downward heat advection from the overlying Socorro-Guaxupé granulites equilibrated at 900°C. Pressures of 13-14 kbar are documented in the underlying metapelite nappe with temperatures of 640-670°C, in which lenses of eclogite indicate P_{max} of ca. 17.5 kbar. Phyllites of the parautochthonous unit are directly overlain by HP granulites in the north and record $P \approx 7$ kbar and $T = 500^{\circ}\text{C}$. The distribution of metamorphic facies is reminiscent of inverted metamorphism with eclogites from subduction-related metamorphism and kyanite granulites from early extrusion of subducted continental crust. The metamorphic conditions of the parautochthon may represent a stage achieved during late metamorphic thinning of the nappe pile. The overall picture suggests that high-pressure units recrystallised in a subduction zone located to the WSW. The frontal thrusts of the nappe system show a late, north northeastward transported thin-skinned pattern.

Keywords: Brasilian/Pan-African; collision tectonics; nappe system; high-pressure metamorphism; kyanite granulite.

2-1. Introduction

Most granulites formed in the lower crust of collisional orogens generally underwent late-kinematic recrystallisation because they were eventually maintained during a long time at elevated temperatures close to hot mantle. Sillimanite kinzigites are normal end products of most metapelitic granulites formed within the lower crust of former mountain roots. The exhumation of the lower crust either results from regional extension and/or asthenospheric doming (i.e. Permian-Mesozoic exhumation of the Ivrea zone, Zinng et al., 1990).

In himalayan-type collisions that generally result from continuous plate convergence and continental subduction, the lower crust is exposed through piling-up of crystalline nappes displaced 100 km or more over less metamorphic allochthons, giving rise to metamorphic inversion (Le Fort et al., 1986; Burg et al., 1987). Mineral assemblages in high grade metamorphic rocks from such nappes may register a severe high-temperature decompression with low-pressure recrystallisation and anatexis that overprints most of the

earlier higher pressure mineral assemblages. In central Himalaya maximum pressures around 9 kbar have been calculated for most metapelites by Vannay and Hodges (1996), with values up to 12 kbar in Langtang (Macfarlane, 1995). Indeed, the occurrence of kyanite in the primary assemblage of metapelites associated with dry leucosomes towards the base of the main crystalline allochthon in central Nepal (Caby et al., 1983) leads to the assumption that much higher pressure rocks may be present at depths. Such is the case of northern Pakistan where high-pressure metapelites (650-700°C and 8-13 kbar) were exhumated under decreasing temperatures in the kyanite stability field (Pognante et al., 1993). Also lenses of medium-temperature eclogites survived enclosed in gneisses and metatexites (Pognante and Spencer, 1991; Tonarini et al., 1993; Le Fort et al, 1997). Liu and Zhong (1997) have described in eastern Himalaya relics of high-pressure granulites. In the Tso Morari dome at the North Himalayan Massif a high-pressure and low-temperature mafic and pelitic eclogites was recently described, implying in a continental subduction at the onset of the Indian-Eurasian collision (Guillot et al., 1997 and Sigoyer et al., 1997).

Slightly retrogressed mafic eclogites with preserved low to medium-temperature prograde minerals such as lawsonite have been reported elsewhere in granulites and anatetic metapelites (Biino, 1994), showing that early high-pressure metamorphic conditions may survive retrogression even at high temperatures. There are however very few examples of outcropping slightly or unretrogressed kyanite granulites (see Pin and Vielzeuf, 1983). The occurrences of kyanite granulites described are all associated with eclogites but kyanite is invariably overgrown by sillimanite as in the Iberian massif (Ibarguchi et al., 1990; Arenas, 1991; Abalos et al, 1996) or in the Bohemian massif (Carswell and O'Brien, 1993). In contrast, kyanite is the only Al-silicate present in rocks adjacent to all reported ultra high-pressure rocks in the world. This may suggest that subduction settings with low geothermal gradients (<12°C/ km) represent the only site where high-pressure granulites can form and be exhumed rapidly, thus escaping reequilibration in the sillimanite stability field.

We describe in this paper the tectonic setting and metamorphic evolution of kyanite kinzigitites and associated rocks that form the base of himalayan-type nappes with associated reverse metamorphism in the Neoproterozoic Brasiliano belt, south of the São Francisco craton. We then discuss the tectonic implication of the reconstructed P/T paths of granulites and adjacents units and we propose a scenario for nappe stacking and exhumation according to the available U-Pb and Sm-Nd geochronological data.

2-2. Geological setting

The Archaean-Paleoproterozoic São Francisco Craton in SE Brazil (Fig. 2-1) is bounded in its western and southern margins by nappes involving Proterozoic rift and continental margin sequences (Brasília and Alto Rio Grande belts, Brito Neves et al, 1995; Paciullo et al., 1998). It comprises from top to bottom: a giant high-temperature granulite-migmatitic allochthon (the Socorro-Guaxupé nappe) that is part of the Apiaí-Guaxupé terrane (Campos Neto and Figueiredo, 1995); an upper kyanite-granulite nappe with high-pressure metamorphism (Vasconcellos, et al. 1991; Trouw, 1992; Trouw and Castro, 1996; Campos Neto and Caby, 1997, Trouw et al., 1998); a lower metapelite nappe with medium-temperature, high-pressure metamorphism; a quartzite nappe with passive continental margin affinity (Ribeiro et al., 1995), and a parautochthonous unit overlying the southern edge of the São Francisco craton (Fig. 2-1). This Neoproterozoic nappe system exposed

south of the São Francisco craton is the extension of the Brasilia belt (Trouw et al., 1984a; Fuck et al., 1994; Valeriano et al., 1995 and 1998; Simões, 1995; Seer et al., 1998). The nappes that underlie the Socorro-Guaxupé nappe have been named the "Alto Rio Grande belt" and their lithostratigraphy, structure and metamorphism were first studied by Trouw et al. (1980, 1982, 1983, 1984b, 1986), Ribeiro and Heibron (1982), Campos Neto et al. (1990), Junho et al. (1992), and Ribeiro et al. (1995). The nappe system is bounded to the southeast by major syn to late-metamorphic shear zones that were active till 570 Ma (Machado et al., 1996).

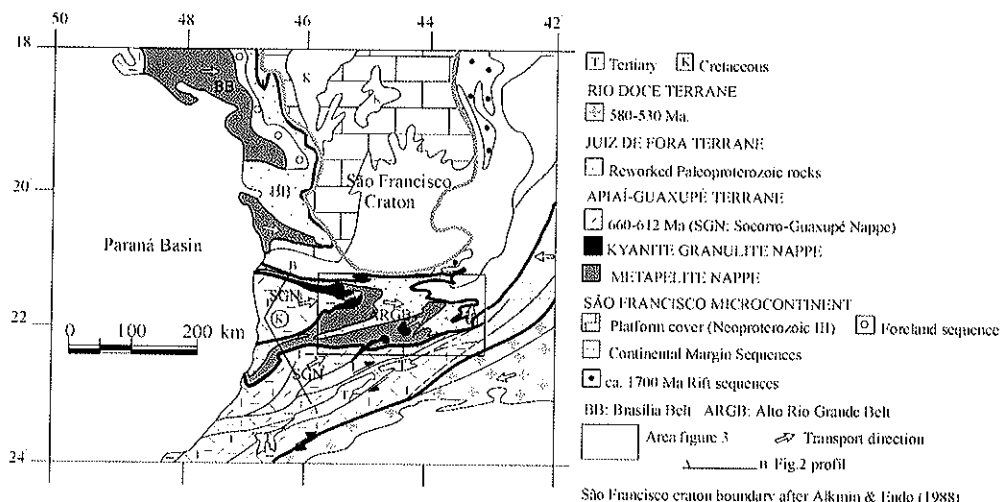


Figure 2-1: Sketch tectonic map of Southeast Brazil.

2-2.1 The Socorro-Guaxupé nappe

The Socorro-Guaxupé nappe comprises a flat-lying to gently southwestward dipping sole of enderbitic granulites ca. 3 km thick. These granulites grade upward into grey to pink, biotite-hornblende diatexesites ca 6 km thick interlayered at their top with pelitic to semi-pelitic migmatites and subordinate lenses of quartzite, calc-silicate gneiss, rare marbles and mafic metaintrusives. Peraluminous muscovite-bearing granites intrude the top of the allochthon (Fig. 2-2). The basal green-colored, medium-grained, garnet bearing banded granulites of enderbitic modal composition are metaluminous, low-K rocks of calc-alkaline affinity with lower amounts of large ion lithophile elements (Campos Neto et al., 1996) than the other granulitic plutonic rocks of the nappe unit (Fernandes et al., 1987; Iyer et al., 1996). The anhydrous enderbitic light-coloured leucosomes and the coarse-grained grey to pink hololeucocratic charnockite veins are interpreted as *in situ* dry melts. Decimetre-thick dark gabbro-noritic layers considered as syn-metamorphic intrusives are common. The Neoproterozoic age of granulitic metamorphism is constrained by a 629 ± 14 Ma Sm-Nd garnet-biotite-whole rock isochron age from a granulite sample from the Piranguinho quarry (Fig. 2-3, Teixeira, written communication, data from Centro de Pesquisas Geocronológicas, Universidade de São Paulo, Brazil). The protoliths of these enderbitic granulites give a Sm/Nd T_{dm} model age of 1290 Ma, with ε_{Nd} (0.640) = -1.2. These results are in agreement with the isotopic primitive composition of the Mara Rosa arc in the hinterland of the Brasilia belt, where the main metamorphism also took place around 630 Ma (Pimentel et al., 1997). The intrusive charnockites dated at 640 Ma by the U-Pb

zircon method (Basei et al, 1995) grade upward into biotite-hornblende granitoids, both rock types exhibiting porphyritic texture. The granitoids with a high-K calc-alkaline trend were emplaced as syn-metamorphic batholiths (630-625 Ma, Ebert et al., 1996; Töpfner, 1996) and are coeval with stratoid mangerites (Campos Neto et al., 1988; Janasi, 1997).

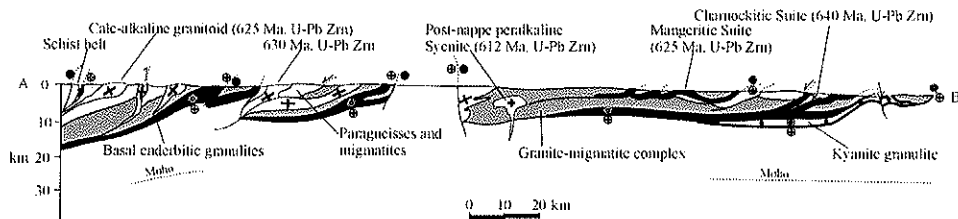


Figure 2-2: Schematic cross-section of Socorro-Guaxupé nappe.

The basal granulites are characterised by garnet-clinopyroxene-orthopyroxene-plagioclase-quartz assemblages in mafic rocks and garnet-sillimanite-cordierite-green spinel-biotite-plagioclase-quartz as reequilibrated assemblage in metapelites. Previous petrologic studies (Table 2-1) point to initial high-pressure, high-temperature metamorphism at $P= 12.5$ Kbar, $T= 900^{\circ}\text{C}$ followed by partial reequilibration at $P= 7.5$ Kbar and $T= 850^{\circ}\text{C}$. Only high temperature-low pressure conditions prevail on the top of the nappe.

| NAPPE POSITION | MAIN MINERAL ASSEMBLAGE | P (KBAR) | T (°C) | REFERENCE |
|----------------|---------------------------|----------|--------|----------------------------------|
| Top | Grt-Crd-Sil-Bt-Pl-Kfs | 4.5 | 820 | Vasconcellos et al, 1991 |
| | Grt-Crd-Sil-Bt-Spl-Pl-Kfs | 7.5 | 850 | Oliveira & Ruberti, 1979 |
| | Grt-Cpx-Pl-Qzt | 8.5 | 850 | Iyer et al, 1996 |
| | Grt-Cpx-Hbl-Bt-Pl-Qzt | 12.5 | 900 | Del Lama et al, 1994 |
| Base | Grt-Cpx-Opx-Pl-Qzt | 12.0 | 890 | Campos Neto & Caby (unpublished) |

Table 2-1: Summary of thermobarometric data of Socorro-Guaxupé terrane. Mineral name abbreviations from Kretz (1983).

The whole Socorro-Guaxupé nappe maintained a near horizontal foliation, and the ENE trending lineations with E-directed shear sense indicators throughout the nappe argue for its eastward displacement (around 200 km, Fig.2-3). To the south, a major NE-trending dextral shear belt truncates the Socorro-Guaxupé nappe. Syn-metamorphic structures in the nappe are cut by undeformed circular high-K diorite to syenitic plutons emplaced at ca.10 km depth (Janasi et al, 1993) at 612 Ma (Töpfner, 1996) that belong to ultrapotassic suites. An alkaline intrusive suite adjacent to a graben filled with molassic and volcanic sequences (ca. 600 Ma, Siga Jr. et al, 1995) at the southwestern boundary of Apiaí-Guaxupé Terrane also reflect this last extensional regime.

2-3. The kyanite-granulite nappe

2-3.1 Lithology

This ca. 5 km thick high-pressure nappe comprises mainly coarse-grained kyanite-garnet granulites with lesser amounts of kyanite quartzites, impure quartzites, few calc-silicate rocks and garnet-rich quartzites. The typical granulites are derived from potassic,

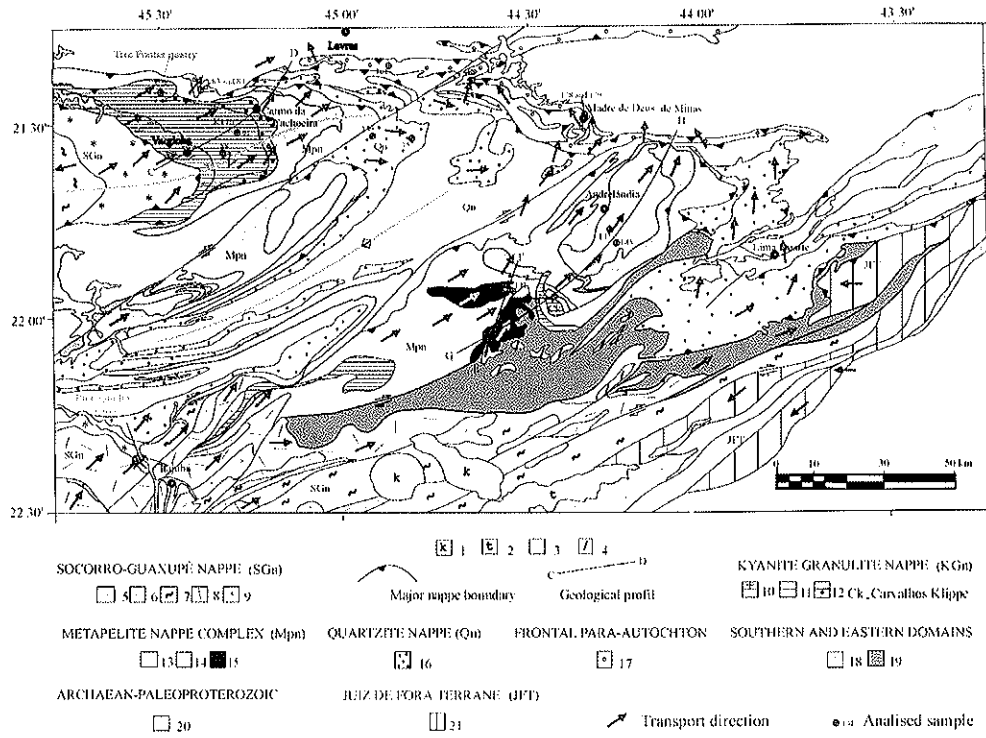


Figure 2-3: Geological map of nappe system South of São Francisco craton

1. Cretaceous, 2. Tertiary, 3. plutonic rocks (ca. 595-570 Ma), 4. tourmaline-bearing granites. Socorro-Guaxupé nappe: 5. high-K calc-alkaline granitoids (ca. 630 Ma), 6. schist belt, 7. paragneisses and migmatites, 8. granite-migmatite complex, 9. granulites. Kyanite-Granulite nappe (Kgn): 10. sillimanite-kyanite migmatites, 11. kyanite granulite, 12. metabasic-quartzitic association. Metapelite nappe complex (Mpn): 13. metapelites, 14. metagreywackes, 15. kyanite-bearing migmatites. Quartzite nappe (Qn): 16. quartzitic-schist assemblage. Frontal Para-autochthonous units: 17. interbedded quartzites and phyllites. Southern and Eastern domains: 18. metavolcanosedimentary sequence, 19. migmatite terrain. Archaean-Paleoproterozoic: 20. orthogneisses, migmatites and metamafic-ultramafic sequence. Juiz de Fora terrane: 21. Paleoproterozoic reworked enderbites.

hyper-Al and Ca-poor pelites (Três Pontas type). This sequence devoid of significant retrogression grades upward into sillimanite-garnet granulites (Varginha-type) approaching the basal contact of the Socorro-Guaxupé nappe (Fig. 2-4). At Três Pontas, these granulites form a moderately boudinaged sequence in which the compositional layering inherited from sedimentary bedding is outlined by the variable proportion of kyanite, garnet and minor micaceous layers. Layers a few centimetres thick with up to 80% of garnet, others a few millimetres thick with kyanite as the main mineral, grey quartzites, various amphibole and calc-silicate-bearing rocks, and rare mafic/ultramafic rocks are intercalated within the main kyanite-garnet granulite type. To the south two klippen made up of the same kyanite granulites are preserved, thus arguing for a minimum of 100 km of eastward displacement of the nappe (Fig. 2-1 and 2-3). One Sm/Nd whole-rock from a kyanite granulite of the Três Pontas and one from the Varginha types give T_{dm} model ages of 1.4 and 1.55 Ga respectively with ϵ_{Nd} (0.625) of -3.6 and -2.1 (Janasi verbal communication, data from Isotope Research Laboratory, Kansas University, USA). Such values seems to indicate that the source of the sediments had a mixed Proterozoic-Archaean age different from the

terrigenous cover of São Francisco craton, and had active continental margin characteristics (McLennan et al., 1990).

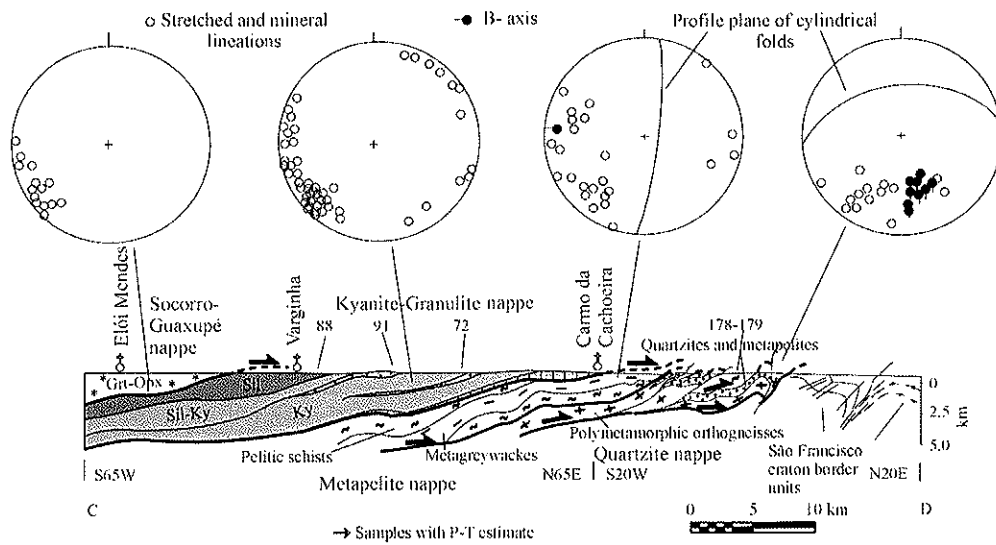


Figure 2-4: Cross-section of kyanite-granulite nappe and Carmo da Cachoeira nappe with equal-area stereographic lower hemisphere projection of mineral and stretching lineations.
91 – analysed sample for P-T.

2-3.2 Kinematics

The main structural pattern is similar to that of the Socorro-Guaxupé nappe and is characterized by a sub-horizontal foliation. ENE trending mineral and stretching lineations (kyanite, rutile, white mica, quartz ribbons, Fig. 2-4), whereas in the Carvalhos Klippen lineations are oriented E-W (Fig. 2-5). The most common structures are asymmetrical boudins (up to 5 m long) even in metapelites of similar rheology, and rare interfolial folds. The ENE direction of ductile flow is evidenced by asymmetric structures such as winged porphyroclasts, decimetric metabasic swells of pull-apart type and small isoclinal a-type folds. Mylonitic bands are associated with in-plane type winged porphyroclasts and tight small-scale folds with stretched limbs.

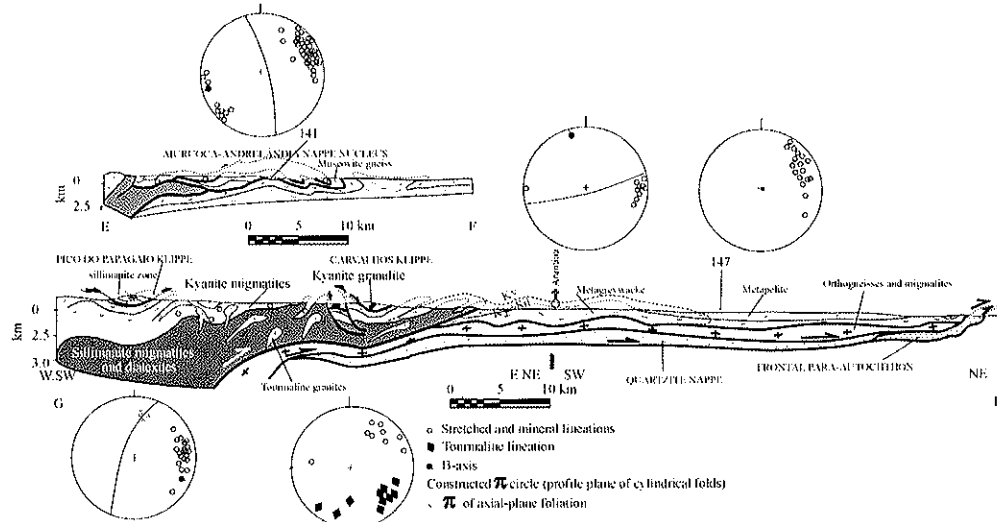


Figure 2-5: Cross-sections of Aiuruoca-Andrelândia nappe complex with equal-area stereographic lower hemisphere projection of mineral and stretching lineations.
141 – analysed sample for P-T.

2-3.3 Microstructures and mineral assemblages

The Três Pontas type kyanite-garnet granulites are light-gray to bluish, coarse-grained massive rocks with 0.5 cm mean grain size. Bands with porphyroblastic structure containing garnet, kyanite and rutile alternate with thinner bands of more massive granoblastic, calc-silicate-rich and mica-poor rocks that did not undergo through post mineral deformation and/or recrystallization.

An early prograde stage is preserved in pyrope-rich garnets that display cores with unrecrystallized microdomains containing relics of a folded cleavage defined by minute acicular rutile crystals. The syn-kinematic foliation is defined in most granulites by quartz ribbons, by the planar disposition of rare micas and platy kyanite prisms, the elongations of which defines the lineation in hand specimen. Most layers display porphyroblastic microstructures except for a few massive, garnet-rich rocks and calc-silicate rocks collected from boudin cores. Feldspar and kyanite augen up to 2 centimetres long and minute augen enclosed in coarse monocrystalline quartz up to 1-2 cm long register pervasive ductile flow at rather high pressures, since sillimanite is absent in most samples. Minute prismatic sillimanite (125μ) has only been observed along grain boundaries from a few samples. On the basis of the textural relationships, it is possible to distinguish an early stage of crystallisation reaching coarse grain size, followed by synkinematic granoblastic recrystallisation.

The first stage assemblage comprises quartz, mesoperthite, rare plagioclase, almandine-pyrope garnet, white mica, rutile, ankerite, graphite, monazite and rare primary biotite. Quartz-feldspathic lenses formed by up to 80% of centimetre size mesoperthitic feldspar, quartz, and some kyanite, primary white mica and garnet, are regarded as metamorphic segregates representing recrystallized dry melts extracted from underlying aluminous granulites, and affected by further solid-state deformation. Garnet-free, kyanite-bearing granitic layers may represent a younger generation of stromatic leucosomes. Larger, better preserved garnets have pyrope-rich rings surrounding domains with fossilized early stages of growth that contain numerous inclusions of prismatic rutile, monazite, quartz and kyanite, the latter being more abundant towards the rims of the garnet. Rutile, monazite and quartz drops, as well as rare small grains of primary white mica are included in kyanite. White mica flakes are occasionally in contact with garnet rims, some being rarely included in garnet outer zones. Locally layers a few centimetres thick contain up to 30 % of white mica, associated with quartz, kyanite, garnet and rutile. Such a mineral assemblage is reminiscent of white-schists. Pseudomorphs after Na-pyroxene (albite+chlorite+carbonate) have been observed in one sample.

The second syn-kinematic stage assemblage comprises quartz, discontinuous almandine-rich garnet rims, biotite, kyanite, microcline, plagioclase, myrmekite, ilmenite, white mica and calcite. High-temperature plastic flow has deformed and partly destroyed the coarse grain minerals formed during the previous stage. Perthites are plastically deformed and mantled by minute sub-grains of recrystallised microcline, quartz, myrmekite and plagioclase. Primary white mica is bent and rimmed by brown biotite. Kyanite may be plastically microfolded or kinked, though it is mostly unaltered in mica-poor samples.

However in white mica-rich layers the kyanite is partly replaced (though in textural equilibrium) by aggregates of secondary muscovite or by a finer and randomly oriented to radiating aggregate of white mica. Secondary muscovite is the main mineral of some non foliated, feldspar and garnet-poor layers, in which all stages of replacement after kyanite can be observed, in equilibrium with plagioclase and calcite. Most of the brown biotite grew during this stage: in the fine-grained matrix; as large undulose flakes in the pressure shadows of garnet; or like a strain cap of quarter structures (Hanmer and Passchier, 1991). The biotite also occurs in fractures and deep embayments in garnet, in equilibrium with polygonal plagioclase, ilmenite and recrystallized kyanite, thus giving the appearance of primary biotite nucleation in garnet cores.

Medium-temperature synkinematic retrogression occurred in selected bands with protomylonitic fabrics in which garnet is flat and crushed. Total replacement of garnet by biotite occurs approaching cross cutting fissures filled with biotite. Kyanite from such bands is however only slightly retrogressed into white mica. Such features indicate that a fluid phase percolating in cracks promoted the synkinematic retrogression and caused rehydration of granulites. Lower temperature retrogression, though negligible in analysed samples, is evidenced in greenish samples by the nucleation of green biotite and chlorite, calcite and albite. Millimetre-thick veinlets filled with such minerals may be also present.

Mafic rocks form layers and boudins. They comprise both metabasites and more complex Fe-Mg-Ca calc-silicate rocks of metasedimentary origin. One ultramafic rock consists in ca. 40% of plastically deformed orthopyroxene prisms in equilibrium with clinopyroxene, set in a fine-grained mosaic of tremolite. Another metabasite lens (ca. 2 metres-thick) cut by leucocratic segregations comprises garnet, clinopyroxene clasts in a fine-grained biotitic matrix. Calc-silicate layers interbedded with grey Fe-Mg quartzite are amphibole-rich. Some plagioclase-free samples contain predominant brownish amphiboles and biotite, quartz, sphene and garnet with rutile inclusions. Other Mg-rich amphibolites contain clinopyroxene, plagioclase, quartz, phlogopite and scapolite. A garnet-amphibole-rich rock displays the unusual coexistence of kyanite+ankerite in a coarse grain assemblage of quartz, plagioclase and scapolite.

A sillimanite overprint is conspicuous in Varginha-type granulites that contain microcline, plagioclase, myrmekite, rutile and/or ilmenite as well as pyrope-rich garnet. Abundant syn-kinematic sillimanite has substituted most of the kyanite. Unaltered kyanite prisms may however survive in more resistant layers and in garnet cores. Recrystallisation of deformed kyanite into tiny prisms may also occur, in association with the blastesis of minute prismatic sillimanite along small shear bands and in equilibrium with newly formed prismatic rutile. The nucleation of prismatic sillimanite also progressed in the form of fine-grains or replacement of kyanite prisms. Rutile in these rocks is entirely replaced by ilmenite. Inclusions of prismatic sillimanite occur towards the rims of pyrope-rich garnet. A few feldspathic bands similar to those from the Tres Pontas granulites are also present.

2-3.4 Mineral chemistry and P/T estimation

Garnet cores from Três Pontas metapelites without biotite nucleation have the mean composition Alm50-Prp42-Grs7. Towards the rim garnet (Alm48-Prp45-Grs7) is in equilibrium with biotite, kyanite, mesoperthite and white mica. The discontinuous <500 μ rim in equilibrium with biotite is almandine rich up to 62 mole %, with a corresponding pyrope decrease to 34 mole %. Grossular content is always about 5-7 mole %, and

| | 72b | | 72 H | | 88b | | 91b | | 141.2 | | 141c | | 147.2 | | 147c | | 145i | | 178a | |
|---|-------|-------|-------|-------|-------|-------|-------|-------|-------|-----------------------|-------|-------|-------|-------|--------------------------|-------|-------|-------|-------|--|
| | C | R | C | R | C | R | C | R | C | R | C | R | C | C | R | C | R | C | R | |
| SiO ₂ | 38.00 | 37.76 | 37.62 | 37.24 | 39.91 | 39.99 | 38.64 | 37.62 | 38.00 | 38.13 | 37.34 | 37.31 | 36.92 | 37.99 | 37.65 | 37.59 | 37.57 | 36.31 | 36.18 | |
| TiO ₂ | 0.07 | 0.03 | 0.08 | 0.00 | 0.00 | 0.06 | 0.00 | 0.00 | 0.00 | 0.00 | 0.00 | 0.00 | 0.00 | 0.13 | 0.01 | 0.00 | 0.05 | 0.00 | 0.14 | |
| Al ₂ O ₃ | 21.40 | 21.37 | 22.23 | 22.48 | 22.04 | 22.27 | 22.62 | 22.21 | 22.41 | 22.39 | 22.16 | 22.12 | 21.53 | 21.32 | 21.61 | 21.16 | 20.90 | 21.21 | 21.65 | |
| Cr ₂ O ₃ | 0.01 | 0.04 | 0.03 | 0.01 | 0.05 | 0.00 | 0.00 | 0.00 | 0.00 | 0.00 | 0.00 | 0.00 | 0.00 | 0.00 | 0.04 | 0.01 | 0.00 | 0.02 | 0.00 | |
| FeO ^t | 33.90 | 34.48 | 28.14 | 28.45 | 23.63 | 23.55 | 25.06 | 28.79 | 26.68 | 27.87 | 26.72 | 25.56 | 36.61 | 33.10 | 34.67 | 35.58 | 35.56 | 29.84 | 32.14 | |
| MnO | 0.28 | 0.27 | 0.45 | 0.47 | 0.56 | 0.56 | 0.52 | 0.66 | 0.54 | 0.69 | 0.59 | 0.55 | 0.71 | 1.19 | 1.26 | 0.90 | 0.82 | 3.10 | 0.86 | |
| MgO | 5.04 | 5.17 | 8.42 | 8.61 | 10.28 | 10.20 | 12.06 | 9.19 | 4.44 | 4.23 | 4.91 | 4.46 | 4.52 | 3.19 | 2.80 | 3.32 | 3.20 | 1.58 | 2.44 | |
| CaO | 1.00 | 0.92 | 2.53 | 2.47 | 2.46 | 2.33 | 1.52 | 1.52 | 9.67 | 8.04 | 7.66 | 9.26 | 0.69 | 2.95 | 1.80 | 1.30 | 1.35 | 7.24 | 5.78 | |
| Na ₂ O | 0.04 | 0.00 | 0.00 | 0.06 | 0.11 | 0.12 | 0.00 | 0.00 | 0.00 | 0.00 | 0.03 | 0.02 | 0.00 | 0.10 | 0.15 | 0.00 | 0.00 | 0.03 | 0.06 | |
| Total | 99.74 | 100.0 | 99.48 | 99.79 | 99.04 | 99.08 | 100.7 | 99.99 | 101.9 | 101.4 | 100.7 | 99.28 | 101.2 | 99.97 | 99.99 | 99.86 | 99.45 | 99.33 | 99.25 | |
| Structural formulae normalised to 12 oxygen with ferric iron calculated | | | | | | | | | | | | | | | | | | | | |
| Si | 3.02 | 3.00 | 2.92 | 2.88 | 3.06 | 3.06 | 2.91 | 2.90 | 2.920 | 2.95 | 2.93 | 2.93 | 2.92 | 3.04 | 3.02 | 3.02 | 3.04 | 2.93 | 2.91 | |
| Al ^T | 0.00 | 0.00 | 0.08 | 0.12 | 0.00 | 0.00 | 0.09 | 0.10 | 0.08 | 0.05 | 0.07 | 0.07 | 0.08 | 0.00 | 0.00 | 0.00 | 0.00 | 0.06 | 0.08 | |
| Al ^{IV} | 2.00 | 1.99 | 1.95 | 1.92 | 1.99 | 2.01 | 1.91 | 2.09 | 1.945 | 1.99 | 1.98 | 1.98 | 1.93 | 2.01 | 2.04 | 2.00 | 1.99 | 1.95 | 1.96 | |
| Fe ³ | 0.11 | 0.11 | 0.09 | 0.09 | 0.07 | 0.07 | 0.18 | 0.181 | 0.135 | 0.05 | 0.09 | 0.08 | 0.14 | 0.11 | 0.11 | 0.12 | 0.12 | 0.10 | 0.11 | |
| Fe ² | 2.14 | 2.17 | 1.73 | 1.74 | 1.44 | 1.43 | 1.40 | 1.676 | 1.580 | 1.75 | 1.66 | 1.59 | 2.28 | 2.10 | 2.21 | 2.27 | 2.28 | 1.91 | 2.05 | |
| Mg | 0.60 | 0.61 | 0.97 | 0.99 | 1.17 | 1.16 | 1.35 | 1.056 | 0.509 | 0.49 | 0.57 | 0.52 | 0.53 | 0.38 | 0.33 | 0.40 | 0.38 | 0.19 | 0.29 | |
| Mn | 0.02 | 0.01 | 0.03 | 0.03 | 0.03 | 0.03 | 0.03 | 0.043 | 0.035 | 0.05 | 0.04 | 0.03 | 0.05 | 0.08 | 0.08 | 0.06 | 0.05 | 0.21 | 0.06 | |
| Ca | 0.08 | 0.08 | 0.21 | 0.20 | 0.20 | 0.19 | 0.12 | 0.125 | 0.796 | 0.67 | 0.64 | 0.78 | 0.06 | 0.25 | 0.15 | 0.11 | 0.11 | 0.62 | 0.50 | |
| X _{Fe} | 0.75 | 0.75 | 0.58 | 0.58 | 0.50 | 0.51 | 0.48 | 0.58 | 0.54 | 0.59 | 0.57 | 0.54 | 0.78 | 0.74 | 0.79 | 0.80 | 0.80 | 0.65 | 0.70 | |
| X _{Mg} | 0.21 | 0.21 | 0.33 | 0.33 | 0.41 | 0.41 | 0.47 | 0.36 | 0.16 | 0.17 | 0.19 | 0.18 | 0.18 | 0.13 | 0.12 | 0.14 | 0.14 | 0.06 | 0.10 | |
| X _{Ca} | 0.03 | 0.03 | 0.07 | 0.07 | 0.07 | 0.07 | 0.04 | 0.04 | 0.27 | 0.23 | 0.22 | 0.26 | 0.02 | 0.09 | 0.05 | 0.04 | 0.04 | 0.21 | 0.17 | |
| GRANULITE FACIES ROCKS | | | | | | | | | | ECLOGITE FACIES ROCKS | | | | | AMPHIBOLITE FACIES ROCKS | | | | | |

Table 2-2: Selected analyses of garnets. C: core, R: rim. FeO^t: total Fe as FeO

| | 72b Mc 18 | 72h Mc 14 | 91b Mpth22 | 91b Pl30 | 88b Pl 23 | 141.2 Pl ² 37 | 141c Pl ¹ 30 | 141c Pl ² 4 | 141c Pl ³ 6 | 147c Pl 31 | 145i Pl 18 | 178a Pl 11 |
|--|------------------------|--------------|---------------|-------------|-----------------------|-----------------------------|----------------------------|---------------------------|---------------------------|---------------|---------------|---------------|
| SiO ₂ | 64.14 | 64.22 | 62.12 | 61.80 | 60.89 | 64.01 | 65.14 | 64.06 | 59.46 | 60.90 | 63.99 | 62.60 |
| Al ₂ O ₃ | 18.70 | 18.83 | 22.16 | 24.14 | 24.25 | 23.69 | 22.34 | 23.07 | 25.87 | 24.47 | 22.27 | 24.17 |
| FeO ^T | 0.00 | 0.00 | 0.03 | 0.04 | 0.09 | 0.20 | 0.07 | 0.04 | 0.02 | 0.05 | 0.01 | 0.00 |
| MnO | 0.00 | 0.00 | 0.00 | 0.00 | 0.04 | 0.00 | 0.00 | 0.00 | 0.00 | 0.00 | 0.00 | 0.00 |
| MgO | 0.00 | 0.00 | 0.00 | 0.00 | 0.07 | 0.00 | 0.01 | 0.00 | 0.00 | 0.00 | 0.01 | 0.00 |
| BaO | 0.42 | 0.42 | - | - | 0.00 | - | 0.00 | 0.00 | 0.08 | 0.00 | 0.05 | 0.00 |
| CaO | 0.00 | 0.00 | 3.50 | 5.25 | 6.08 | 4.16 | 3.08 | 4.30 | 7.65 | 5.72 | 3.31 | 5.10 |
| Na ₂ O | 0.46 | 1.89 | 7.15 | 8.57 | 7.99 | 9.41 | 9.12 | 8.48 | 6.82 | 8.35 | 9.30 | 8.09 |
| K ₂ O | 16.33 | 13.83 | 3.84 | 0.29 | 0.36 | 0.02 | 0.00 | 0.08 | 0.06 | 0.07 | 0.06 | 0.04 |
| Total | 100.05 | 99.19 | 98.80 | 100.09 | 100.37 | 101.5 | 99.76 | 100.03 | 99.96 | 99.56 | 98.94 | 100.00 |
| Structural formulae normalised to 8 oxygen | | | | | | | | | | | | |
| Si | 2.97 | 2.97 | 2.81 | 2.74 | 2.70 | 2.79 | 2.86 | 2.82 | 2.65 | 2.71 | 2.84 | 2.76 |
| Al | 1.02 | 1.03 | 1.18 | 1.26 | 1.30 | 1.22 | 1.15 | 1.19 | 1.36 | 1.28 | 1.16 | 1.25 |
| Ca | 0.00 | 0.00 | 0.17 | 0.25 | 0.29 | 0.19 | 0.14 | 0.20 | 0.36 | 0.27 | 0.16 | 0.24 |
| Na | 0.04 | 0.17 | 0.63 | 0.74 | 0.68 | 0.79 | 0.77 | 0.72 | 0.59 | 0.72 | 0.80 | 0.69 |
| K | 0.96 | 0.82 | 0.22 | 0.02 | 0.02 | 0.00 | 0.00 | 0.00 | 0.00 | 0.00 | 0.00 | 0.00 |
| Ab | 4.1 | 17.2 | 62.0 | 73.0 | 64.0 | 80.0 | 84.3 | 77.7 | 61.5 | 72.3 | 83.3 | 74.0 |
| An | 0.0 | 0.0 | 17.0 | 25.0 | 29.0 | 20.0 | 15.7 | 21.8 | 38.1 | 27.3 | 16.4 | 25.8 |
| Or | 95.9 | 82.8 | 21.0 | 2.0 | 2.0 | 0.0 | 0.0 | 0.4 | 0.3 | 0.4 | 0.3 | 0.2 |
| | Granulite facies rocks | | | | Eclogite facies rocks | | | | Amphibolite facies rocks | | | |

Table 2-3: Selected analyses of feldspars. Mc: microcline; Mpth: mesoperthite; Pl: plagioclase; Pl¹: symplectite intergrowth with cpx; Pl²: coronitic garnet ring; Pl³: amphibole intergrowth.

| | 72B Ms 33 | 147.2 Prg137 | 147C Ms23 | 145i Ms23 | 179B Ms11 | 178A Ms21 | 159C Ms13 | 157 Ms4 | 161C Ms9 | 161E Phg43 | 84C Phg60 | 84A Phg26 | 188A Ms6 |
|---|------------------|-----------------|--------------|--------------|-----------------|--------------|--------------|--------------------------------|-------------|---------------|--------------|--------------|-------------|
| SiO ₂ | 46.25 | 46.72 | 45.90 | 46.22 | 46.35 | 46.50 | 47.04 | 47.28 | 46.16 | 48.33 | 47.26 | 46.78 | 46.69 |
| TiO ₂ | 0.99 | 0.06 | 0.44 | 1.01 | 0.50 | 0.13 | 0.32 | 0.42 | 0.14 | 0.24 | 1.14 | 0.86 | 0.33 |
| Al ₂ O ₃ | 34.41 | 41.36 | 36.29 | 35.49 | 36.84 | 37.03 | 35.90 | 35.68 | 37.47 | 32.56 | 25.82 | 27.83 | 36.28 |
| Cr ₂ O ₃ | 0.02 | 0.00 | 0.00 | 0.04 | 0.11 | 0.07 | 0.02 | 0.00 | 0.07 | 0.00 | 0.00 | 0.00 | 0.00 |
| FeO ^t | 1.15 | 0.97 | 0.84 | 1.47 | 0.96 | 0.73 | 1.43 | 1.10 | 0.24 | 1.13 | 7.88 | 6.78 | 1.17 |
| MnO | 0.00 | 0.01 | 0.00 | 0.01 | 0.00 | 0.00 | 0.03 | 0.00 | 0.00 | 0.05 | 0.02 | 0.00 | 0.06 |
| MgO | 0.74 | 0.00 | 0.62 | 0.61 | 0.57 | 0.60 | 0.86 | 0.88 | 0.19 | 0.74 | 1.81 | 1.43 | 0.66 |
| CaO | 0.00 | 0.00 | 0.00 | 0.00 | 0.00 | 0.00 | 0.01 | 0.00 | 0.02 | 0.00 | 0.00 | 0.00 | 0.04 |
| Na ₂ O | 0.26 | 7.68 | 1.14 | 1.12 | 1.91 | 1.49 | 0.76 | 0.92 | 1.81 | 1.44 | 0.13 | 0.17 | 0.88 |
| K ₂ O | 10.65 | 0.44 | 9.76 | 8.72 | 8.49 | 9.10 | 10.52 | 10.60 | 7.85 | 8.33 | 10.78 | 10.56 | 9.65 |
| H ₂ O | 4.47 | 4.77 | 4.51 | 4.51 | 4.57 | 4.57 | 4.58 | 4.58 | 4.53 | 4.45 | 4.31 | 4.33 | 4.55 |
| Total | 98.94 | 102.1 | 99.50 | 99.20 | 100.3 | 100.2 | 101.2 | 101.46 | 98.46 | 97.27 | 99.15 | 98.74 | 100.3 |
| Structural formulae normalised to 12 oxygen | | | | | | | | | | | | | |
| Si | 3.10 | 2.93 | 3.05 | 3.07 | 3.04 | 3.05 | 3.08 | 3.09 | 3.05 | 3.25 | 3.29 | 3.24 | 3.07 |
| Al ^{IV} | 0.89 | 1.06 | 0.95 | 0.93 | 0.96 | 0.94 | 0.92 | 0.91 | 0.94 | 0.75 | 0.71 | 0.76 | 0.92 |
| Al ^{VI} | 1.82 | 2.00 | 1.89 | 1.85 | 1.89 | 1.92 | 1.85 | 1.84 | 1.98 | 1.83 | 1.40 | 1.51 | 1.88 |
| Ti | 0.05 | 0.00 | 0.02 | 0.05 | 0.02 | 0.00 | 0.01 | 0.02 | 0.00 | 0.01 | 0.06 | 0.04 | 0.01 |
| Fe ² | 0.06 | 0.05 | 0.04 | 0.08 | 0.05 | 0.04 | 0.08 | 0.06 | 0.01 | 0.06 | 0.46 | 0.39 | 0.06 |
| Mg | 0.07 | 0.00 | 0.06 | 0.06 | 0.05 | 0.06 | 0.00 | 0.08 | 0.02 | 0.07 | 0.19 | 0.15 | 0.06 |
| Na | 0.03 | 0.94 | 0.14 | 0.14 | 0.24 | 0.19 | 0.10 | 0.12 | 0.23 | 0.19 | 0.02 | 0.02 | 0.11 |
| K | 0.91 | 0.04 | 0.82 | 0.74 | 0.71 | 0.76 | 0.88 | 0.88 | 0.66 | 0.72 | 0.96 | 0.93 | 0.81 |
| X _{ms} | 0.83 | 0.03 | 0.89 | 0.85 | 0.89 | 0.91 | 0.85 | 0.84 | 0.98 | 0.84 | 0.49 | 0.57 | 0.88 |
| X _{Prg} | - | 0.88 | - | - | - | - | - | - | - | - | - | - | - |
| X _{cel} | 0.13 | 0.0 | 0.11 | 0.11 | 0.10 | 0.11 | 0.15 | 0.15 | 0.04 | 0.15 | 0.26 | 0.22 | 0.11 |
| Gnl np | Metapelite nappe | | | | Quartzite nappe | | | Frontal parauthochthonous unit | | | | | |

Table 2-4: Select analyses of white mica. Ms: muscovite, Prg: paragonite, Phg: phengite. Gnl np: kyanite granulite nappe.

spessartine < 1 mole % (Table 2-2). Primary plagioclase is oligoclase as porphyroclasts with An 14 to 17 mole % (Table 2-3), and as strings in mesoperthite. Primary white mica (Table 2-4) has low Si content (3.10 p.f.u.) and low molar fraction of celadonite ($X_{\text{cel}}=0.13$). Secondary muscovite has similar low Si and celadonite content but is less titaniferous. Biotite inclusions from pyrope-rich rings have higher phlogopite (X_{Phl} up to 0.16) and TiO_2 (up to 4 wt%) than matrix biotite (Table 2-5). Garnet from the sillimanite-containinn Varginha-type granulites also has high pyrope content of around 40-mole % in equilibrium with phlogopite-rich, titaniferous biotite (up to 4 wt% TiO_2) and plagioclase (ca. An28).

| | 72b Bt32 | 91b Bt31 | 72h Bt2 | 88b Bt11 | 147.2 Bt146 | 147c Bt*28 | 145i Bt7 | 178a Bt19 |
|---|-------------|-------------|------------|-------------|--------------------------|---------------|-------------|--------------|
| SiO_2 | 35.07 | 36.73 | 37.17 | 36.84 | 35.57 | 36.40 | 36.19 | 36.38 |
| TiO_2 | 3.23 | 2.74 | 4.41 | 4.01 | 0.95 | 1.44 | 1.62 | 1.63 |
| Al_2O_3 | 17.31 | 17.05 | 17.69 | 16.40 | 19.70 | 19.96 | 19.51 | 19.31 |
| Cr_2O_3 | 0.00 | - | 0.00 | 0.09 | - | 0.01 | 0.05 | 0.07 |
| FeO^t | 24.10 | 10.54 | 13.60 | 12.62 | 19.57 | 17.71 | 19.42 | 17.71 |
| MnO | 0.02 | 0.02 | 0.00 | 0.00 | 0.00 | 0.00 | 0.02 | 0.00 |
| MgO | 6.45 | 14.78 | 13.26 | 15.00 | 9.60 | 10.59 | 10.40 | 11.95 |
| BaO | 0.10 | - | 0.11 | 0.10 | - | 0.18 | 0.06 | 0.00 |
| Na_2O | 0.02 | 0.05 | 0.05 | 0.09 | 0.63 | 0.25 | 0.18 | 0.23 |
| K_2O | 9.35 | 10.73 | 9.95 | 10.4 | 9.95 | 9.11 | 8.42 | 8.96 |
| H_2O | 3.85 | 3.96 | 4.07 | 4.04 | 3.95 | 4.01 | 4.00 | 4.03 |
| Total | 99.50 | 96.61 | 99.91 | 99.23 | 99.92 | 99.66 | 99.87 | 100.2 |
| Structural formulae normalised to 12 oxygen | | | | | | | | |
| Si | 2.76 | 2.78 | 2.74 | 2.73 | 2.70 | 2.72 | 2.71 | 2.70 |
| Al^{IV} | 1.23 | 1.06 | 1.26 | 1.26 | 1.25 | 1.27 | 1.28 | 1.29 |
| Al^{VI} | 0.33 | 0.46 | 0.27 | 0.16 | 0.51 | 0.48 | 0.44 | 0.39 |
| Ti | 0.18 | 0.16 | 0.22 | 0.22 | 0.05 | 0.08 | 0.09 | 0.09 |
| Fe^2 | 1.54 | 0.67 | 0.84 | 0.78 | 1.24 | 1.11 | 1.22 | 1.10 |
| Mg | 0.73 | 1.66 | 1.45 | 1.66 | 1.09 | 1.18 | 1.16 | 1.32 |
| Na | 0.00 | 0.01 | 0.00 | 0.01 | 0.09 | 0.03 | 0.02 | 0.03 |
| K | 0.91 | 1.04 | 0.93 | 0.95 | 0.96 | 0.87 | 0.80 | 0.85 |
| X_{ann} | 0.14 | 0.01 | 0.02 | 0.01 | 0.06 | 0.05 | 0.06 | 0.046 |
| X_{phl} | 0.01 | 0.16 | 0.11 | 0.16 | 0.04 | 0.06 | 0.06 | 0.08 |
| Granulite facies rocks | | | | | Amphibolite facies rocks | | | |

Table 2-5: Selected analyses of biotites. Bt*: biotite included in garnet.

The restricted occurrence of rutile (Table 2-6) in both prograde and primary assemblages implies that initial and peak pressures were higher than the GRAIL net transfer reaction (Bohlen et al., 1983). Temperatures were estimated using Fe-Mg partitioning between coexisting garnet and biotite, or garnet and phengite in metapelitic rocks from KFMASH system. The available models for this thermometer (Ferry and Spear, 1978; Hodges and Spear, 1982, Green and Hellman, 1982, and Indares and Martignole, 1985) were applied and results are shown with its estimated errors in Table 2-7. The equilibrium temperatures between two pairs of primary biotite and pyrope-rich rims from the Três Pontas metapelites are between 690 and 780°C (Indares and Martignole, 1985) and are 730°C for primary muscovite and almandine-rich garnet rims

(Green and Hellman, 1982). Such values argue for initial minimum pressures around 12.0 kbar according to GRAIL in pyrope-rich garnets (Alm48-Prp47). Taking into account the coexistence of mesoperthite and primary plagioclase, a minimum pressure of about 13.0 kbar can be deduced from the GRIPS reaction using matrix ilmenite activity=0.93 (Bohlen and Liotta, 1986). The experimentaly calibrated garnet-biotite Fe-Mg exchange thermometer of Ferry and Spear (1978) and the revised model of Hodges and Spear (1982) do not take into account the presence of Al^{VI} and Ti in natural biotites as was done by Indares and Martignole (1985) for granulitic rocks. Thus the scattered and unrealistically high temperatures obtained for some granulites from Ferry and Spear and Hodges and Spear model's (Table 2-7) is attributed to the presence of appreciable Ti in biotite (up to 4.4% of TiO₂, Table 2-5). For these samples the Indares and Martignole (1985) formulation was used instead, furnishing values of T=890°C for the sillimanite-bearing Varginha-type granulite, and T=780°C for the kyanite-bearing Três Pontas-type granulite, both with white mica.

| | 72B | 147.2 | 178A | 179B | 157 | 159C | 161E | | |
|--------------------------------|-------------------|--------|-------------------|-------|-------|-----------------|-------|---------------|-------|
| | Rt 35 | IIm 48 | IIm131 | St11 | St 8 | St 1 | St21 | St 30 | Ctdl |
| SiO ₂ | 0.03 | 0.03 | 0.28 | 28.35 | 28.62 | 29.12 | 28.21 | 28.66 | 24.20 |
| TiO ₂ | 94.67 | 50.90 | 46.01 | 0.60 | 0.60 | 0.42 | 0.68 | 0.46 | 0.00 |
| Al ₂ O ₃ | 0.02 | 0.00 | 0.12 | 53.42 | 54.45 | 55.29 | 54.89 | 55.60 | 41.05 |
| Cr ₂ O ₃ | 0.05 | 0.02 | 0.04 | 0.13 | 0.05 | 0.00 | 0.25 | 0.00 | 0.00 |
| FeO ^T | 3.66 | 44.78 | 47.18 | 13.48 | 13.11 | 13.19 | 14.26 | 10.37 | 21.63 |
| MnO | 0.02 | 0.6 | 0.07 | 0.05 | 0.10 | 0.13 | 0.44 | 0.18 | 0.30 |
| MgO | 0.03 | 0.10 | 0.43 | 1.86 | 1.15 | 0.90 | 1.21 | 1.25 | 4.05 |
| CaO | 0.01 | 0.00 | - | 0.04 | 0.04 | 0.00 | 0.00 | 0.00 | 0.03 |
| Na ₂ O | 0.00 | 0.00 | - | 0.08 | 0.03 | 0.00 | 0.00 | 0.00 | 0.01 |
| K ₂ O | 0.01 | 0.01 | - | 0.00 | 0.00 | 0.00 | 0.00 | 0.00 | 0.00 |
| ZnO | - | - | - | 0.00 | 0.00 | 0.20 | 0.18 | 1.88 | - |
| Total | 98.50 | 96.44 | 94.13 | 98.01 | 98.19 | 99.08 | 99.95 | 98.43 | 91.27 |
| X _{Fe} | - | 0.97 | 0.91 | 0.78 | 0.85 | 0.87 | 0.82 | 0.71 | 0.74 |
| X _{Mg} | - | - | - | 0.19 | 0.13 | 0.10 | 0.12 | 0.15 | 0.25 |
| X _{Zn} | - | - | - | - | - | 0.01 | 0.01 | 0.11 | - |
| | Ky granulite nap. | | Metapelitic nappe | | | Quartzite nappe | | Parautochthon | |

Table 2-6: Selected analyses of chloritoid, staurolite, rutile and ilmenite. FeO^T: total Fe as FeO.

| Sample | T ₁ ±50°C | T ₂ ±50°C | T ₃ ±5°C | T ₄ °C | T ₅ ±40°C | P ₁ ±0.5kbar | P ₂ ±1.0kbar | P ₃ ±0.8kbar |
|-------------|-------------------------|-------------------------|------------------------|-------------------|-------------------------|----------------------------|----------------------------|----------------------------|
| 91B Alm r | 621.9 | 640.0 | 614.3 | | | 11.3-10.9 | | |
| 91B Alm r | 672.5 | 692.0 | 643.3 | | | 12.0-12.5 | | |
| 91B Py | 719.0 | 730.0 | 691.5 | | | 13.0-12.5 | | |
| 72H Py | 874.7 | 903.0 | 781.2 | | | | 12.3 min. | |
| 72B Alm | | | | 733 | | | 12.2 min. | |
| 88B Py | 994.6 | 1022. | 891.1 | | | 12.2 | | 11.5 |
| 147C Alm r | 582.0 | 615.0 | 618.7 | | | 12.1 | | |
| 147C Alm r | 574.0 | 606.0 | 608.8 | | | 11.9 | | |
| 147C Alm c | | | | 665 | | 13.0 | | |
| 147C Alm c | | | | | 500.0 | | 7.0 | |
| 147.2 Alm r | 567.0 | 598.0 | | | | | 9.2 | |
| 147.2 Alm c | | | | | 541.3 | | 8.6 - 8.9 | |
| 178A Grs c | | | | 571 | | | | 7.3 |
| 178A Alm r | 463.7 | | 514.2 | | | | | 5.9 |
| 179B Alm r | | | | 682 | | | | |
| 159C Alm r | | | | 627 | | | | |

Table 2-7: Thermobarometry for the KFMASH system. Alm r: almandine rich rim; Alm c: almandine rich core; Grs c: grossular rich core; Prp: pyrope rich garnet; min.: minimum pressure; T₁: Ferry & Spear (1978), T₂: Hodges & Spear (1982); T₃: Indares & Martignole (1985), T₄: Green & Hellman (1982); T₅: Pownceby et al. (1991); P₁: Bohlen et al (1983); P₂: Bohlen & Liotta (1986); P₃: Newton & Haselton (1981).

The Fe-Mg exchange between the thinner and incomplete garnet outer rim (Alm61) and the low titanium phlogopite-rich biotite ($TiO_2=1.5\%$ and Phl21) is related to a retrograde equilibrium at up to $T=640^\circ C$ and $P=11.3$ kbar (Table 2-7).

The Varginha type granulite (sample 88) displays recrystallised mylonitic bands with a oligoclase, sillimanite, phlogopite-rich biotite ($X_{Phl}=0.16$) and ilmenite assemblage, which deflect around pyrope-rich garnet porphyroblasts. Contacts between high-Ti biotite and garnet are straight and remains of kyanite and rutile are present in the non-mylonitic assemblage. The Indares and Martignole geothermometer gives temperature up to $890^\circ C$ (Ferry and Spear and Hodges and Spear models yield temperatures above the mineral assemblage equilibrium). The pressure estimated by the GRIPS assemblage is in agreement with Newton and Haselton (1981) garnet-plagioclase- Al_2SiO_5 -quartz geobarometer: 12.0 kbar and 11.5 kbar respectively (Table 2-7).

The approximate P/T (Fig. 2-6) path is based on assumed chemical equilibrium between minerals from the garnet inner-rim to almandine-rich outer-rim assemblages (sample 91B). The near-isobaric heating corresponds to a late metamorphic trajectory towards sillimanite replacement (Varginha-type granulite, sample 88).

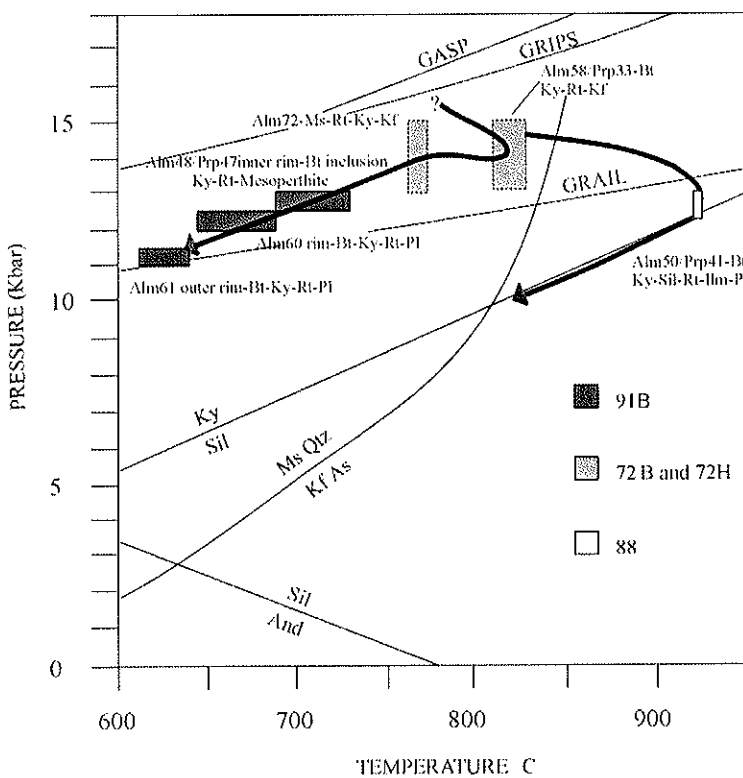


Figure 2-6: Kyanite-granulite P-T path. 91B: analysed thin section; GASP: Koziol & Newton (1988); GRIPS: Bohlen & Liotta (1986); GRAIL: Bohlen et al (1983); $Ms+Qtz \rightarrow Kf+As$ and Al_2SiO_5 triple point: Xu et al (1994).

2-4. The metapelite nappe complex

This nappe complex is chiefly made up of aluminous micaschists and garnetiferous paragneisses. It essentially comprises a layered sequence of aluminous mica-schists and

dark-gray, massive and medium-grained garnet-biotite-plagioclase gneiss/schists containing rutile and kyanite concentrated in syn-kinematic quartz veinlets. Coarse-grained kyanite blasts up to 5 cm, centimetric garnet and rutile in a matrix of white mica, quartz and late biotite are characteristic of most mica-schists. The garnet-biotite-plagioclase gneiss/schists interpreted as calc-alkaline volcanoclastics (Campos Neto et al, 1990) may represent metagraywackes. Lenses of garnet amphibolites derived from probable sills have retroeclogites (Trouw, 1992) in their cores, and retrogressed plagioclase-rich amphibolites at the borders. The retroeclogites have given a Sm-Nd garnet/whole rock age of 604 Ma (Trouw and Pankhurst, 1993).

The metapelite nappe complex forms two distinct near-horizontal sheets above the quartzite nappe (Fig. 2-3). The Carmo da Cachoeira nappe in the west (Fig. 2-4) is chiefly made up of metagraywackes and staurolite-free micaschists associated with thin beds of Mn-rich garnet-quartz rocks, calc-silicate gneiss and slices of meta-ultramafic/mafic rocks. This nappe went through a non-coaxial deformation as shown by the development of symmetamorphic S/C foliation fabric with mica-fish and well-developed mineral and stretching lineations showing a northeastward flow direction. The lineations are scattered in SW low-plunging dispersion pattern (Fig. 2-4) controlled in part by later buckling of large synformal fold (Fig. 2-3). Allochthonous metapelites from the Madre de Deus region are also considered as part of this nappe, but they were overthrust later by the quartzite nappe. The canoe-like Aiuruoca-Andrelândia nappe transported to the NE (Figs. 2-3 and 2-5) comprises an inner refolded root zone ca. 10-km thick and a stretched thinned front up to 2 km thick. Migmatites with garnet-kyanite bearing dry stromatic leucosomes, grading upwards into two-mica well-banded plagioclase-(kyanite)-garnet gneiss, are observed in the root zone and form a km-scale a-type recumbent fold towards the front of the nappe. They are detached over biotite diatexites and sillimanite-bearing stromatic migmatites that occur in the deeper part of the nappe and are cut by several muscovite-tourmaline bearing granite plutons that also form stocks in the upper part of the nappe. Small klippen of sillimanite-bearing schists with relict kyanite and with a sole of retrogressive, colder mylonites were emplaced on top of the kyanite schists in the southern part of the Aiuruoca-Andrelândia nappe (Fig. 2-5). Lineations throughout the nappe pile indicate ENE-directed displacement.

2-4.1 Petrology of eclogitic rocks and kyanite metapelites

Garnet clinopyroxenites collected from the core of mafic lenses are green coloured with medium-grained porphyroblastic texture. The garnet porphyroblasts ca. 4 mm in diameter are often surrounded by a thin plagioclase (An16 mole %) ring and by a 1 mm wide corona of brown amphibole (pargasite or hornblende). The ca. 3-mm poikiloblastic grains of clinopyroxene have blebs of quartz and plagioclase, contain both rutile and ilmenite mostly mantled by sphene, and are also surrounded by amphibole. Garnet is slightly zoned with Alm57-44, Prp19-22 and Grs22-31 mole % in the cores and Alm59-54, Prp17-18 and Grs23-26 mole % toward the rims. Rutile, apatite and prismatic blue Fe-pargasite, blue-green Mg-horblende and rare clinopyroxene are the more common inclusions. The largest ca. 1-mm clinopyroxene inclusions which cause semi-radial cracks in garnet have diopside or diopside-omphacite compositions at the contact with garnet and enclose relict lamellas of jadeite (Table 2-8). The matrix diopside re-equilibrated during the early stages of the decompression is devoid of significant Na-content and the intergrown plagioclase contain An16 mole %. The plagioclase enclosed in brown amphibole has up to

An38 mole %. Such a complex pattern may suggest the re-equilibration of former omphacitic pyroxene.

| | 72.V | | 141C | | 141.2 | | 141.2 | | 141C | | |
|--------------------------------|--------|--------|--------|--------|-------|--------|--------|--------------------|--------------------|---------------------|---------------------|
| | Opx162 | Cpx161 | Cpx3 | Cpx 29 | Jd 33 | Omp 40 | Cpx 48 | Pg ¹ 12 | Pg ² 35 | Hbl ¹ 24 | Hbl ² 42 |
| S iO ₂ | 56.60 | 53.39 | 53.01 | 52.51 | 62.89 | 55.52 | 52.48 | 38.35 | 43.97 | 46.18 | 45.02 |
| TiO ₂ | 0.00 | 0.00 | 0.00 | 0.05 | 0.00 | 0.00 | 0.05 | 0.00 | 0.38 | 0.83 | 1.04 |
| Al ₂ O ₃ | 0.09 | 0.07 | 1.38 | 1.48 | 23.54 | 8.64 | 3.35 | 21.34 | 13.47 | 10.09 | 11.86 |
| Cr ₂ O ₃ | 0.03 | 0.00 | 0.03 | 0.00 | 0.00 | 0.00 | 0.03 | 0.00 | 0.02 | 0.07 | 0.14 |
| FeO ^T | 8.94 | 2.37 | 9.00 | 9.33 | 0.17 | 6.78 | 8.73 | 16.69 | 15.42 | 16.73 | 16.07 |
| MnO | 0.31 | 0.16 | 0.05 | 0.13 | 0.01 | 0.06 | 0.07 | 0.08 | 0.06 | 0.14 | 0.05 |
| MgO | 33.22 | 17.77 | 12.81 | 12.48 | 0.05 | 8.28 | 11.87 | 7.83 | 11.07 | 11.08 | 10.29 |
| CaO | 0.11 | 24.83 | 23.82 | 23.32 | 4.73 | 18.19 | 22.76 | 11.19 | 11.15 | 11.43 | 11.94 |
| Na ₂ O | 0.00 | 0.10 | 0.54 | 0.50 | 9.41 | 3.99 | 0.90 | 2.84 | 2.26 | 1.02 | 1.49 |
| K ₂ O | 0.00 | 0.00 | 0.00 | 0.00 | 0.00 | 0.00 | 0.00 | 0.00 | 0.12 | 0.09 | 0.10 |
| Total | 99.33 | 98.72 | 100.64 | 99.89 | 100.8 | 101.4 | 100.3 | 98.33 | 97.93 | 97.59 | 97.86 |
| Si | 1.98 | 1.96 | 1.96 | 1.96 | 2.20 | 1.99 | 1.95 | 5.64 | 6.44 | 6.76 | 6.26 |
| Ti | 0.00 | 0.00 | 0.00 | 0.00 | 0.00 | 0.00 | 0.00 | 0.00 | 0.04 | 0.09 | 0.11 |
| Al | 0.004 | 0.003 | 0.06 | 0.06 | 0.97 | 0.36 | 0.15 | 3.69 | 2.32 | 1.74 | 2.05 |
| Cr | 0.001 | 0.00 | 0.00 | 0.00 | 0.00 | 0.00 | 0.00 | 0.00 | 0.00 | 0.00 | 0.01 |
| Fe ³⁺ | 0.03 | 0.00 | 0.04 | 0.03 | 0.00 | 0.00 | 0.02 | 0.47 | 0.36 | 0.44 | 0.16 |
| Fe ²⁺ | 0.235 | 0.046 | 0.23 | 0.25 | 0.01 | 0.20 | 0.25 | 1.58 | 1.52 | 1.60 | 1.82 |
| Mn | 0.009 | 0.005 | 0.00 | 0.00 | 0.00 | 0.00 | 0.00 | 0.01 | 0.01 | 0.02 | 0.00 |
| Mg | 1.74 | 0.97 | 0.71 | 0.69 | 0.01 | 0.44 | 0.66 | 1.72 | 2.42 | 2.42 | 2.26 |
| Ca | 0.004 | 0.98 | 0.94 | 0.93 | 0.18 | 0.70 | 0.91 | 1.76 | 1.75 | 1.79 | 1.88 |
| Na | 0.00 | 0.01 | 0.04 | 0.03 | 0.64 | 0.28 | 0.06 | 0.81 | 0.64 | 0.29 | 0.02 |
| K | 0.00 | 0.00 | 0.00 | 0.00 | 0.00 | 0.00 | 0.00 | 0.00 | 0.02 | 0.01 | 0.02 |

Table 2-8 Selected analyses of pyroxenes and amphiboles. Structural formulae of Px normalised to 6 oxygen; structural formulae of Amp: average normalised to 15 cations excluding K, Na and Ca. FeO^T: total Fe as FeO. ¹: amphibole included in garnet; ²: coronitic amphibole. Opx: orthopyroxene, Cpx: clinopyroxene, Jd: jadeite, Omp: omphacite, Pg: pargasite, Hbl: hornblende.

Metapelitic schists from the upper part of the nappe are staurolite free, Ky-Rt-Grt-Ms-Pl-Qtz assemblages. From this zone downwards staurolite becomes stable and ilmenite is found instead of rutile. Kyanite is the only Al-silicate of high-Al metapelites. Synkinematic muscovite generally mantles garnet, staurolite and kyanite. It has a high X_{Ms}/X_{Cel} ratio (ca. 8.0) although the Si-content remains low and constant (3.05 p.f.u.). Biotite overgrows and/or partially replaces the muscovite. Garnet may contain composite inclusions of kyanite, rutile, ilmenite, paragonite (X_{Prg}=0.9) and staurolite (Tables 2-4 and 2-6) in a strain sensitive fabric. Muscovite and biotite also occur as inclusions towards clear garnet rims. Garnet is almandine rich with higher grossular content in the core (Fig. 2-7A). Plagioclase (An16-27) is a late phase in equilibrium with muscovite, biotite and ilmenite.

Metapelites from the Madre de Deus de Minas region (Fig. 2-3) contain abundant staurolite and ilmenite as well as kyanite. Staurolite seems to precede kyanite according to Ribeiro and Heilbron (1982) and Heilbron (1985) who have mapped NE-oriented isograds oblique to nappe contours. Fe-staurolite (Table 2-6) and kyanite up to 1-cm size show straight boundaries with optical continuity. The staurolite often displays several fabric-sensitive inclusions of ilmenite and quartz. The garnet, also porphyroblastic, with ilmenite, white mica, albite and quartz inclusions, is zoned (Fig. 2-7 B). Chlorite also may be abundant and is associated with sulfides.

2-4.2. P-T estimates

The garnet-clinopyroxenite seems to record a pre-eclogite stage as evidenced by the bluish pargasite and Mg-hornblende inclusions in garnet. The garnet-amphibole

thermometer of Graham and Powell (1984) yields 569°C for the garnet (Alm45-Prp22-Grs31)-hornblende pair and 660°C for the garnet (Alm59-Prp13-Grs26)-pargasite pairs.

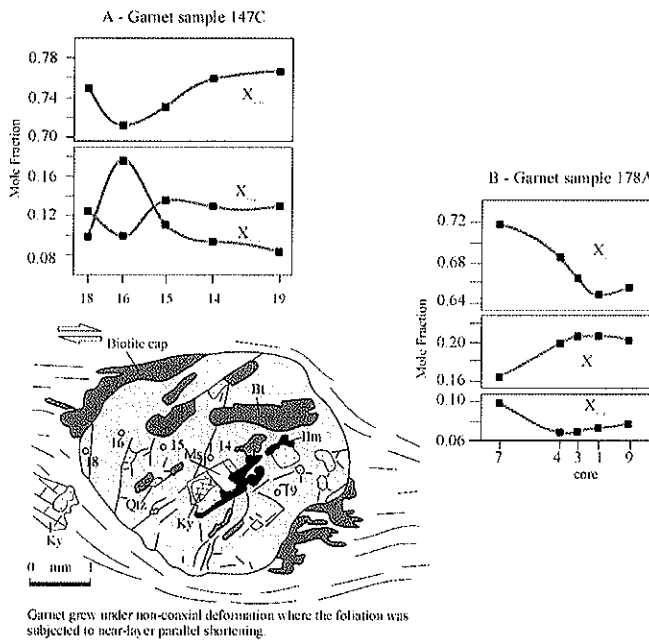


Figure 2-7: Garnet compositional profiles. A: sample 147C with garnet sketch; Bt=biotite, Ms=muscovite, Ilm=ilmenite, Ky=kyanite, dotted=quartz. B: sample 178A.

Although the igneous Al-in hornblende geobarometer (Hammarstrom and Zen, 1986 and Hollister et al., 1987) gives ca. 11.5 kbar the pressure from pargasite bound 14 kbar. The pressure peak recorded by the unzoned jadeite lamella in Cpx included in garnet (X_{Jd} up to 0.76) reaches 17.5 kbar (Meyre et al., 1997) for a T fixed at 660°C. The garnet core (Alm58-Prp17-Grs23) and omphacite inclusion ($X_{Jd}=0.3$) furnishes ca. $T= 716^{\circ}\text{C}$ (based on Powell, 1985) and $P=15$ kbar (Meyre et al., 1997) also for the eclogite stage. The Fe-Mg exchange between coexisting garnet (core compositions of Alm57-Prp18-Grs23 from thin section 141.2 and Alm45-Prp22-Grs31 from thin section 141.C) and diopside (respectively either as inclusion or as matrix assemblage with high-Na oligoclase simplectitic texture) is the first record of eclogite retrogression at a mean $T= 650\pm 33^{\circ}\text{C}$ and $P=13.7\pm 1.9$ kbar (Eckert et al, 1991). The garnet outer-rim, plagioclase ring and outer amphibole assemblage in a well-developed coronitic texture is the final record of retrograde stage. Garnet-amphibole thermometry (Graham and Powell, 1985) gives a mean temperature of about $632\pm 35^{\circ}\text{C}$ compatible, within the errors, with the temperature by amphibole-plagioclase thermometry (Blundy and Holland, 1990), $T=650\pm 75^{\circ}\text{C}$ (Table 2-9). The pressure is up to 11.6 kbar (Khon and Spear, 1990).

The eclogitic rocks may have passed through a prograde metamorphic stage with strong isothermal loading followed by heating and decompression in a clockwise P-T loop. Their retrogression history included a near-isobaric cooling stage (Fig. 2-8).

P-T estimation for the metapelites in the Aiuruoca-Andrelândia nappe have been attempted on the kyanite-staurolite gneiss/schist. Garnet (Alm71-Grs18) cores $\text{Fe}/(\text{Fe}+\text{Mg}) \text{ mol} = 0.83$ indicate a temperature of about 580°C (Spear and Cheney, 1989), and the temperature

approach decrease to 540°C applying the Fe-Mn partitioning between coexisting garnet and ilmenite (Ilm activity=0.92) as inclusion (Pownceby et al., 1991) in spite of the low Mn content of garnet (Alm79-Grs1-Sps1), both in agreement with the presence of staurolite and paragonite inclusions. The garnet core assemblage (also kyanite and rutile inclusions) gives a pressure up to 8.9 kbar based on GRAIL barometry (Table 2-7). The assumed equilibrium

| Sample | T ₁ °C | T ₂ ±75°C | T ₃ ±5°C | T ₄ °C | P ₁ ±0.5 kbar | P ₂ ±1.9 kbar | P ₃ kbar |
|-------------------|----------------------|-------------------------|------------------------|----------------------|-----------------------------|-----------------------------|------------------------|
| 141.2 corona | 668 | 671.3 | | | 11.1 | | |
| 141.2 corona | 597 | 654.4 | | | 10.9-11.6 | | |
| 141.2 Di incl | | | 667.3 | 646 | | 13.5±1.9 | |
| 141.2 Di incl | | | 640.4 | 618 | | 13.0±1.9 | |
| 141.2 Di incl | | | 704.5 | 684 | | 14.2±1.9 | |
| 141.2 Omp incl | | | 736.5 | 716 | | | 15.0 |
| 141.2 Jd incl | | | | | | | 17.5 at 660°C |
| 141.2 Prg incl | 653-675 | | | | | | |
| 141.C corona | | 620.0 | | | | | |
| 141.C Di/Grt core | | | 661.6 | 641 | | 14.2±1.9 | |
| 141.C Di/Grt rim | | | 696.8 | 677 | | 12.9±1.9 | |
| 141.C Hbl incl | 569 | | | | | | |

Table 2-9: Thermobarometry for eclogitic rocks. Di incl: diopside inclusion; Omp incl: omphacite inclusion; Jd incl: jadeite inclusion; Pg incl: pargasite inclusion; Di/Grt-Prp: diopside and grossular-pyrope rich garnet pair; Hbl incl: hornblende inclusion; T₁:Graham & Powell (1984); T₂: Blundy & Holland (1990); T₃: Ellis & Green (1979); T₄: Powell (1985); P₁: Kohn & Spear (1990); P₂: Eckert et al (1991); P₃: Meyre et al. (1997).

between near rim almandine-rich garnet, matrix muscovite and plagioclase would occur at T≈665°C (Green and Hellman, 1982) and P≈13.0 kbar using the GRAIL barometer, and the GRIPS reaction. The almandine-rich rim and biotite mantle both in contact with plagioclase imply T≈610°C and P≈12.0 kbar, respectively using Indares and Martignole (1985), Bohlen et al (1983) and Bohlen and Liotta (1986). A higher-pressure stage in these metapelites, consistent with the eclogitic assemblage recorded in mafic lenses, is inferred from the occurrence of chlorite+albite+carbonate pseudomorphs possibly after Na-Ca pyroxene. These data suggest a clockwise P-T loop and are in agreement with the high-pressure amphibolite facies decompression path of eclogitic mafic lenses (Fig. 2-8).

In the kyanite-staurolite schists near Madre de Deus the asymmetrical portions of Alm-poor, Gros-rich garnets having straight contacts with muscovite furnish a temperature of 580°C (Green and Hellman, 1982). The incomplete clean Alm-rich garnet rim in textural equilibrium with synkinematic and late biotite gives T ca. 517°C by Indares and Martignole (1985) thermometer. The garnet-kyanite-plagioclase-quartz barometer (Newton and Haselton, 1981, modified by Koziol and Newton, 1988) applied to Alm-poor garnet-muscovite pairs with low-Ca oligoclase porphyroclasts furnish 7.3 kbar, while the Alm-rich garnet-biotite pairs accompanying polygonal oligoclase crystals indicate P≈5.9 kbar (Table 2-7). Although no information is deduced about the peak pressure, the metapelites seems to show the same metamorphic path of the eclogites (Fig. 2-8).

2-5. The quartzite nappe complex

The quartzite nappe complex is a lower allochthon cropping out as a window surrounded by the metapelite nappe. White and green-mica quartzites, with locally

preserved detrital grains grade upward and westward into well bedded to laminated quartzites interlayered with graphitic metapelites (ca. 100 m thick). A cratonic area is the

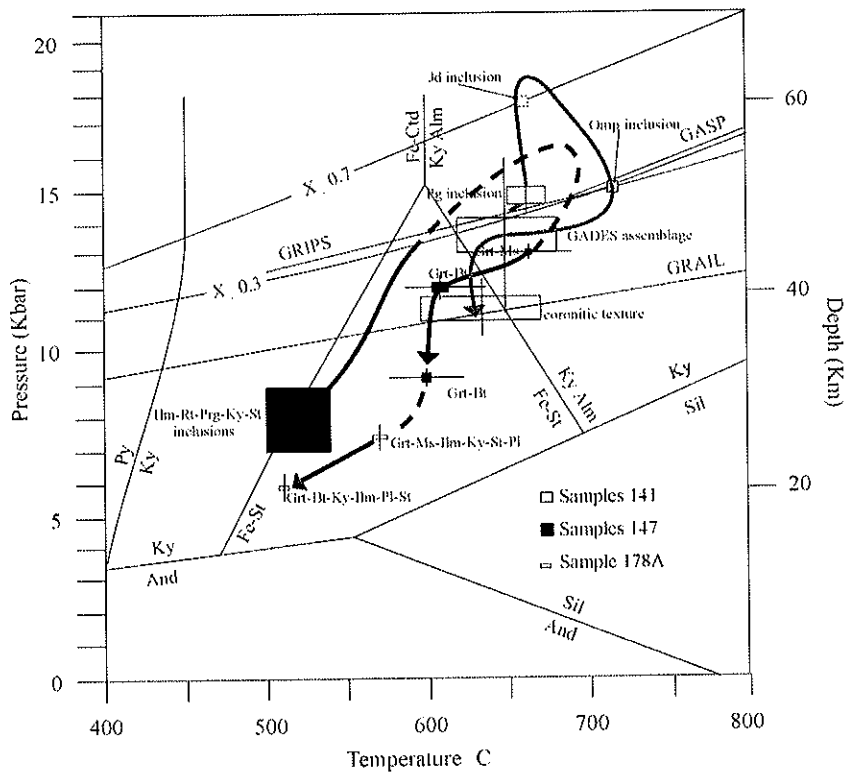


Figure 2-8: Aiuruoca-Andrelândia nappe P-T path. $X_{\text{d}}=0.7$ based on the reaction $\text{Ab}=\text{Jd}+\text{Qtz}$: Meyre et al. (1997); GASP: Koziol & Newton (1988); GRIPS: Bholen & Liotta (1986); GRAIL: Bholen et al (1983); staurolite field: Powell et Holland (1990); Al_2SiO_5 triple point: Xu et al (1994); 141C and 141.2: analysed thin sections.

assumed source of these metasediments, which were deposited in a shelf/ramp environment after 1.87 Ga (minimum U-Pb age of detrital zircons, Söllner and Trouw, *in* Ribeiro et al., 1995). The syn-metamorphic foliation is axial-plane of kilometric, a-type recumbent and E-SE verging folds (Trouw et al., 1980; 1983). S/C-type structures and associated strong E-SE mineral and stretching lineations (Fig. 2-3) were formed during eastwards synmetamorphic transport (Trouw et al., 1982). The quartzite nappe also includes a large volume of polymetamorphic orthogneisses ascribed to the basement of the quartzites. The basement consists of migmatites and meta-ultramafic slices, but the quartzitic sequence is allochthonous above the orthogneisses, except for a few remnants of possibly undetached cover. In the quartzite nappe, in the Lima Duarte region 50-km southeast of Andrelândia, only sillimanite is found in quartzites and metapelites.

Metapelite samples (157-159) ca. 30-km southeast of Lavras have a staurolite-ilmenite-garnet-muscovite-quartz assemblage with abundant tourmaline. The garnet is compositionally zoned ($\text{Alm}_{70-81}\text{Prp}_{15-11}\text{Sps}_{14-6}$ from core to rim), the staurolite is Fe-rich (mean $X_{\text{Fe}} = 0.85$), the muscovite has low Si and Cel contents (mean $\text{Si} = 3.06$ p.f.u., $X_{\text{Cel}} = 0.13$) and ilmenite has a high Fe activity (0.94). Almandine-rich garnet and stable muscovite pairs furnish a temperature of 620 to 636 °C (Green and Hellman, 1982 calculated for $P = 6.5$ kbar, Table 2-7-sample 159).

2-6. The parautochthonous unit

This frontal unit crops out in a narrow belt between Paleoproterozoic rocks of the São Francisco craton and the nappes. It was affected by the lowest temperature metamorphism and has a thin-skinned structural behaviour. It comprises a shelf-type series made up of interbedded quartzites and gray phyllites. The main metamorphic cleavage defined by chloritoid and white micas is deformed by tight, near isoclinal and N-verging folds generally with wavelengths up to some tens of metre, with an associated axial-planar crenulation cleavage developed in metapelites. Most stretching lineations observed in quartzites are related to these folds. Southeast of Lavras the crenulation cleavage progressively flattens downward approaching a rarely outcropping low-angle mylonitic sole thrust. Hundreds of metre scale duplex structures with flat-ramps and antiformal stacks have also been observed.

Al-Fe-Mg metapelites contain abundant Fe-chloritoid and variable amounts of Mg and Fe-chlorite, phengite, Zn-rich staurolite (Table 2-6), kyanite, rutile, and ilmenite. Xenomorphic kyanite shows an asymmetrical chloritoid-muscovite fringe. Kyanite and chloritoid show apparent gradational boundaries. Staurolite ($X_{Fe} = 0.71$, $X_{Zn} = 0.11$) occurs as idioblastic and twinned crystals with abundant dark dusty inclusions free of appendages, and displays inclusion-free overgrowths. In these rocks the Si content of phengite reaches 3.25 p.f.u. and the X_{Ce} reaches 0.28 (sample 161E, Table 2-4), resulting in a pressure around 7 kbar for temperature around 500°C (Oberhänsli et al., 1995) that may control the appearance of Zn staurolite in the absence of garnet and biotite. Maximum Si content up to 3.3 has been measured in white mica from samples east of Três Pontas quarry (Table 2-4).

2-7. Discussion

The nappe system exposed south of the São Francisco craton shows a coherent metamorphic pattern with T-max decreasing downward beneath the Socorro-Guaxupé nappe, and is therefore similar to that reported from the Central Himalayas (Caby et al., 1983; Le Fort et al., 1986; Burg et al., 1987; Macfarlane, 1995; Vannay and Hodges, 1996; Hodges et al., 1996). The Guaxupé basal granulites record T-max around 900°C at 630 Ma, coeval with the emplacement of noritic magmas. These high temperatures were reached regionally at P-max around 12 kbar, and coincided with the emplacement of charnockitic/mangeritic magmas extracted from underlying granulites. Geochemical data suggest that the Socorro-Guaxupé granulites derive mainly from igneous protoliths in the mafic roots of a Neoproterozoic arc assemblage. The strong decompression down to 4.5 kbar observed at the top of the Socorro-Guaxupé nappe relates to tectonic unroofing through southeast-directed normal shearing.

The kyanite granulites nappe ca. 6 km-thick under the Socorro-Guaxupé nappe displays the same foliation and ENE-verging kinematics records P-max around 13 kbar and T around 750°C increasing upward to 890°C (Varginha-type granulites), thus similar to that of overlying Guaxupé granulites. Rare ultramafic cumulates were emplaced in the kyanite granulites. Lower temperatures of about 650°C were attained in the lower high-pressure nappe (P=12-14 kbar) related to the decompression stage of eclogitic basic rocks at 17.5 kbar (T=660°C). T decreases to ca. 600°C and P to 7 kbar downward in the quartzite nappe and only reaches 500°C at ca. 7 kbar in the parautochthons. Since the kyanite granulites are

separated from the parautochthons by only a few hundreds of metres (15 km north of Varginha), a major post metamorphic displacement of the granulites may have taken place in agreement with a temperature gap of about 250°C. This late contact is responsible for the truncation of the quartzite nappe southwest of Lavras. The maximum thickness of the metapelitic nappe (ca. 11 km) occurs south of Adrelândia where klippen of kyanite granulites are preserved on top of this nappe showing that the still-hot granulites were displaced more than 100 km towards the ENE. ENE to NE-directed syn-metamorphic transport is well constrained in both the Varginha and the Andrelândia regions. The metapelitic nappe records fast exhumation from eclogitic to amphibolite facies conditions and its re-equilibration at T=660°C and P=13 kbar could be interpreted as representing the maximum nappe stacking before thinning. The lack of evidence for high-pressure conditions in the lower parts of the nappe system, together with E-directed and N-directed transport directions in the quartzite nappe and in the Madre de Deus region, respectively, suggest that the emplacement of the high-pressure overlying nappes is a late event that occurred after significant thinning of the allochthons.

Apparently high thermal conductivity may be inferred from eclogitic metamorphic assemblages from the metapelitic nappe. Such a value is typical for subduction-related metamorphism (Ernst, 1988) suggesting an open oceanic domain to the west. This is supported by the occurrence of a mafic-ultramafic sequence with podiform chromite (Petunia complex) exposed below the Socorro-Guaxupé nappe 130-km WNW of Varginha. These rocks were considered as a fragment of Neoproterozoic oceanic crust by Choudhuri et al. (1995) although not supported by available geochronological data. The Neoproterozoic ca. 800 Ma Maratá Sequence with podiform chromite has been described in the Brasilia Belt (Fuck et al., 1994).

The metamorphic conditions from both the kyanite granulite nappe and the metapelitic nappe could represent the early exhumation process of subducted continental crust material.

The lack of evidence for Neoproterozoic high-pressure conditions in the basement rocks of the southern part of the São Francisco craton (rare minute brown biotite and white micas) implies that the nappes had been significantly thinned when they overrode this area of the craton margin. In contrast, rocks of the eastern domain around Lima Duarte underwent a high temperature imprint with formation of sillimanite.

The Socorro-Guaxupé nappe shows a rather different temperature evolution with T_{max} as high as 900°C possibly connected with heat advection by noritic magmas corresponding to a high heat flow and steep paleothermal gradients. The near-isothermal decompression recorded on the top of Socorro-Guaxupé nappe necessarily requires regional heating during extension that may have been connected with mantle upwelling, as suggested by the occurrence of lenses of ultramafics interleaved with granulites in the middle part of the nappe.

2-8. Conclusions

The high-pressure nappe system at the southern border of the São Francisco Craton represents part of the history of Neoproterozoic Gondwana assembly between the São Francisco microcontinent and a western plate that included magmatic arc assemblages. The roots of this magmatic arc are represented by the Socorro-Guaxupé granulites whereas the upper part could be represented by the 860 Ma old Mara Rosa arc of oceanic affinities

(Pimentel et al., 1997), with possible relics of oceanic lithosphere. The P-T conditions deduced from mineral assemblages of both the high-pressure granulite and the metapelitic nappes strongly suggests that these have been exhumed eastward from a west-dipping subduction complex deduced from eclogitic rocks. Early ENE-directed syn-metamorphic transport around 630 Ma stacked the HP-HT thick-skinned arc terrane (Socorro-Guaxupé nappe) over metapelitic units (kyanite-granulites and metapelitic nappe) that were subjected to nearly synchronous high-pressure metamorphic conditions. These metapelitic units are not considered as belonging to the cover of the São Francisco craton in the light of ϵ_{Nd} (0.630) between -2 and -3.5 and T(dm) 1.4 and 1.55. The whole high-pressure pile may have been exhumed from the subduction prism through the return-flow mechanism proposed by Chemenda et al. (1995). Metamorphic facies thus record an inverted metamorphism. Sillimanite overprint visible only on top of the kyanite granulites records a T increase due to downward heat advection from the overlying hotter Socorro-Guaxupé granulites during its eastward displacement. The excellent preservation of kyanite granulites that form a 4.5-km sheet devoid of overprinting in the sillimanite stability field is exceptional. This pile was subsequently thrust onto the lower portion of the nappe system that according to lithologic considerations and age of the source may derive from the São Francisco passive continental paleo-margin (quartzite nappe and parautochthons).

The late dextral movement along the strike-slip shear zones in the south may have controlled final displacements of the nappes, both parallel and radial to the craton boundary.

Acknowledgements

This research is supported by FAPESP grants 95/4652-2, 95/2622-9 and 96/12320-2 and CNPq grant 95/523944. Discussions with V. A. Janasi and M. A. S. Basei and valuable reviews by M. Babinsky, I. McReath, P. Le Fort, T. Horscroft and an anonymous referee greatly improved this paper. This manuscript were written while the first author was on research leave at the Tectonophysics Laboratory of the Montpellier II University, France: the support and hospitality received are also appreciated.

CAPÍTULO 3

TERRANE ACRETION AND UPWARD EXTRUSION OF HIGH-PRESSURE NEOPROTEROZOIC NAPPES OF THE SOUTHEAST BRAZIL: PETROLOGIC AND STRUCTURAL CONSTRAINTS

Abstract

The high-grade crystalline nappes exposed southeast of the São Francisco craton comprise two distinct units of mainly granulite-facies rocks that represent a composite section of Neoproterozoic deep continental crust: the Socorro-Guaxupé nappe above, derived from an arc terrane, and the Três Pontas-Varginha nappe below. Metamorphism in the Três Pontas-Varginha nappe is characterized by the exceptional preservation of kyanite granulites ($700\text{-}750^\circ\text{ C}$, 15 kbar), and experienced limited retrogression. Maximum temperatures around $900\text{-}950^\circ\text{ C}$ were reached towards the base of the overlying Socorro-Guaxupé nappe, during the intrusion of charnockitic-mangeritic magmas. Lower pressure metamorphism, accompanied by anatexis, prevailed at shallower crustal levels. Our petrological results document an inverted thermal structure with isobaric heating of the top of the high-pressure granulite nappe. Both granulite nappes were transported more than 200 km eastward above lower nappes involving reworked basement and passive margin units, both metamorphosed to high pressure but lower temperature conditions. Significant thinning and cooling of the two granulite nappes may have occurred before their emplacement onto the lower nappes. The proposed geodynamic scenario considers that continental subduction took place westward underneath Neoproterozoic oceanic lithosphere. The two granulite units crystallised at ca 45 km depths under distinct paleogeotherms within this subduction zone around 630 Ma. The kyanite granulites were rapidly exhumed through the mechanism of low-angle "forced" extrusion, whereas syn-collisional collapse affected the soft, anatexic middle crust of the overlying arc terrane. The final emplacement of the thinned nappe pile onto the cold São Francisco craton and its platform cover, with at most, anchizonal to greenschist-facies metamorphism, occurred around 600 Ma.

3-1. Introduction

Recent advances in deciphering the geometry, kinematics and orogenic development of deeper crustal levels of major Proterozoic collisional orogens have revealed increasing similarities with Phanerozoic orogens such as the Himalaya, but observed at much deeper crustal levels. Crystalline nappes with associated reverse metamorphism, displaced at low angle onto less metamorphosed units, have been documented in several segments of Mesoproterozoic belts (*Rivers et al.*, 1989) and Neoproterozoic orogens of the Gondwana (*Caby*, 1989; *Castaing et al.*, 1993; *Caby*, 1994; *Attoh*, 1998). The occurrence of preserved high-pressure granulites and eclogites in continental margin units gives the opportunity to better constrain the P/T regimes from subducted continental crust. As pointed out by *Myashiro* (1973), paired metamorphic belts involving low-pressure rocks adjacent to high-pressure terrains imply rather contrasted paleogeotherms that may allow delineation with former suture zones. Perturbed paleogeotherms $<15^\circ\text{C/km}$, reconstructed from continental units, are in agreement with subduction underneath cold oceanic lithosphere (*Peacock*,

1992), whereas those $>45^\circ$ C/km require the major role of mantle upwelling at shallow depths to account for the genesis of low-pressure granulites (Spear, 1993).

In this respect, the giant crystalline nappes thrust eastward onto the southern edge of the São Francisco craton (SFC) in SE Brazil include both high-temperature, medium to low-pressure units, and high-pressure (HP) terrains with the uncommon occurrence of unretrogressed felsic kyanite granulites (Campos Neto & Caby, in press). In this paper, we present new detailed metamorphic studies on the HP-granulites that allow to reconstruct two contrasting, nearly synchronous P-T paths. We document the syn-collisional collapse of the western hot allochthon intruded by a huge volume of charnockitic *sl* plutons and we propose a mechanism of low-angle extrusion for the exhumation of the deeper, HP-granulite nappe displaced 200 km eastwards onto lower temperature nappes derived from a passive margin. Then we present a new geodynamic and kinematic scenario for the evolution of SE Brazil that requires a west-dipping subduction setting.

3-2. Geological setting

Southeast and central Brazil records two major episodes of continent assembly on the western and southern edges of the SFC (Fig. 3-1) during Neoproterozoic-Cambrian times (Campos Neto & Figueiredo, 1995; Pimentel *et al.*, 1996; Paciullo *et al.*, 1998; Heilbron *et al.* 1998). The crustal roots of a magmatic arc accreted on the southeastern edge of SFC between 590-570 Ma (Söllner *et al.*, 1987, 1989 and 1991) essentially form the younger Rio Doce terrane. Steep foliations with overall subhorizontal stretching lineations, forming the 60 km wide axial zone, represent the frontal feature of this transpressive system (the Ribeira belt). West of the Archean-Paleoproterozoic SFC, the Brasilia belt (Fuck *et al.*, 1994) comprises the external zones parautochthons and lower allochthons with greenschist-facies metamorphism derived from the rift-type to passive continental margin metasedimentary sequences that were deposited on the SFC margin. HP-metagreywackes and metapelites forming the middle nappes (Valeriano *et al.*, 1995; Seer *et al.* 1998; Valeriano *et al.*, 1998; Simões, 1995), were transported eastward more than 100 km onto the anchizonal carbonates and glaciogenic rocks (Bambui Group). The internal tectonic units comprise a juvenile island arc terrane 900-750 Ma old (Pimentel *et al.*, 1991; Pimentel & Fuck, 1992; Pimentel *et al.*, 1997). Regional metamorphism at 630 Ma (Pimentel *et al.*, 1997) was related to ocean closure and continental collision. Post-kinematic granites were emplaced in Late Cambrian time (Pimentel *et al.*, 1996).

The nappe system south of the SFC represents deeper crustal equivalents to the Brasilia belt (Trouw *et al.*, 1984). It comprises a flat-lying package of east-verging nappes with HP-metamorphism including retroeclogites (Trouw, 1992; Campos Neto & Caby, in press) overlying the allochthonous-parautochthonous units related to passive continental margin (Ribeiro *et al.*, 1995). No occurrences of metaluminous granites have been reported from these nappes. In contrast with the Brasilia nappe edifice, the upper allochthon (the Socorro-Guaxupé nappe - SGN) comprises mainly mafic granulites and a syn-kinematic suite of intrusions of charnockitic affinity. These high-grade units have been interpreted as the root of a magmatic arc formed along an active continental paleo-margin of a western plate (Campos Neto & Figueiredo, 1995) possibly connected with the Rio de la Plata/Parana craton. Major strike-slip shear zones connected with the Ribeira belt bound the SGN to the southeast. High-K post-kinematic granites and syenites were intruded in the SGN during the 612-590 Ma time span (Töpfner, 1996; Pimentel *et al.*, 1996). Lithostratigraphy, structure

and metamorphism of the units that underlie the SGN were summarised by Trouw *et al.* (1983 and 1986), Campos Neto *et al.* (1990), Ribeiro *et al.* (1995) and Paciullo (1997).

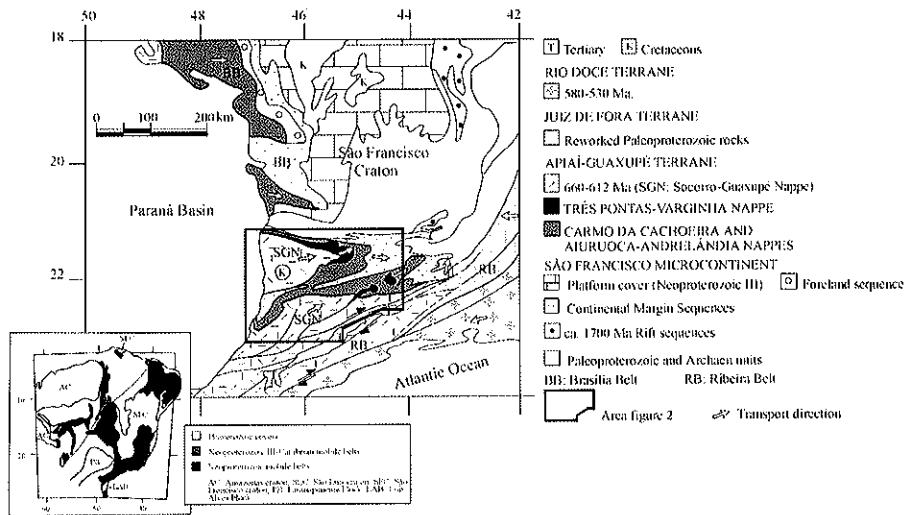


Figure 3-1. Regional tectonic map of part of southern Brazil.

3-3. Tectonic Units

3-3. 1. The Socorro-Guaxupé nappe – SGN

The SGN is a giant allochthon showing a right way up crustal section of hot and partially-melted, layered crust. Its basal sole thrust cuts across various terrains of the lower nappes, both the passive margin units and the reworked basement with Archean age protoliths. It comprises a Basal Granulitic Unit (ca. 3 km thick) that grades upward into grey to pink, metaluminous migmatites (Middle Diatexitic Unit, ca. 6 km thick) indenting at their top with pelitic to semi-pelitic migmatites (Upper Migmatite Unit). Normal faulting and dextral strike-slip shear zones control a major metamorphic jump between these migmatites and the green-schist facies unit in the southwest (Fig. 3-2).

3-3. 1. 1. The Basal Granulitic Unit

Green-coloured, banded Grt±Opx (symbols after Kretz, 1983) granulites of enderbitic modal composition are the main rock types of the Basal Granulite Unit, interleaved with decimetre-thick layers of gabbro-noritic gneiss considered as synmetamorphic intrusives. The well-developed stromatic structures are present as anhydrous hololeucocratic leucosomes (light-coloured enderbitites and coarse-grained grey to pink charnockites). Concordant veins (0.10 to 1.0 m thick) of Grt-bearing mangerite also occur. The top of this unit is marked by the gradual transition into amphibolite facies, where the predominate rock types are Hbl and Bt-Hbl-bearing tonalite to granodiorite gneisses containing many decametre-thick metabasic lenses and white stromatic bands of leucotonalitic to trondhjemitic composition. Field and petrographic relations show that these amphibolite facies rocks are not the products of granulite retrogression (Fernandes *et al.*, 1987). Based on major and trace elements, Campos Neto *et al.* (1996) have established

that the enderbitic granulites may derive mainly from magmatic arc igneous protoliths. A few lenses of well-banded Grt-Bt-Spl-mesoperthite (Mph)-Pl gneisses of pelitic composition are interlayered with the mafic granulites. These aluminous rocks also show major element chemical relationships compatible with sedimentary protoliths deposited along an active margin. However, their restitic character in part, may disguise the primary chemical trend. The enderbitic granulites from the Piranguinho quarry (Fig. 3-2) show a preliminary Sm/Nd T(dm) age around 1290 Ma with e_{Nd} (0.640)= -1.2 (Table 3-1) that constrains the Meso-Neoproterozoic age of the assumed magmatic arc. The Grt-Bt whole rock Sm-Nd date of 630 Ma (Table 3-1) constrains the age of granulite facies metamorphism.

3-3. 1. 2. The Middle Diatectic Unit

Anatetic granitic-gneisses characterize the Middle Diatectic Unit. Here, discontinuous stromatic migmatites are enclosed by widespread grey to pinkish nebulites and deformed porphyritic granitoids. Stromatic migmatites predominate as a dark-grey Hbl-Bt (Cpx) gneissic mesosome of dioritic-tonalitic composition. Light-grey hololeucocratic Bt-leucosomes (cm to m thick veins) of throndhjemite composition alternate with Fe-Mg melanosomes. Pervasive grey to pinkish nebulites are leucocratic and coarse grained Bt (Hbl)-bearing granites showing transitional contacts with irregular and batholithic size bodies of deformed porphyritic granites. These contain enclaves of dioritic-monzonodioritic gneisses and xenoliths of Grt-Di-Scp calc-silicate rocks. Lenses of Sil-Crd metapelites (=kinzigites), ca. 100 m thick and 3 km long occur among these granitic rocks.

3-3.1.3. The Upper Migmatitic Unit

This upper unit mainly consists of a migmatized metasedimentary sequence in which degree of anatexis decreases upward (southwestward). Grt±Sil-Bt banded gneisses, mostly with light-grey, Bt-Grt-bearing leucosomes grade upward into peraluminous mica schist locally interleaved with Ms-bearing leucosomes. Subordinate Sil-Ms feldspathic quartzites and Qtz-rich gneisses, calc-silicate gneisses, rare marbles, Hbl gneisses and mafic metaintrusives are intercalated. Zircons from a high-grade metapelite have yielded a U/Pb upper intercept age in the range 1.9-2.1 Ga (*Ebert et al.*, 1996), a date that we interpret as the mean age of the inherited zircons incorporated in the sediment.

3-3.1.4. The syn-kinematic plutonic intrusives

Various intrusives occur throughout the nappe pile. They are strongly stretched and linear, ca. 2 km thick bodies of charnockites concentrated towards the base of the allochthon. Higher in the pile occur large and well-oriented bodies of Hbl-Bt bearing granitoids. The porphyritic-porphyroclastic charnockitic rocks comprise a high-K calc-alkaline suite with a modal trend towards norite to enderbite-opdalite-charnockite compositions. Mc and subordinated Pl are the main megacrysts and Opx-Bt-Hbl are the mafic minerals. Pyroxene-bearing pegmatites occur in crosscutting veins. The mangeritic-granitic suite (625 Ma, Table 3-1) has a tabular shape and occurs within the migmatites of the Middle Diatectic Unit. It comprise green-coloured, medium to coarse grained gneisses

from hypersthene (Hy)-bearing mangerite and charnockite, interleaved with pink, laminated and coarse-grained hornblende granite and hololeucocratic granite. These rocks have a mean chemical composition relatively high in Al, Fe, Na and K, low Ca, Sr and Mg# and characteristically higher Zr content, up to 1300 ppm (Campos Neto *et al.*, 1988; Janasi, 1997).

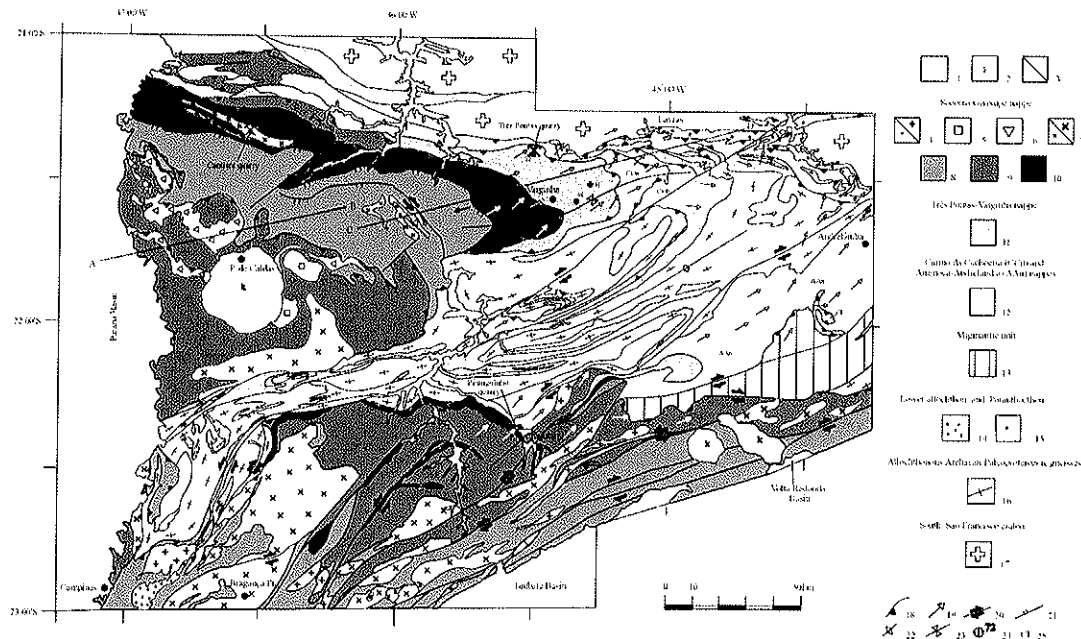


Figure 2. Geological map of the nappe system south of the São Francisco craton.

1. Phanerozoic basins; 2. Cretaceous alkaline plutons; 3. Small pull-apart basins. Socorro-Guaxupé nappe: 4. (small crosses) K-granites (ca.580 Ma) and (crosses) shear zone related granites (ca. 600-580 Ma); 5. Syenitic plutons (612 Ma); 6. Mangeritic-Granitic suite (625 Ma); 7. (x) K calc-alkaline porphyritic granitoids (ca.630 Ma) and (small x) Charnockitic suites; 8. Upper Migmatitic unit; 9. Middle Diatexitic unit; 10. Basal Granulitic unit. Três Pontas-Varginha nappe: 11. Ky-Grt granulites grading upward to Sil-bearing diatexites. Carmo da Cachoeira (CCn) and Aiuruoca-Andrelândia (AAn) nappes: 12. Metapelites and metagreywackes. Migmatitic unit: 13. Migmatites. Lower allochthon and parautochthon: Quartzite-schist assemblage of the Quartzitic nappe 14 and the Parautochthon 15. Allochthonous Archaean-Paleoproterozoic gneisses: 16. Grey-gneisses and migmatites. South São Francisco Craton: 17. Grey-gneisses and mafic-ultramafic series. 18. Major thrusts; 19. Displacement vectors; 20. Strike-slip shear-zone; 21. Major ductile normal fault; 22. Antiform; 23 Synform; 24. Analysed sample; 25. Carvalhos klippe.

The granites forming the upper batholiths (dated around 630 Ma, Table 3-1) follow modally and chemically an expanded high-K calc-alkaline trend. Porphyritic Hbl-Bt-Qtz monzonites and monzogranites with abundant mafic enclaves and less abundant small bodies of gabbro prevail (Campos Neto *et al.*, 1984; Wernick *et al.*, 1984; Janasi & Hulbrich, 1991; Haddad, 1995). Monzodiorites, tonalites and granodiorites occur subordinately. Their isotopic signature (Sm-Nd and Rb-Sr) strongly suggests they formed above a subduction zone (Janasi *et al.*, 1997). The metaluminous pink to grey anatetic granites crop out in the Middle Diatexitic Units as pervasive large masses with poorly defined boundaries. Plutons of Ms-granites (625 Ma, Table 3-1) and light-grey Grt-Bt agmatitic granites prevail in the Upper Migmatitic Unit. The youngest plutons (612 Ma, Table 3-1) are undeformed ellipsoidal syenitic massifs, with local ring-like structure composed of unsaturated syenite (Janasi *et al.*, 1993; Janasi & Vlach, 1997).

3-3.2. The Três Pontas-Varginha nappe - TPVN

The TPVN (ca. 5 km thick) comprises mainly coarse-grained and granoblastic Ky-Grt granulites, lesser Ky-quartzites, impure quartzites, few calc-silicates and manganiferous beds (gondites). From its base, where decametre lenses of metabasic rocks and quartzite occur, granulites form a moderately boudinaged sequence (Três Pontas-type) in which the compositional layering inherited from sedimentary bedding is outlined by the variable proportion of Ky, Grt and minor micaceous layers (Figs. 3-6). Layers a few centimetres thick with up to 80% of Grt, others a few millimeters thick with Ky as the chief mineral, grey quartzites and various amphibole-calc-silicates are intercalated in common kyanite granulites. Rare lenses of mafic/ultramafic rocks among which orthopyroxenite may represent synmetamorphic intrusives. Ductilely deformed kyanite-mesoperthite bearing leucosomes and younger kyanite-bearing granitoid veins are parallel to compositional layering. This sequence devoid of significant retrogression grades upward into Sil-Grt (Ky) granulites (Varginha-type) approaching the basal contact of the SGN. Bt-Grt-Sil anatectites also occur at the highest level.

| Unit | Method | Age (Ma) | Ref. |
|--|--------------------------|-------------------------------------|------|
| Piranguinho basal Grt-granulite | Sm-Nd T_{dm} model age | 1290 $\epsilon_{Nd} (0.640) = -1.2$ | 1 |
| | Sm-Nd Grt-Bt-whole rock | 629±14 | 1 |
| Cantière Charnockitic suite | U-Pb zircon evaporation | 667±17 | 2 |
| | U-Pb zircon | 643±12 | 3 |
| S. J. Rio Pardo Mangeritic suite | U-Pb zircon evaporation | 630±16 | 2 |
| | U-Pb zircon | 625±7 | 3 |
| Sil-Grt migmatite Socorro Porfritic Granitoid Bragança Paulista Porfiroclastic Granitoid Tico-Tico Peraluminous Granite | U-Pb zircon (lower int.) | 650 | 4 |
| | U-Pb zircon | 629±3 | 5 |
| | U-Pb zircon | 655 ±2 | 4 |
| | U-Pb zircon | 625±18 | 5 |
| Pedra Branca peralkaline Syenite | U-Pb zircon | 612±2.5 | 5 |
| Shear zone-related Serra do Lopo Granite | U-Pb zircon | 595±12 | 4 |

Table 1. Recent U-Pb and Sm-Nd geochronological data from Socorro-Guaxupé nappe 1. Teixeira (personal communication); 2. Kröner (written communication); 3. Basei et al. (1995); Ebert et al. (1996); 5. Topsner (1996).

The Três Pontas-type granulites are mainly derived from Al-rich and Ca-poor pelites (low Na₂O/K₂O ratio <1.0). Layers with a high content of Ca, Mg and Ti may represent impure carbonates. Other common intercalations are derived from relatively medium-Ca and high-Mg greywackes (high Na₂O/K₂O ratio 1.1). The Varginha type granulites show a variable Na₂O/K₂O ratio (both pelites and greywackes) and low Ti. Geochemical investigations in progress suggest that these rocks may derive from calc-alkaline, or high-Ca chemical sources possibly resulting from reworked magmatic arc rocks, whereas those with high-Al, low-Ca character may derive from Al-rich clays. One Sm/Nd whole-rock date from a granulite of Três Pontas and one from the Varginha type (both with chemical affinity of an active margin provenance) give T_{dm} model ages at 1.4 and 1.55 Ga respectively with ϵ_{Nd} (0.625) of -3.6 and -2.1 (*Janasi*, unpublished result). Such values argue for a derivation of the sediments from a distinct Meso-Neoproterozoic terrane and show a broad incompatibility with a unique source from the Archean/Paleoproterozoic rocks of SFC. These data further constrain the foreign origin of both the Socorro-Guaxupé and the Três Pontas-Varginha granulites, that we therefore regard as two distinct terranes.

3-4. Nappe geometry, kinematics and metamorphic evolution

The sinuous tectonic front of the Brasilia nappes progressively overlaps to the south the southern edge of the SFC (Fig. 3-1). The flat geometry of the nappes in the south is that of spoon-like structures displaced eastward. These are separated by lateral ramps that were commonly reactivated as strike-slip faults after the main displacements. This argues for a greater tectonic transport from the west to the east (200 km), and this accounts for deeper crustal levels progressively exposed in the western nappes

| Sample | T ₁ ±50°C | T ₂ ±50°C | T ₃ (°C) | T ₄ (°C) | T ₅ (°C) | T ₆ (°C) | T ₇ (°C) | T ₈ ±75°C | T ₉ (°C) |
|--------------|-------------------------|-------------------------|------------------------|------------------------|------------------------|------------------------|------------------------|-------------------------|------------------------|
| 81.B Opx-Cpx | | | | | | | | | |
| 81.B Ca↑ Grt | | | 810-833 | 792-817 | 777-786 | 848 | 869 | | 756 |
| 81.B Fe↑ Grt | | | 775-797 | 755-778 | 765-775 | | | | 720 |
| 81.B Amp-Pj | | | | | | | | 755-756 | |
| 34.A Grt-Opx | | | | | 861 | | | | |
| 34.A matrix | 890 | 919 | | | | | | | |
| 34.A matrix | 954 | 982 | | | | | | | |
| 34.A rim | 730 | 760 | | | 721 | | | | |

Table 3-2. Thermometry of the granulites from the hanging wall of the main thrust. T1: Ferry & Spear (1978); T2: Hodges & Spear (1982); T3: Ellis & Green (1979); T4: Powell (1984); T5: Harley (1984); T6: Wells (1977); T7: Sen & Jones (1989); T8: Blundy & Holland (1990); T9: Graham & Powell (1984).

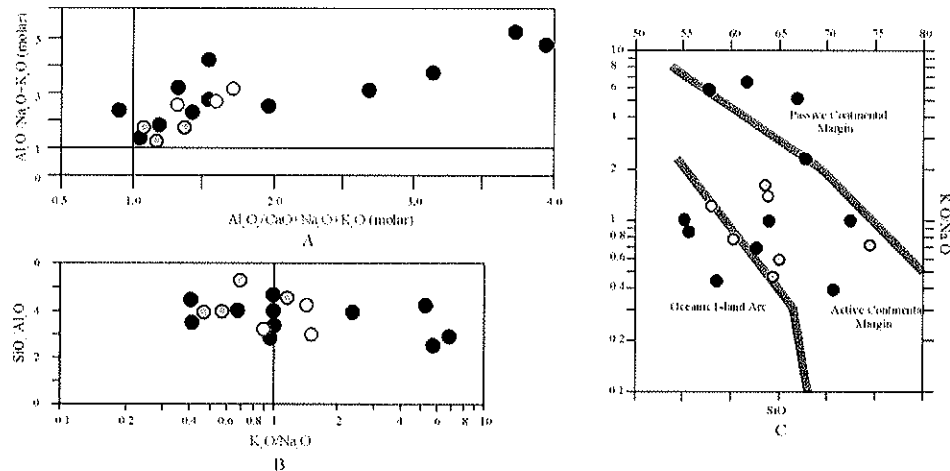


Figure 3-3. Chemical diagrams for rocks with metasedimentary affinities: 3.A- A/CNK (Shand Al-saturation index versus A/NK, Debon & Le Fort, 1983), 3.B- SiO₂/Al₂O₃ versus K₂O/Na₂O (active margin field from McLennan et al., 1990), 3.C- K₂O/Na₂O versus SiO₂ (Roser & Korsch, 1986). Open circles: Varginha-type granulites and black circles: Três Pontas-type granulites of Três Pontas-Varginha nappe; grey circles: granulites from Basal Granulitic unit of Socorro-Guaxupé nappe.

3-4.1. The Socorro-Guaxupé nappe (SGN)

Two major lobes bounded westward by the Phanerozoic Paraná Basin form the Socorro-Guaxupé nappe. Narrow and curved slices of reworked basement rocks and metasediments that are connected with the lower, less metamorphic nappes, the bulk representing an antiformal structure (Fig. 3-2) separate these two lobes. The northern lobe (ancient “Guaxupé Massif” of Almeida et al., 1981), is a ca. 10 km thick nappe with flat-lying to gently southwestward dipping foliation. The southern lobe also comprises large domains with recumbent foliation that was only refolded close to younger, late-metamorphic NE-oriented strike-slip shear zones. The main metamorphic foliation that maintains a recumbent attitude throughout the major part of the nappe is thus the earliest tectonic feature related to progressive non-coaxial deformation having taken place during the east-

northeast displacement of the nappes. Petrostructural and kinematic observations in the northern lobe (Fig. 3-2) allow to recognise distinct tectonometamorphic features that may have formed in three stages.

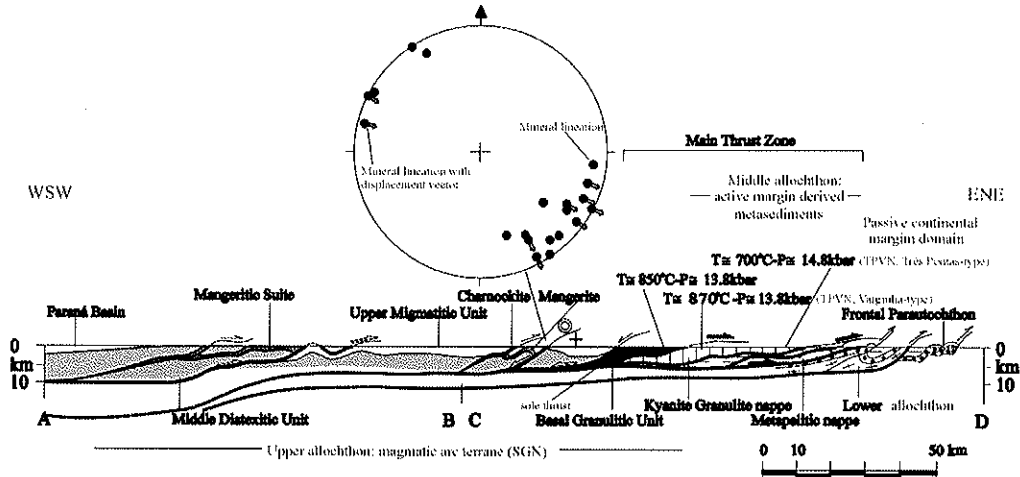


Figure 3-4. Cross-section of the northern nappe system (location in Fig. 2).

3-4.1.1. Basal sole thrust

The base of SGN (ca. 3 km thick) essentially consist of mafic granulites displaying a strong plano-linear fabric (mainly low plunging W-SW mineral and stretching lineations) and bearing several top-northeast shear sense indicators (Figs. 3-6 C and D). Isoclinal and sheath folds record the main movement of the nappe during wanishing granulite-facies conditions (630 Ma). In the southern lobe, the shear zone of the hanging wall of the main thrust reaches 1 km of thickness, with linear tectonites showing the same northeast-directed direction of transport.

Microstructures and mineral assemblages. Mafic granulites exposed south of Varginha City, close to the base of the northern lobe of SGN, contain centimetre size pyroxene-rich black layers. Metric bands of leucocratic granulite with Grt-poor, Qtz- norite composition and decimetre size lenses of mesocratic norite predominate among the main enderbitic composition. At the southern segment NW of Itajuba City, irregular, small (cm size) lenses of white Grt-trondhjemite leucosome also occur. The main enderbitic granulites exhibit a porphyroclastic structure defined by up to 1 cm in size stretched poikilitic phases with primary lobate boundaries: Opx, Grt, Pl and Qtz ribbons. These relict phases document HP granulite-facies conditions. They are surrounded by a recrystallized matrix essentially composed of Qtz, andesine and minor Bt with triple point microstructure resulting from late-kinematic annealing. The green amphibole can occur in textural equilibrium with both pyroxenes (hypersthene and a pleochroic pale greenish brown salite (up to 24% FeO), but normally it grew in the matrix and hardly replaces the pyroxenes displaying local equilibrium with outermost garnet-rims. Subordinate brown biotite (Bt-2) is Ti and Al^{VI}-rich (ca. Phl11-Ann2.5, Al^{VI}=0.215 p.f.u.). It is concentrated in shear bands (C'). Inclusions in garnet are represented by Ilm, Pl and Bt1 of different composition than that of the matrix (Phl-rich and relatively low Al^{VI}=0.18 p.f.u.). The Grt (Alm49-Prp26-Grs22)

occasionally occurring as a ring around earlier Pl shows increased $\text{Fe}^2/(\text{Fe}^2+\text{MgO})$ ratio towards rims: (Alm52-Prp28-Grs18) when adjacent to Opx, and Alm58-Prp30-Grs7 garnet-rim when adjacent to Bt. The $\text{Fe}^2/(\text{Fe}^2+\text{MgO})$ ratio may decrease in small garnet grains from the matrix (Alm55-Prp35-Grs5).

3-4.1.2. Syn-metamorphic normal shearing and Late-metamorphic NE-directed thrusting

NW-SE oriented mineral and stretching lineations, associated with many asymmetrical kinematic indicators consistent with top to the west, normal movements, occur towards the top of the basal granulites (Fig. 3-4). A major detachment, locally accommodated by a NW-oriented, oblique sinistral strike-slip faulting marks the contact between the Upper Migmatitic Unit and the Basal Granulitic Unit (Fig. 3-2). SE-plunging syn-metamorphic mineral and stretching lineations have been mapped widely in the Middle Diatectic Unit (*Campos Neto et al.* 1985; *Ebert et al.*, 1996). These features which record top to the SW movements may result from the syn-metamorphic unroofing of the granulites and the collapse of the hot anatetic rocks, in which heat advection occurred through the large volume of charnockite-mangeritic magmas emplaced at mid-crustal levels.

| Sample | T (°C) | P ₁ - gads (±1.9 Kbar) | T (°C) | P ₂ - gapes (±1.5 Kbar) | T (°C) | P ₃ (±0.5 Kbar) |
|----------------|-----------|--------------------------------------|-----------|---------------------------------------|-----------|-------------------------------|
| 81.B Grs-rich | 850 | 13.8±1.9 | | | | |
| 81.B Grs-rich | 820 | 13.3±1.9 | | | | |
| 81.B Grs-rich | | | 775 | 11.5±1.5 | | |
| 81.B inner rim | 780 | 11.9±1.9 | | | | |
| 81.B rim | | | | | 720 | 9.3-9.0 |
| 34.A matrix | | | 860 | 11.5±1.5 | | |
| 34.A matrix | | | 920 | 11.7±1.5 | | |
| 34.A inclus. | | | 755 | 10.6±1.5 | | |
| 34.A rim | | | 720 | 10.5±1.5 | | |
| 34.A rim | | | 760 | 10.9±1.5 | | |

Table 3. Barometry of the granulites from the hanging wall of the main thrust. P1 and P2: Eckert et al. (1991); P3: Kohn & Spear (1990).

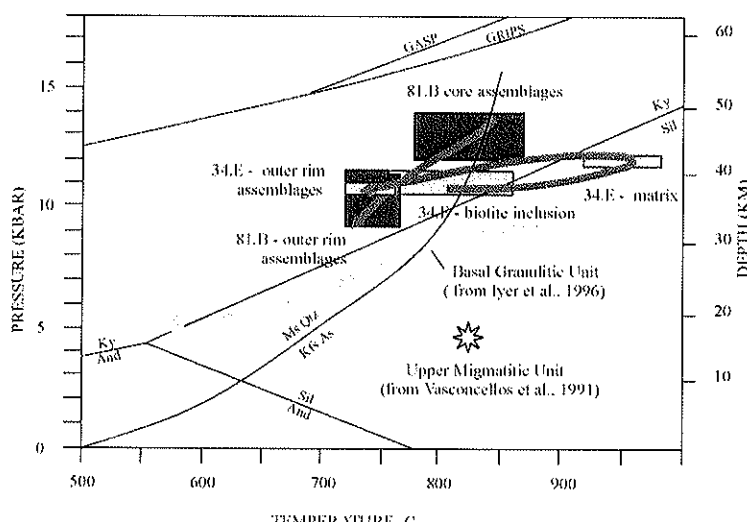


Figure 3-5. P-T trajectories for the granulites from the hanging wall of the main thrust - Basal Granulitic unit of the Socorro-Guaxupe nappe.

Large exposures of the Middle Diatectic Unit representing the roof anatetic metasediments are controlled by thrusts. Reverse faults are well evidenced by the basal truncation of 625-630 Ma old granitic and mangeritic plutons. A pure-shear component of this thrust-shearing was responsible for the folding (up to 3.5 km of wavelenght) of the main foliation as a near-recumbent and asymmetrical, NE-verging fold system developed under amphibolite facies conditions (Bt and/or Hbl locally in axial planes).

3-4.1.3. P/T estimation for SGN

Previous P/T estimates have revealed that the SGN and the TPVN have suffered two contrasting P/T evolutions. Values of $T=820^{\circ}\text{C}$ and $P=4.5$ kbar (Crd-Sil-Grt-Bt) have been obtained on metapelites from the Upper Migmatite Unit (*Vasconcellos, et al.*, 1991). Similar mineral assemblages occurring near the contact with the Basal Granulitic Unit record P-T conditions of 800°C and 7.5 kbar (recalculated data from *Oliveira & Ruberti*, 1979). HP/HT granulitic conditions were obtained on basal granulites from the SGN by *Iyer et al.*, (1996) and *Del Lama et al.*, (1994).

At the northern segment of the SGN, the Grt-Bt1 assemblage shows consistent $T=755^{\circ}\text{C}$, still higher than the Grt-rim/Opx thermometry ($T=721^{\circ}\text{C}$). The Opx-Cpx pairs from mafic granulites indicate T around 870°C and T between 820°C and 775°C for garnet-pyroxene pairs and are interpreted as peak temperatures. A temperature of 720°C is obtained from amphibole-garnet rim pairs (see Table 3-2 for the available thermometers). For the higher temperatures, the pressure varies from 14.0 to 11.5 kbar (GADS and GAPES barometers, Eckert et al., 1991) and 9.0 kbar for the lower temperatures (Grt-Amp-Pl-Qtz barometer, Kohn & Spear, 1990; Table 3-3). In the Socorro lobe, the temperatures obtained from Grt-Bt (*Hodges & Spear*, 1982) are scattered and some of them give unrealistically high values (up to 980°C), perhaps due to non-ideal mixing (Fe-Mg-Ca-Mn) in garnet and/or to the too high Ti and Al^{VI} content of biotites (*Neogi et al.*, 1998). T-max of 920°C can be assumed, whereas the Grt-Opx pairs furnish $T=860^{\circ}\text{C}$. These paleotemperatures are interpreted as indicating an isobaric heating scenario ($P=11.7$ to 10.5 kbar, Fig. 3-5) consistent with dry melting and with the emplacement of anhydrous charnockitic/mangeritic magmas.

3-4.2. The Três Pontas-Varginha nappe (TPVN)

This flat -lying nappe emerges from below the Guaxupé mafic granulites. It crops out for at least 170 km parallel to its displacement direction and is characterised by a recumbent primary foliation (Fig. 3-6). Two klippen made up of the same lithology of unretrogressed Ky-granulites are preserved above slightly anatetic metasediments (Fig. 3-2). Regular W-SW plunging mineral and stretching lineations, mostly defined by the shape fabric of Ky, Rt, Ms and Qtz-ribbons, are widespread. They result from homogeneous E-directed transport during HP-granulite facies conditions. Grt-Ky leucosomes formed in the pressure shadows of boudins of more rigid, less deformed and anhydrous granulites document renewed, syn-granulitic deformation. This thicker nappe (ca. 5 km) represents

the footwall of the main thrust zone. The E-NE direction of displacement is evidenced by asymmetry of boudins of winged, decimetric metabasic swells of pull-apart type and S-C composite shear fabrics. Renewed eastward tectonic transport related to exhumation toward amphibolite facies conditions keep the foliation on metric tight-inclined to recumbent, NE-verging a-type folds and sheath-folds coeval to mylonitic-forming ductile shear bands.

3-4.2.1. Microstructures of kyanite granulites

The Três Pontas type Rt-Ky-Grt granulites are light-gray to bluish, coarse-grained massive rocks with 0.5 cm mean grain size. A recumbent syn-kinematic foliation is defined in most granulites by the ribbon quartz fabric and the planar disposition of rare micas. Aligned Ky prisms define the lineation. In mica-poor layers, mesoperthite is concentrated in the pressure shadows of garnet and also in leucosomes. Horizons with feldspar and kyanite augen up to 2 centimetres long and minute ones enclosed in coarse monocrystalline quartz up to 1-2 cm long suggest pervasive ductile flow at rather high temperatures and pressures. Minute prismatic Sil (100m) growing along grain boundaries has been observed only in two samples around Varginha city. Only a few granoblastic calcsilicate, psammitic rocks and rare kyanite granulites are free of post mineral deformation.

3-4.2.2. Successive mineral assemblages and P/T estimates of kyanite and sillimanite granulites

Trouw (1992), *Trouw & Castro* (1996) and *Vasconcellos et al.* (1991) have described the high-pressure conditions of these rocks. *Campos Neto & Caby* (in press) report conditions of T=730°C and P=13 kbar from the Três Pontas-type Ky-granulites, and an isobaric heating (up to T=890°C) toward its top in the Varginha-type granulites.

The new results summarized below - which will be presented in another paper- are based upon microprobe analyses of a larger number of metapelitic samples from different localities, which show distinct mineral chemistry. Coupled with textural arguments, these data allow to recognize in a few rocks both microdomains with a prograde evolution, and other rocks which registered at varying degree part of the retrograde evolution related to exhumation. Several stages can thus be recognized in the metamorphic evolution of kyanite and sillimanite granulites, allowing us to reconstruct provisional P/T paths (Fig. 3-9). The available thermometers and barometers for each analysed sample from KFMASH (Table 3-4) and CMFASH (Table 3-5) systems of Três Pontas-type, and KFMASH system (Table 3-6) from Varginha-type granulites, always in presence of quartz, are indicated. Wherein the Ilm activity (0.93 to 0.95) is always used (even if it lacks in Grt rings) by GRAIL and GRIPS barometers, such values argue for initial minimum pressures.

An early prograde metamorphic stage has been fossilised in garnets from massive samples from the Três Pontas quarry. Cores ($\text{Fe}^2/(\text{Fe}^2+\text{Mg})$)=0.86 display unrecrystallized micro domains revealed by relics of a vestigial cleavage defined by minute acicular Rt and a dense halo of both quartz and fluid inclusions. Composite inclusions (150 m) of Prl-Sd-Rt and Qtz-Ilm-Ky-Bt (Bt with low-Ti and Phl8-Ann2) have been found in one sample. If primary, such mineral assemblages would argue for fossilised low temperatures. The only occurrence of rutile implies that pressure was higher than the GRAIL reaction.

| Sample | Mineral assemblage | T ₁ (±50 °C) | T ₂ (±50°C) | T ₃ (±5°C) | T ₄ (°C) | P ₁ GRIPS (±1.0kbar) | P ₂ GASP (kbar) | P ₃ GRAIL (±0.5 kbar) |
|-----------------|------------------------|----------------------------|---------------------------|--------------------------|------------------------|------------------------------------|-------------------------------|-------------------------------------|
| 72.3 core | Alm82-Ann | 459 | 468 | | 700 | | 7.5 | |
| 72.3 inner rim | Alm80 Ms78-An0 | | | | | | 14.8 | |
| 72.3 inner rim | Alm82 Ms73-An0 | | | | 688 | 14.9 | 14.6 | |
| 72.3 outer rim | Alm81 Ann8-An2 | 574 | 600 | | | | 10.9 | |
| 72.H | Prp40 Phl11-Mc | 875 | 903 | 781 | | | | |
| 72.B outer rim | Alm76 Ann14 Ms83-An0.6 | 1082 | 1355 | 1203 | 770 | | | |
| 72.Z leucosome | Alm82- Ms72-An19 | | | | 782 | 13.5 | | |
| 72.Z melanosome | Alm85-Ann11-An19 | 741 | 747 | 684 | | 10.6 | | |
| 91.B inner rim | Prp47-Phl27 An17 | 719 | 730 | 691 | | 13.0 | | |
| 91.B outer rim | Alm60-phl19-An24 | 672 | 692 | 643 | | 12.0 | | |
| 91.B outer rim | Alm61-Phl21-An24 | 622 | 640 | 614 | | 11.3 | | |

Table 3-4. KFMASH P-T conditions of Très Pontas-type granulites. Mineral assemblage in mole % of the main end-members. T1: Ferry & Spear (1978); T2: Hodges & Spear (1982); T3: Indares & Martignole (1985); T4: Green & Hellman (1982); P1: Bohlen & Liotta (1986); P2: Newton & Haselton (1982) modified by Koziol & Newton (1988); P3: Bohlen et al. (1983).

| Sample | Mineral assemblage | T ₁ (±75°C) | T ₂ (°C) | T ₃ (°C) | T ₄ (°C) | T ₅ (±50°C) | P ₁ (±0.5 Kbar) | P ₂ gads (±1.9 Kbar) | P ₃ (±0.5 Kbar) |
|----------------|---------------------|---------------------------|------------------------|------------------------|------------------------|---------------------------|-------------------------------|------------------------------------|-------------------------------|
| 72.5 near core | Alm45Grs 39-Di-An34 | | | 641 | 623 | | | 12.6±1.9 | |
| 72.5 inner rim | Alm45Prp 30-Di-An34 | | | 680 | 660 | | | 12.7±1.9 | |
| 72.5 inner rim | Alm47Prp 28-Di-An34 | | | 637 | 615 | | | 11.7±1.9 | |
| 72.5 outer rim | Alm46Prp 31-Pa-An35 | 735 | 690 | | | | 10.8 | | |
| 72.U core | Alm47Prp 27-Pa-An34 | 754 | 723 | | | | 12.1 | | |
| 72.U inner rim | Alm50Grs 26-Pa-An37 | 763 | 638.6 | | | | 11.9 | | |
| 72.U inner rim | Alm50Prp 23-Pa-An37 | 750 | 636.1 | | | | 11.8 | | |
| 72.U outer rim | Alm61-Phl12-An31 | | | | 668 | | | 9.2 | |
| 72.U outer rim | Alm64-Phl14-An31 | | | | 681 | | | 9.0 | |

Table 3-5. CMFASH P-T conditions of Très Pontas-type granulites. Mineral assemblage in mole % of the main end-members. T1: Blundy & Holland (1990); T2: Graham & Powell (1984); T3: Ellis & Green (1979); T4: Powell (1985); T5: Hodges & Spear (1982); P1: Kohn & Spear (1990); P2: Eckert et al. (1991); P3: Bohlen et al. (1983). Pressures are calculated from Blundy & Holland, Powell and Hodges & Spear's thermometers.

The high-pressure granulite facies assemblage is fairly preserved in massive lithologies from the core of boudins in the Très Pontas quarry. Only a few layers comprises the anhydrous mineral assemblage Qtz, Msp, Alm-Prp, Ky, Rt, Graph, Mnz. Rare Bi, Ms and Pl, Fe sulphides and Ank seem to be also primary in other samples. Quartzo-feldspathic lenses formed by up to 80% of one cm in size mesoperthitic feldspar and quartz (few Ky, primary Ms and Grt) are regarded as early synmetamorphic leucosomes extracted from adjacent aluminous granulites and affected by further solid-state high-temperature shear.

Larger, best preserved garnets from garnetiferous layers (up to 2,5 cm) display Mg enrichment in rings (Alm50-Prp38-Grs9) that surround domains with the fossilized prograde stage. They also contain numerous inclusions of prismatic Rt, Mnz, Qtz and Ky, the latter mineral being more abundant towards the rims. Kyanite prisms up to 2 cm long contain Rt, Mnz and Qtz inclusions, as well as rare small grains of possibly primary white-mica. Muscovite flakes are occasionally in contact with garnet rims in some samples, some being rarely included in garnet outer zones. A few layers some centimeters thick contain up to 30 % of Ms associated with Qtz, Ky, Grt and Rt. Possible pseudomorphs after Na-Cpx (albite+carbonate+Fe-rich alteration followed by kaolinite and Na-illite) have been observed in one sample.

This first granulitic stage is related to mineral equilibrium between the homogeneous Prp-enriched composition of larger garnet rings, Pl strings from mesoperthite, Pl porphyroblast, Ky and Rt, Ms and rare Ti-rich Bt. Conditions of T max around 700°C and P about 15 kbar have been calculated for samples from the Três Pontas quarry (Fig. 3-9).

The second syn-kinematic mineral assemblage. Plastic flow has deformed and partly destroyed the coarse grain minerals formed during the previous stage, except in the core of a few boudins. Mesoperthite clasts are plastically deformed and mantled by minute subgrains of recrystallized Mc, Qtz, Pl and myrmekite. Early white mica is bent or completely recrystallized as polygonal arcs and rimmed by elongated Ms and Ky. Large (up to 7 mm) Ms flakes from polygonal arcs may include lobate Ky and show Ms-Qtz lamellae with symplectitic boundaries. Kyanite can be plastically microfolded or kinked, though it is mostly unaltered in mica-poor samples, and Rut is replaced by Ilm. Secondary Ms is the chief mineral of some non foliated, feldspar and garnet-poor layers, in which all stages of its replacement after kyanite (no margarite) can be observed, in equilibrium with plagioclase and calcite. Most of the brown biotite grew during this stage at the expenses of Grt. Alm-rich garnet rims may result of Fe-Mg exchange between both minerals at high temperatures. The biotite also occurs in fractures and deep embayments within garnet, in equilibrium with polygonal Pl, Ilm and recrystallized Ky, thus giving the false appearance of primary biotite inclusions in garnet cores. P/T conditions for this stage are estimated from Fe-Mg exchange between Bt and thin Grt outermost rims with higher $\text{Fe}^{2+}/(\text{Fe}^{2+}+\text{Mg})$ ratio. The conditions for this stage for the Três Pontas granulites are estimated at $T=690^{\circ}\text{C}$ - 600°C , and P around 11 kbar. A distinct P/T path with progressive T increase to $760 \pm 20^{\circ}\text{C}$ and P around 10.5 to 13.5 kbar is recorded in other samples with minute intergranular fibrolite, collected at higher crustal levels 15 km northeast of Varginha.

Sillimanite overprint in the Varginha area is present in all samples collected towards the upper part of the allochthon, about 2.5 km above the main thrust boundary at several localities around the Varginha city. These sillimanite granulites with distinct evolution contain Msp, Mc, Pl, myrmekite, Rt and/or Ilm as well as Prp-rich garnet but no muscovite. Unaltered Ky prisms may however survive in resistant layers and are mainly preserved in Grt cores. Recrystallization of deformed Ky prisms along small shear bands into tiny prisms may also occur, in association with the blastesis of minute prismatic Sil neoblasts in equilibrium with newly formed prismatic Rt. Plurimillimetre in scale pismatic Sil is included towards the rims of Prp-rich garnet. In other rocks, the nucleation of prismatic Sil also progressed in the form of a fine-grain, progressive replacement of Ky prisms displaying dactylitic fringes, whereas Rt of such rock is entirely replaced by Ilm.

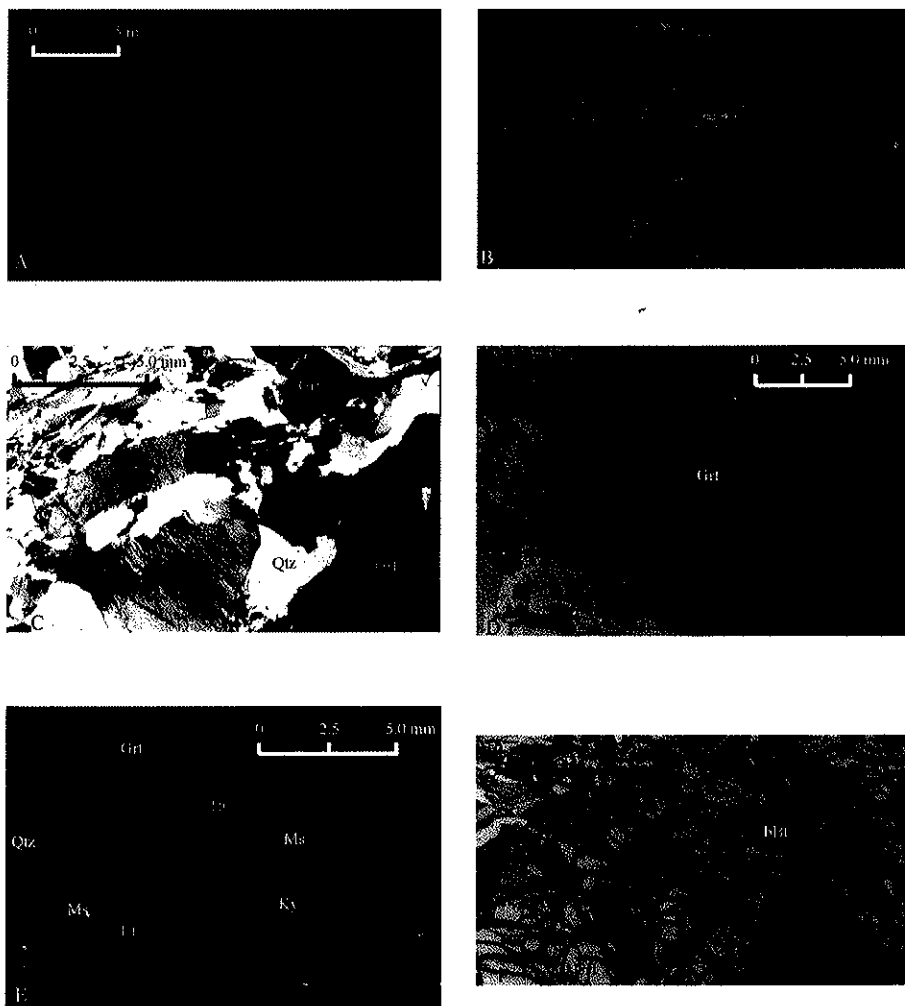


Figure 3-6. Plate of photos

- A. Três Pontas quarry cliff. Well-banded granulites with massif boudinaged layer. B. Kyanite-garnet granulite of Três Pontas-type. C. Garnet-mesoperthite-kyanite-quartz assemblage surrounded by biotite, quartz and small garnets. Sample nesg 93 A2. D. Garnet porphyroblast with internal foliation drawn by minute rutile inclusions. Note the discontinuous and clean garnet rim. E. Kyanite porphyroblast (rutile and monazite inclusions) showing corroded seriate boundary with surrounding muscovites; garnet-biotite and quartz. Sample nesg 72.3. F. Crushed garnet partially replaced by green-biotite after brown biotite.

Prismatic Sil is in textural equilibrium with garnet (Prp up to 45), Ky, Bt (Phl 15 to 17), oligoclase, Mc, Rt and Ilm. The temperatures furnished by Grt-Bt pairs from three samples give 830 and 950°C at pressures around 12 kbar, the last figure being likely overestimated.

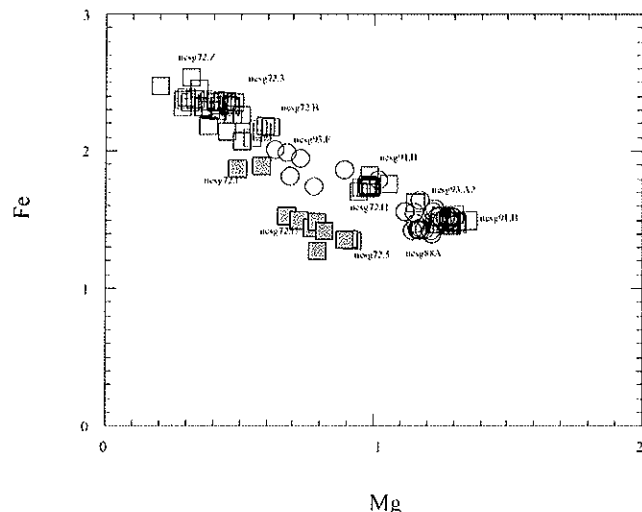


Figure 3-7. Fe₂ X Mg diagrams for garnets from Três Pontas-Varginha nappe.

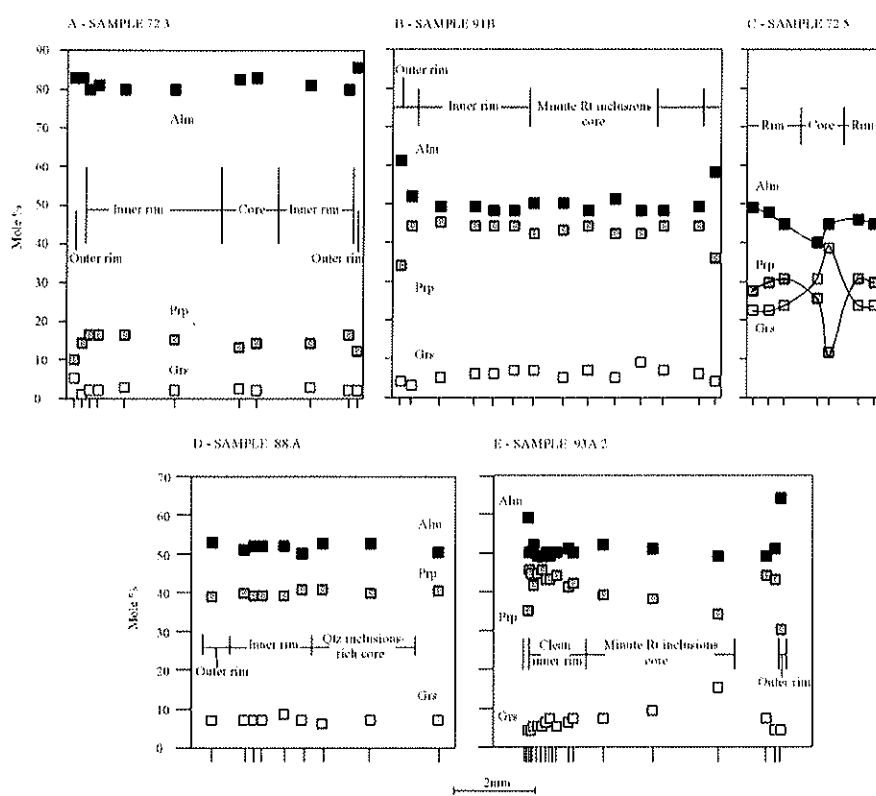


Figure 3-8. Core to rim garnet compositional profiles from Três Pontas and Varginha types granulites.

Some HT mylonites are characterised by sigmoid Qtz monocrystalline ribbons with undulose extinction, S-shaped and elongated clasts of garnet possibly resulting from its plastic deformation and showing different stages of replacement by abundant biotite (Phl 23) in textural equilibrium with sillimanite. This mineral occurs as minute acicular and spherolitic framework, as well as prismatic grains rimmed by Bt-Qtz symplectite in a quartz-oligoclase fine-grained seriate-interlobate matrix. Both relict Rt and Ilm also occur. Mineral equilibria from these mylonitic bands suggest a near-isothermal decompression toward T=765°C and P=9 kbar. Another sample with crushed garnet (Alm60) in several sharp fragments intensively rimmed and replaced by brown-Bt crowded by abundant Sil inclusions and oligoclase neoblasts give T= 795°C and P=7.9 kbar.

Syn-kinematic retrogression of granulites is well expressed in selected bands with protomylonitic fabrics 15 km northeast of Varginha. In such rocks, garnet was flattened and crushed. Its partial to total replacement by biotite occurs approaching cross-cutting fissures strongly enriched in Bt. Kyanite from such biotitized rocks is however partly retrogressed into Ms. Such features indicate that a fluid phase percolating in cracks assisted the synkinematic retrogression and caused the rehydration of granulites. Lower temperature retrogression, though negligible in all our analysed samples, is evidenced by green, Ti-free Bt and Chl, Cal and Ab. Such late lower temperature fabrics were assisted by low temperature fluid infiltration along fissures.

| Sample | Mineral assemblage | T ₁ (±50°C) | T ₂ (±50°C) | T ₃ (±5 °C) | T ₄ (°C) | P ₁ grips ±1kbar | P ₂ grail ±0.5kbar | P ₃ gasp |
|-----------------|---------------------|---------------------------|---------------------------|---------------------------|------------------------|--------------------------------|----------------------------------|------------------------|
| 88.A outer rim | Alm53-Phl 15-An29 | 933 | 950 | 830.6 | | | | 12.2 |
| 93.A2 inner rim | Prp40-Phl 17-An23 | 850 | 869 | | | 13.8 | | 11.5 |
| 93.A2 inner rim | Prp44-Phl 22-An 22 | 800 | 822 | | | 11.9 | | 11.5 |
| 93.A2 mylonite | Prp42-Phl 23-An24 | 748 | 764 | | | | | 8.8 |
| 93.A2 mylonite | Prp45-Phl 24-An23 | 756 | 771 | | | | | 9.2 |
| 93.A2 outer rim | Alm64-Phl 19.5-An23 | 564 | 580 | | | | | 6.4 |
| 93.A2 outer rim | Alm59-Phl 29-An23 | 516 | 533 | | | | | 6.5 |
| 93.F prograde | Alm59-Ms 71-An37 | | | 730 | | 13.0 | | |
| 93.F inner rim | Alm62-Phl 8-An37 | 800 | 839 | | | 12.4 | | 9.9 |
| 93.F outer rim | Alm68-Phl 8-An28 | 774 | 795 | | | | | 7.9 |
| 93.F outer rim | Alm68-Phl 10-An28 | 611 | 639 | | | 7.8 | | 6.8 |
| 93.F outer rim | Alm66-Phl 11-An28 | 666 | 697 | | | | | 7.6 |

Table 3-6. KFMASH P-T conditions of Varginha-type granulite. Mineral assemblage in mole % of the main end-members. T1: Ferry & Spear (1978); T2: Hodges & Spear (1982); T3: Indares & Martignole (1985); T4: Green & Hellman (1982); P1: Bohlen & Liotta (1986); P2: Bohlen et al. (1983); P3: Newton & Haselton (1982) modified by Koziol & Newton (1988).

3-4.3. The southern shear-belt

The southern part of the SGN was involved in the NE-trending southern shear-belt (or Ribeira Belt, Fig. 3-1), formed during a younger event (the Rio Doce orogeny). Several E-NE trending granitic plutons were emplaced into transpressional bends or segments of shear

zones according to *Ebert et al.*, (1996). The zircon ages of these shear-zone related plutons are bracketed between 595 and 580 Ma (*Ebert et al.*, 1996; *Machado et al.*, 1996; *Töpfner*, 1996), whereas monazites cluster between 580 and 563 Ma, suggesting a long-lived event closely related to shear zone activity. A sinistral movement during high temperature deformation has been documented (*Garcia & Campos Neto*, 1998), in agreement with the opening of molassic pull apart basins. In contrast, lower temperature renewed displacements along the major shear zones are clearly dextral. Cataclasites and pseudotachylites also account for possibly younger, Phanerozoic reactivations in the core of the shear zones. High-temperature dextral movements also predominate in the Ribeira belt (*Vauchez et al.*, 1994). The shortening propagation of the transpressional system toward the north was accommodated by small NW-directed brittle-ductile thrusts and by a continuous set of gently W-SW-plunging normal buckle folds with small amplitude/wavelength ratio and cylindrical geometry. These folds grade to upright tight folds close to the shear zones.

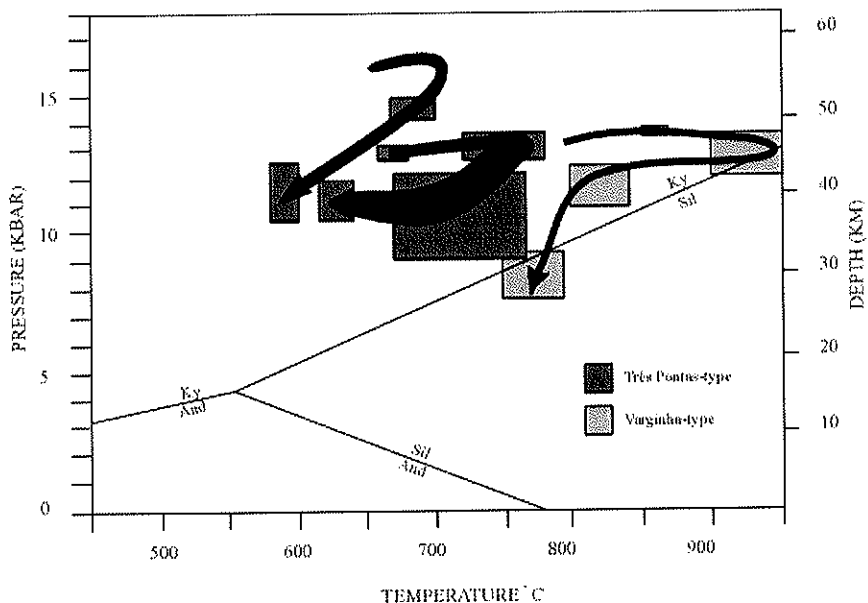


Figure 3-9. P-T trajectories for the granulites from the Três Pontas-Varginha nappe.

3-5. Age constraints on high-grade metamorphism and nappe emplacement

Imprecise U/Pb, zircon ages around 650-700 Ma (lower intercept) have been interpreted as related to the Neoproterozoic HT metamorphism by *Ebert et al.* (1996). The lower intercept age of 655 Ma obtained on a migmatite has also been interpreted by the same authors as dating the thermal peak. U-Pb zircon ages of 660 Ma (by evaporation process) and 640 Ma were also obtained (Table 3-1). In the southern lobe of SGN, upper intercept ages of 625 Ma and bracketed between 624 and 630 Ma were obtained on a peraluminous granite and on calc-alkaline granites, respectively (*Töpfner*, 1996). The Grt-Bt-whole rock Sm-Nd alignment at 630 Ma (Table 3-1) further constrains the age of granulite facies metamorphism in the deeper parts of the SGN. A post-kinematic peralkaline syenite emplaced at about 3 km depths (*Janasi et al.*, 1993) has given a nearly concordant age of 612 Ma (*Töpfner*, 1996) that gives a younger limit for the HT/HP metamorphism in the Socorro-Guaxupé terrane.

3-6. Summary of data and discussion

Lithology and preliminary geochemical and isotopic constraints from high-grade units of the nappe system exposed at the southwestern edge of the São Francisco craton suggest that three major geodynamic environments were juxtaposed during collisional processes: 1- a long-lived Late Mesoproterozoic to Neoproterozoic immature to mature magmatic arc terrane, represented by the HT upper allochthon (SGN); 2- a metasedimentary assemblage with geochemical affinities suggestive of its derivation from an active margin environment, possibly representing an accretionary prism: it forms the HP middle allochthon (HP kyanite-granulites of TPVN and the Carmo da Cachoeira and Aiuruoca-Andrelândia nappes, Fig. 3-2); and 3- the metasedimentary passive continental margin assemblage related to the SFC, exposed in the lower nappes and the frontal parautochthons (*Campos Neto & Caby, in press*).

The main thrust evidenced in the high-grade nappe system separates the magmatic arc terrane (SGN) from undelying HP Ky-granulites (TPVN). The hanging wall of the main thrust comprises a ca. 3 km thick syn-granulite shear zone (the Basal Granulitic unit of SGN) that records T-max around 950°C and P= 12 kbar dated at 630 Ma, roughly coeval in time with the emplacement of noritic magmas. Metasediments possibly derived from a Mesoproterozoic active continental margin define the footwall of this main thrust zone; they form the 5 km thick slab of mainly Ky-granulites (TPVN). A maximum temperature of 750 °C was attained at an estimated pressure of 15 kbar in the Três Pontas granulites.

Progressive near-isobaric temperature increase up to 900°C, P=12 kbar occurred towards its top in the Varginha-type granulites. The TPVN is everywhere delimited at its base by a metamorphic gap evidenced by much lower temperatures downwards. These are below 600°C in the lower nappes (*Campos Neto & Caby, in press*). The resulting metamorphic pattern with inverted metamorphism is thus comparable to that reported from several collisional orogens formed after significant subduction of continental crust such as the Greater Himalayan zone (*Le Fort et al., 1986; Burg et al., 1987; Hubbard, 1989; Vannay & Hodges, 1996; Matte et al., 1997*) and the Paleozoic orogens such as the Uralides and Variscides (*Matte, 1998*). Our results suggest an inverted metamorphic field gradient involving a perturbed paleogeotherm of about 13°C/km for the Ky-granulites to an upper steady state paleogeotherm ca. 20°C/km towards the base of the arc terrane. This thermal pattern may be related to diachronic equilibration at different temperatures but constant pressures throughout the metamorphic prism, as evidenced in the Indian Greater Himalayan zone by *Vannay & Grasemann (1998)*. This thermal inversion model ("hot iron" type) also requires the rapid emplacement of the upper hot allochthon onto the TPVN, arguing for a similar age of metamorphic peak slightly before or around 630 Ma.

A SW-dipping detachment controlled by SE-transported sinistral, oblique strike-slip fault, bounds the top of the main thrust shear zone of the upper allochthon. Movement along this HT ductile normal fault was coeval with widespread anatexis and with the emplacement of mangeritic magmas extracted from surrounding granulites around 630-625 Ma. This hinterland-driven detachment may result from internal extension by dynamic compensation in response to the possible broad topographic gradient developed by the collisional extrusion, as reported from the Nepalese Himalayas (*Hodges et al., 1996*). Such

apparent "extensional" regime compares well with the ductile normal fault formed on top of the hot, migmatitic Tibetan slab in the central Higher Himalaya, where it has been interpreted as syn-collisional collapse above the partially melted crust at the time of collection of Himalayan leucogranites (*Caby et al.*, 1983; *Burg et al.*, 1987; *Burchfiel et al.*, 1992; *Chemenda et al.*, 1995; *Vannay & Hedges*, 1996).

Though nearly contemporaneous, the HT/LP metamorphism ($T=820^{\circ}\text{C}$ and $P=4.5$ kbar) at shallow levels of the SGN arguing for a compressed paleogeotherm of about $50^{\circ}\text{C}/\text{km}$ is incompatible with the first syn-kinematic metamorphic stage recorded in the Ky-granulites. This metamorphic relationship argues for initial different tectonic environments for the two granulite nappes, and we therefore regard them as representing two juxtaposed terranes. Paleothermal constraints thus suggest that the closure of an ocean through a W-dipping subduction zone may have occurred in late Neoproterozoic time. Possible ophiolitic complexes (the Petunia complex, *Choudhuri et al.*, 1995) and the Maraba sequence (*Fuck et al.*, 1994), both comprising serpentinites with podiform chromite typical of oceanic mantle, provide strong further evidences for such an open ocean, west of the SFC. The position of the Ky-granulite slab that records much higher pressures than both the overlying and underlying units suggests that it was emplaced as an horizontally extruding slice through the mechanism of upward extrusions (*Chemenda et al.*, 1995; *Chemenda et al.*, 1996). Continental subduction may be responsible for the low-angle exhumation of HP units, as proposed for the Himalayas (*Matte et al.*, 1997) and for several domains of Paleozoic orogens (*Matte*, 1998). The Varginha-type granulites with final equilibration in the sillimanite field record a near-isothermal decompression metamorphic path around 8.5 kbar, whereas the basal Três Pontas-type granulites mainly record decompression in the Ky-field. The major foreland nappe stacking seems to be related to this younger stage of horizontal eastward displacement evidenced by retrogressive mylonites. The outward propagation of the nappe pile subjected to significant thinning was accompanied by T-decrease at each thrusted rock-package ($T=600^{\circ}\text{C}$ in the lower allochton and $T=500^{\circ}\text{C}$ in the frontal parautochthon, *Campos Neto & Caby*, submitted). Since the TPVN practically overrides the parautochthons in its northern part, a major late-metamorphic out-of-sequence thrust is responsible for the final emplacement of the whole nappe pile, as it is the case for the Brasilia nappes in the north, where they overlie the anchimetamorphic Bambui Carbonates of the foreland. (*Simões*, 1995).

The preservation of an inverted metamorphic field gradient in rock units all equilibrated in the Ky-field requires rapid exhumation of the granulite nappes and simultaneous strong erosion and/or tectonic denudation or syn-displacement thinning. Thus the main thrust system could not represent a long-lived extrusion process of part of the lower crust, in which case the kyanite granulites would all have been thoroughly overprinted in the sillimanite stability field and affected by anatexis. The apparent episodic alternation of compressive and extensional structures may suggest progressive pulses of large-scale shortening and extrusion, as reported from the Nepalese Himalayas (*Hedges et al.*, 1996), but further isotopic and petrological data are required to evaluate such a possibility. Our data allow us to propose a short-lived tectonic scenario beginning around or shortly before 630 Ma and achieved by around 625 Ma, since the whole post-orogenic lithospheric extension took place prior to 610 Ma, as shown by U/Pb zircon ages of the cross-cutting syenites emplaced around 3 kbar. Thus, part of the lower crust was upwards exhumed from

a west-dipping subduction prism and driven horizontally above the southern edge of the SFC during the maximum time span of 20 Ma, resulting in a mean cooling rate of about 15–20°C/Ma. The superposed tectonic history after ca. 580 Ma is due to northwestward propagation of the transpressive Ribeira shear belt. K/Ar ages on amphibole of 610 Ma and micas that cluster around 550 Ma (*Teixeira & Cordani, 1979*) suggest a slow cooling rate in the south of SGN related to a long-lived thermal anomaly.

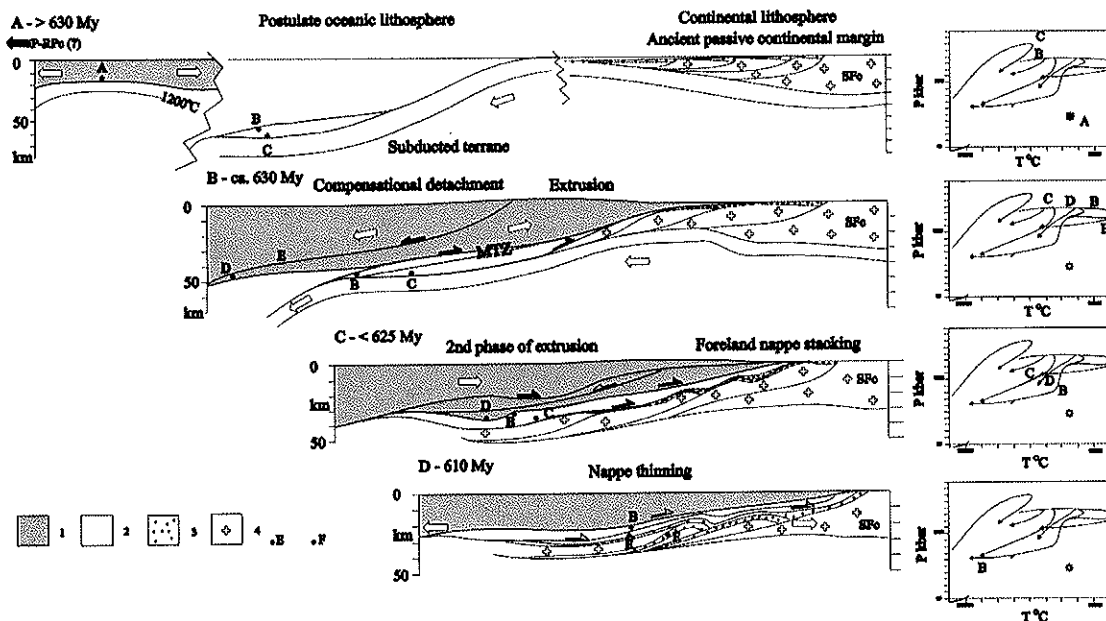


Figure 3-10. Suggested geodynamic model of Neoproterozoic collision SW of São Francisco craton.
 1. Magmatic-arc terrane (Socorro-Guaxupé nappe); 2. Mantle beneath arc; 3. Subducted slab (Três Pontas-Varginha nappe and Carmo da Cachoeira, Aiuruoca-Andrelânia nappes); 4. Passive continental margin deposits; 5. Ancient gneisses; SFC: São Francisco craton; Pb: Paraná block; .B: Thermobarometric conditions.

3-7. Conclusion

The granulite nappes exposed SE of the São Francisco craton derive from two distinct terranes assembled to form a composite section of deep continental crust: the Socorro-Guaxupé nappe above and the Três Pontas-Varginha nappe below. Metamorphism in the lower TPVN is unique by the preservation of High-Pressure Kyanite-granulites (750°C, 15 kbar). The pressure/temperature estimates presented here suggest that these HP granulites crystallized under a perturbed paleogeothermal gradient of about 13°C/km related to a west-dipping subduction zone underneath postulated oceanic lithosphere. Such paleogeotherm is indeed incompatible with metamorphic conditions in the overlying SGN that represents the possible roots of a continental arc and in which the different metamorphic facies at its top relate to a perturbed paleogeothermal gradient of about 50°C/km. Within the lower part of this upper nappe, maximum temperatures around 900–950°C were reached regionally during the intrusion of charnockitic-mangeritic magmas at 630–625 Ma.

The proposed subduction/collision scenario (Fig. 3-10) envisages the west dipping subduction of continental derived units underneath oceanic lithosphere. After complete resorption of the oceanic domain, collision with a magmatic arc related to the Rio de la

Plata craton produced the main crustal thickening. Exhumation of the deeply subducted units occurred then through the mechanism of low-angle, E-directed extrusions. At least 200 km of eastward displacement of the nappes took place along the southern margin of the SFC, an even greater displacement being likely if the HP-metapelitic Airuoca/Andrelândia lower temperature nappes (Fig. 3-2) with eclogites are also taken into account. These new results suggest the Himalayan size and character of the Neoproterozoic nappe system of southeastern Brazil.

Acknowledgments. Supported by FAPESP grants 95/4652-2, 95/2622-9 and 96/12320-2 and CNPq grant 95/523944. Discussions with V.A. Janasi and M.A.S. Basei were helpful. We thank P. Matte and K. V. Hodges for constructive reviews. This manuscript was written while the first author was on research leave at the Laboratoire de Tectonophysique, Montpellier II University, France: their support and hospitality were also appreciated.

CAPÍTULO 4

OROGENIC SYSTEMS FROM SW-GONDWANA: AN APPROACH TO BRASILIANO-PAN AFRICAN CYCLE AND OROGENIC COLLAGE IN SE-BRAZIL

Abstract

The Goianides Ocean was the product of the Tonian taphrogeny acting in the western portion of the São Francisco plate that resulted in the Rodinia Supercontinent break-up. Within this context the intraoceanic juvenile arc-crust accretion (0.90-0.85 Ga) triggered the orogenic collage toward the Gondwana Supercontinent. More evolved subduction-controlled magmatic arcs were generated driving the kinematics of plate convergence up to Rio de la Plata, São Francisco, continent overriding-type collision at 0.63 Ga. The Tocantins orogenic system (product of that Goianides Ocean closure) have involved deep reworking of old continental crust, high-pressure east-direct overthrusting with crustal thickening and indentation processes, having as modern analogues the India-Asia collision. At 0.6 Ga mostly of the orogens were exhumed.

Opposite to that, the Adamastor Ocean resulted from the Cryogenian taphrogeny and global Rodinia break-up. This ocean was populated by several microplates, which had diachronically collided against the just-assembled São Francisco-Rio de la Plata plate in a Cordilleran-style tectonics. These processes are related to the building of the Mantiqueira branching system of orogens, that displays early intra-oceanic juvenile accretionary components and yields average ages for the orogenic events between 0.61 and 0.54 Ga, up to the final oceanic lithosphere consumption at 0.52 Ga.

4-1. Introduction

The geological evolution toward the agglutination of the Gondwana supercontinent started immediately after the Grenvillian orogenies that built the predecessor Rodinia supercontinent. Since the beginning of the Neoproterozoic break-up and drift controlled by taphrogeny has driven plate kinematics toward orogenic interactions. These processes reached the Lower Ordovician and operated for at least 500 Ma, following all the steps of J.T. Wilson's tectonic cycle. An interesting characteristic of these orogenies is the diachronism of events, many of them coeval with taphrogenic processes elsewhere. Many orogenies were controlled by different kinds of plate interaction occurring diachronically at different places. These plurality of processes that converged to the closure of a wide oceanic space populated by small continental fragments (terranes or microplates) may be described by means of orogenic systems or branching systems of orogens, rather than the general and geometry-related mobile belt model. The collection of orogenic systems leading to supercontinent amalgamation represents the "orogenic collage" (Sengor, 1990).

The advance of geochronological knowledge in the SE-Brazil in the last decade, mostly due to U-Pb and Sm-Nd robustly constrained data, helped identify the concurrent metamorphic and plutonic events. The isotopic work revealed major lithospherical mantle accretionary processes and also the contrasting lithospheric signatures between terranes have shown powerful tectonic tools.

Two major orogenic systems could be described in Southeast Brazil. The Tocantins orogenic system was the former and it was related to the closure processes of a Tonian ocean located west of the São Francisco plate, the Goianides Ocean. It comprises several orogens, which have been collectively described as Brasília belt (Fuck et al., 1993) and Alto Rio Grande belt (Hasui, 1982). The global break-up of Rodinia, rifting apart its descendants, took place in the Middle Cryogenian. It accounts for the separation of East-Gondwana from Laurentia (Park, 1994) and the generation of the Adamastor Ocean (Hartnady et al., 1985), facing the Congo, Kalahari and São Francisco plates. The main plate convergence processes controlled several collisions and terrane dockage leading to the southeastward growing of the Brazilian continental crust. These processes were collectively related to the Mantiqueira orogenic system. It comprises the northern Ribeira belt (Almeida et al., 1973) and the southern Dom Feliciano belt (Fragoso-Cesar, 1980). The proposed Tocantins and Mantiqueira orogenic systems were taken from Almeida et al.'s (1981) structural provinces.

The evolution of different types of rifts and related passive continental margins and the role played by their final geometry within a plate kinematics scenario may be explained using Lister et al.'s (1986) model.

4-2. Major continental plates framework

The main geotectonic provinces, with special regard to the Precambrian of the South American Platform (the cratonic area for the Andean orogenic episodes) are shown in Fig. 4-1. These provinces are related to the huge continental lithospheric plates (Brito Neves and Cordani, 1991, Brito Neves et al., 1999), that were rifted apart during the break-up of Rodinia at the beginning of the Neoproterozoic (Dalziel, 1997, Weil et al., 1998). The further amalgamation of these old shields to form the Gondwana supercontinent is recorded by successive collision and plate indentation processes during the global Brasiliano-Pan African orogenies.

The Amazonas plate records roughly NW-trending belts, which are successively younger southwestward and added to an Archaean northeastern province (Tassinari et al., 1996). They comprise Paleoproterozoic belts from the Transamazonian cycle (ca. 2.2-1.8 Ga), which are followed by Statherian magmatic arc, and by the southern Mesoproterozoic collision of the Pampia terrane. A wide settlement of the Grenville province exceed the Neoproterozoic limits of the Amazonas plate, if one takes into account the further rifting apart of the Arequipa-Antofalla terrane and the Eastern Laurentia plate (Ramos and Vujovich, 1995, Bettencourt et al., 1996, Balburg and Hervé, 1997).

The Rio de la Plata plate is almost recovered by the Palaeozoic Paraná basin. Its southeastern edge, chiefly its outcropping domain, comprises a cratonic granite-greenstone province, ca. 2.0 Ga old, crosscut by undeformed mafic dyke swarm of ca. 1.8 Ga. A reworked gneiss-granulitic border is admitted. The Rio Apa granite-gneisses seem to belong to this plate, emerging from the Phanerozoic Paraná basin as a small Paleoproterozoic block. The old rocks of the Rio de la Plata plate first recognised by deep drilling (Cordani et al., 1984) were revealed, as a whole, by geophysical research, such as gravimetry (Mantovani and Shukowsky, 1996), and thermal constraining for P and S-wave velocity perturbations (VanDecar et al., 1995). The paleomagnetic data at the end of the Paleoproterozoic postulate a Laurentia connection of this major continental plate segment (Agrella Filho and Pacca, 1999).

The horse head-shaped São Francisco plate, which represents the northeastern extension of the Congo plate, has been defined since Almeida (1977) and Alkimim et al. (1993).

The remnants of oceanic plate segments between these blocks are still to be recognized.

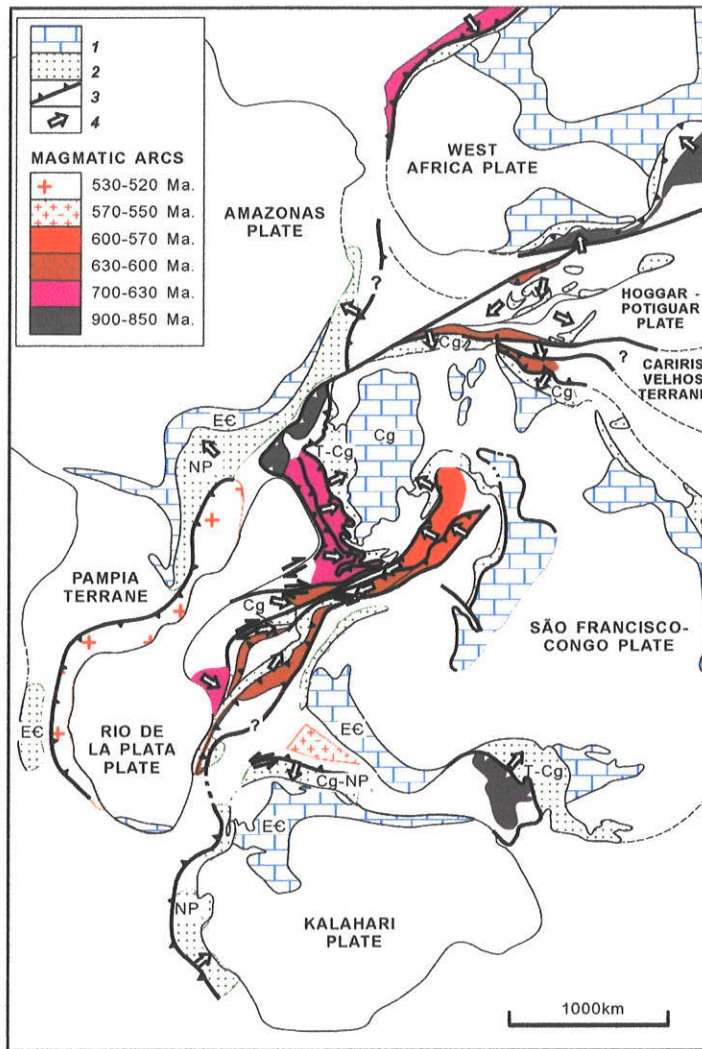


Figure 4-1: Western Gondwana continental plates and magmatic arcs

1. Platform covers, 2. Passive continental margin deposits or thinner continental crust, 3. Subduction zones with sense of dip, 4. Structural vergence.

4-2.1. Statherian taphrogeny: attempts to break-up of the São Francisco plate

Major and widespread upper Rhyacian (ca. 2.1Ga) orogenic collage accompanied by juvenile accretion and rework of the oldest Archaen crust (Teixeira et al., 1998) consolidated the proto-São Francisco plate. After these dramatic plate convergence processes localised zones of intense intraplate extension were collectively integrated in a broad taphrogeny. Failed rifts were responsible for the development of the major NS-elongated Espinhaço basin and the western Araí basin (Fig. 4-2). Rhyolitic rocks occur at

the basal depositional sequences of both basins coeval with off-basin, small tin-bearing granites. These continental, anorogenic volcanic and plutonic suites yield a Statherian age (1.77-1.60 Ga, Brito Neves et al., 1979, Turpin et al., 1988, Machado et al., 1989, Pimentel et al., 1991). The sedimentary sequence (ca. 1,200m thick) of siliciclastic continent-dominated rocks (conglomerates, coarse-grained quartzite and siltstones) constitute the depositional systems of the pre-rift and rift stages. The upper units of the Espinhaço Supergroup represent a seaward connection (wave-ripple quartzite interlayer with shale and few carbonates) covering unconformably the adjacent non-stretched Archaean basement. They were related to a crust downwarping stage of the thermal-flexural type which controlled the change in subsidence regimes without breaking-up the São Francisco plate interior (Dominguez, 1993, Martins-Neto, 1998).

Tabular bodies (up to 110 m thick) of a sub-alkaline to alkaline suite of (Fe-hastingsite and Fe-salite) magnetite-bearing granite, related to anorogenic, extensional tectonic regime occur at the south edge of the São Francisco plate (Taguar granite), yielding an Ectasian age (Rb-Sr isochron of 1.4 Ga, $\text{Sr}^{87}/\text{Sr}^{86}_{(0)}=0.719$, Vasconcellos, 1988). Thus magmatic records of another extensional tectonics during the Ectasian followed the Statherian taphrogeny. However no evidence of an orogen had been registered since the end of the Rhyacian System until the Neoproterozoic in the São Francisco plate.

4-3. Fragments of the Rodinia history

4-3.1. Central Goiás terrane

The western ^{borders} edge of the São Francisco plate is bound by a N.NE-trending belt comprising an Archaean-Proterozoic continental remnant of an older plate against which the Neoproterozoic Mara Rosa island arc docked (see later). This fragment comprises Paleoproterozoic basic-ultrabasic complexes and Paleoproterozoic and Mesoproterozoic vulcanosedimentary sequences (Fig. 4-2).

The Archaean fragment comprises a typical granite-greenstone belt terrain. The metasediments are carbonaceous schist and metarhydromites from turbidite depositional environment. The metavolcanics consist of lower komatiite flows and upper intercalated mafic and felsic flows. The metaplutonic rocks are mainly tonalites and granodiorites (Rivalenti et al., 1989, Jost et al., 1996). Dome-and-keel is the structural framework and the interference geometry was produced by successive episodes of plutonism between 2.85 to 2.70 Ga (Queiroz et al., 1999) coeval with the komatiite lava flows (Arndt et al., 1989). The metamorphic recrystallisation quickly followed magmatism (2.7 Ga) and it was reprinted by the Rhyacian orogeny (2.14 Ga, Queiroz et al., 1999).

Over a narrow mylonitic granite-gneissic belt layered and stratiform mafic-ultramafic complexes (Barro Alto, Niquelândia and Cana Brava) occur discontinuously for 300-km (Danni et al., 1982). Gabbros, melagabbronorites, peridotites, pyroxenites, anorthosites and late diorites are the main rock types of these complexes. They show petrologic gradation from a less differentiated base (pyroxene and olivine cumulates) toward plagioclase cumulates in a more differentiated top. Interlayers of high-degree metamorphic metasediments can be found as well as xenoliths in the mafic rocks. The available data suggest an anorogenic extensional environment for these intrusions (Girardi, et al., 1986, Ferreira Filho et al., 1992) that was rifted apart from an uncertain continental plate. Well constrained U-Pb (SHRIMP) from Niquelândia (Correia et al., 1996) and a Sm-

Nd isochron from Cana-Brava (Fugi, 1989) pointed the emplacement of these complexes at the Rhyacian/Orosirian boundary (2.0 Ga). The quartz-dioritic intrusion at the basal layer of Barro Alto complex yields U-Pb zircon age of 1.7 Ga (Suita et al., 1996).

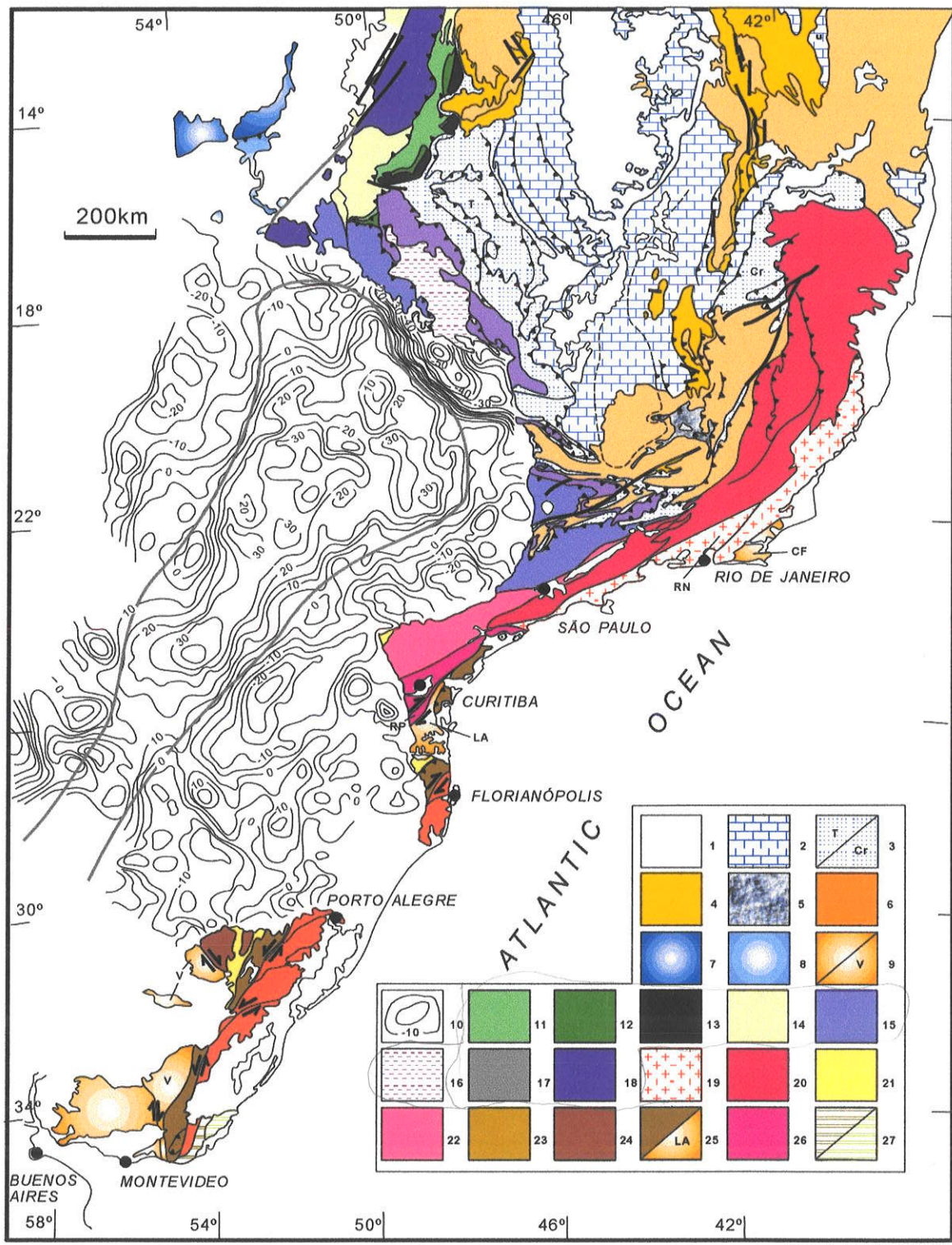


Figure 4-2: Tectonic map of South-Southeast Brazil

Draw by: Thelma Samara/98.

1. Phanerozoic covers. **São Francisco plate:** 2. Cryogenian/Neoproterozoic III platform cover of the cratonic domain (Bambuí Group and correlates), 3. Tonian(T)/Cryogenian(Cr) passive continental margin sequences with remnants of oceanic crust (western Paranoá, Canastra and Carrancas Groups, and eastern Macaúbas Group, Salinas and Ribeirão da Fôlha Formations), 4. Statherian rift-related sequences (eastern Espinhaço Supergroup, western Arai Group and southern São João del Rei Group). Archaean/Paleoproterozoic: 5. Minas and Rio das Velhas Groups, 6. Granite-gneiss basement. **Amazonas plate:** Neoproterozoic III/Cambrian: 7. Platform cover of cratonic domain, 8. Varengian rift-drift sequences. **Rio de la Plata plate:** 9. Paleoproterozoic granite-gneissic cratonic area and granulite-gneiss reworked Valentines terrain (V), 10. Gravimetric record of the basement of the Paraná basin. The gravimetric higher is related to the Rio de la Plata cratonic area. **Central Goiás terrane:** 11. Metasedimentary sequence, 12. Ectasian metavolcanosedimentary sequence displaying rift-to-drift assemblages (Juscelândia, Indaiápolis and Palmeirópolis sequences, including the southernmost Statherian? calc-alkaline related Mossâmedes metavolcanosedimentary sequence), 13. Rhyacian/Orosirian stratiform mafic-ultramafic complexes (Barro Alto, Niquelândia and Cana Brava), 14. Archaean/Paleoproterozoic granite-greenstone belt terrain. **Tocantins orogenic system:** 15. Cryogenian/Neoproterozoic III magmatic arc (Socorro-Guaxupé terrane, including Iporá-Jaupaci area), 16. Cryogenian back-arc related metasedimentary sequence with oceanic crust remnants, 17. Anápolis-Andrelândia terrane (volcano-plutonic arc and related metasedimentary sequence of Araxá Group, Aiuruóca-Andrelândia and Três Pontas-Varginha nappes), 18. Mara Rosa terrane (juvenile island arc crust). **Mantiqueira orogenic system:** 19. Neoproterozoic III/Cambrian Serra do Mar terrane (microplate with Rio Negro – RN, ca. 0.63-0.61 Ga, and Rio Doce – RD, ca. 0.58-0.56 Ga magmatic arcs), 20. Juiz de Fora terrane (Paleoproterozoic crust and Neoproterozoic arc-related metasediments of Embú and Paraíba do Sul complexes) as a microplate setting for (ca. 0.595-580 Ga) Galiléia Magmatic Arc, 21. Foreland basin (ca. 0.60-0.56 Ga Itajaí, Camaquã and Arroyo do Soldado Groups), 22. Apiaí terrane (Ectasian? Passive continental margin as a basement of a ca. 0.61 Ga plutonic magmatic arc (Cunhaporanga, Três Córregos and Agudos Grandes batholiths), 23. Pelotas terrane (ca. 0.62-0.61 Ga plutonic magmatic arc), 24. São Gabriel terrane (upper Cryogenian island arc), 25. Luis Alves terrane comprising the Tijucas belt (rift-to-drift Mesoproterozoic? metavolcanosedimentary sequences: Brusque and Porongos Groups) and the Archaean/Paleoproterozoic Santa Catarina granulitic complex, 26. Curitiba terrane (Paleoproterozoic gneisses and granulites) as a basement of the Rio Pien plutonic magmatic arc (0.615 Ga), 27. Grenvillian-Kibaran migmatites with western Neoproterozoic metasediments of Rojas Group, 28. Cabo Frio terrane.

At the SE extremity of the Archaean fragment, a narrow metavolcanosedimentary belt crops out (the Mossâmedes sequence) and was described by Simões and Fuck (1984). It comprises few metabasalts of low-K tholeiitic affinity followed by a calc-alkaline suite of basic/intermediate and felsic metavolcanic rocks interlain with metatuffs, metacherts and pelitic schist, being in agreement with an active volcanic arc setting (Barbosa and Jost, 1990). The Rb-Sr misgiving ages of this plate convergence felsic volcanism to come across the Paleoproterozoic Orosirian and fini-Statherian with Sm-Nd T_{DM} of ca. 2.2 Ga (Pimentel et al., 1996).

Another metavolcanosedimentary sequence occurs discontinuously as an allochthon over the mafic-ultramafic complexes (Fig. 4-2). These sequences (Juscelândia, Indaiápolis and Palmeirópolis, Marini et al., 1984) are related to a bimodal, continental-type sub-alkaline tholeitic basalt volcanism, and rhyolitic rocks derived from crustal-mantle mixing felsic magma. The uppermost volcanic layer represents basic rocks from N-MORB type basalt (Moraes et al., 1998) ascribing a rift-drift evolution, whose age unfortunately remains unknown. However these rocks were metamorphosed to the upper amphibolitic facies that is coeval with the granulitic facies metamorphism of the mafic-ultramaphic complexes (Moraes and Fuck, 1994, Ferreira Filho et al., 1998). The age of this metamorphic process, first related to the Mesoproterozoic Ectasian by Rb-Sr isochrons (Fuck et al., 1989), has been object of research and interpretation using U-Pb zircon records. Neoproterozoic Cryogenian age have been obtained (Ferreira Filho et al., 1994, Suita et al., 1994), but the SHRIMP data corroborated the Ectasian (1.3 Ga) age (Correia et al., 1999).

Neither of these processes is recorded out of this narrow domain suggest they do not belong to the São Francisco plate. Proterozoic mobile belts formed from 1.95 to 1.0 Ga surround the Archaean cratons of Laurentia and Baltica. In opposition to the São Francisco plate, Paleo-Mesoproterozoic tectonic evolution of the south Amazonas plate (Rio Negro-Juruena Province and Rondonia-San Ignácio Province, Teixeira et al., 1989) show successive accretion of juvenile, volcano-plutonic arc crusts. High-grade metamorphism with a mean U-Pb SHRIMP age at 1.33 Ga (Tassinari et al., 1999) precedes the Grenvillian (1.25-0.9 Ga) Sunsas orogeny. Slightly after all these orogenic events the rapakivi granite

genesis either in Rio Negro-Juruena Province, or in Rondonia-San Ignácio Province took place as an extensional, anorogenic episodes (Bettencourt et al., 1999). Therefore, the correlation between eastern Laurentia and western Amazonas plates (Sadowski and Bettencourt, 1996) is well constrained.

Apparently the latest U-Pb records for Barro Alto granulites and Juscelândia gneiss, and the former Rb-Sr and Sm-Nd data from Moçâmedes arc-related rocks strongly suggest that these sequence fit better in the Laurentia-Amazonas plate from Rodinia Mesoproterozoic Supercontinent.

4-3.2. The Apiaí terrane

Other Ectasian metavolcanosedimentary sequences probably belong to the northeastern boundary of the Rio de la Plata plate. They are the Serra do Itaberaba Group, overlain by the São Roque Group (Juliani, 1993) and encompassing volcanic units that record the transition from rifting to oceanic crust formation, and the Perau (Piekacz, 1981) and the Abapã Formations (Reis Neto, 1994), both basal units of the Açuñui Supergroup (Campanha and Sadowski, 1999).

The Serra do Itaberaba Group (Fig. 4-3) comprises quartzite rocks from marine coastal margins of a rift environment, which almost encompass two major lithostratigraphic formations (Juliani, 1993, Juliani and Beljavskis, 1995, Juliani et al., 1996). The basal ones consist of metavolcanoclastic rocks, metabasalts and metatuffs, calc-silicate rocks, graphite-bearing schists, iron formations and metavolcanic rocks from intermediate to acid compositions. There occur hydrothermally altered tholeiitic basaltic flows of N-MORB type associated with a deep marine rock assemblage. A transition from tholeiitic to calc-alkaline volcanism is depicted by metandesite, metarhyodacite and metarhyolite magmatism, which seem to record a remote subduction of an oceanic crust. This lithostratigraphic unit is unconformity overlain by Mn-rich and Ca-rich metapelites, metavolcanoclastic rocks, carbonaceous rocks and an upper Al-rich metapelites, with intercalations of few amphibolites, metarhyolites and black, fine-grained tourmaline-bearing rocks. This upper unit that show transition to shallow marine environment may be related to the beginning of the closure of the oceanic basin.

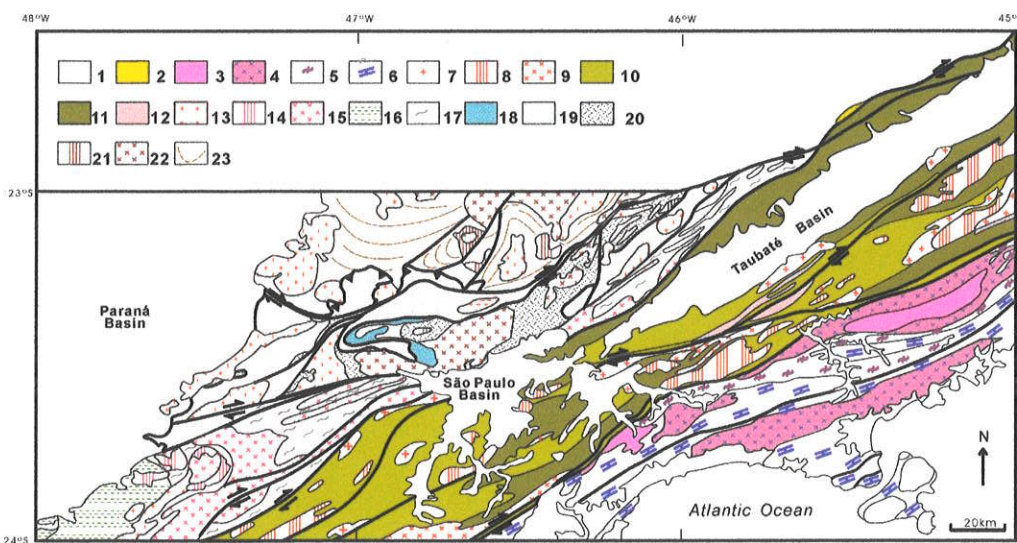


Figure 4-3: Geological Map of the Serra do Itaberaba/São Roque Groups and the Embu Complex

1. Phanerozoic covers. 2. Neoproterozoic III/Cambrian Pico do Itapeva Formation. Serra do Mar terrane: 3. Peraluminous granites (ca. 0.50-0.54 Ga), 4. Metaluminous granitoids and charnockitic suite, 5. Sil-Grt-bearing migmatites with quartzite resisters, 6. Metaluminous migmatites. Juiz de Fora terrane: 7. Shear zone-related metaluminous granites, 8. Peraluminous granites, 9. Hbl-Bt-bearing granitoids. Embu Complex: 10. Shelf-related quartzites and schist-quartzite rhythmic succession, 11. Metavolcanosedimentary sequence, 12. Archaean-Paleoproterozoic grey gneisses. 13. A-type granites (ca. 0.575-0.580 Ga). Apiáí terrane: 14. Peraluminous granites (ca. 0.60 Ga), 15. Metaluminous granitoids (ca. 0.61-0.605 Ga), 16. Terrigenous turbidite deposits of Açungui Group, 17. Schists and gneisses. São Roque Group (back-arc basin?): 18. Upper continental and shallow water quartzite, limestone bioherm and metavolcanic rock association, 19. Metarhythmites, quartzites, metalimestones and metabasaltes with pillow-lava structure (ca. 0.61 Ga), 20. Serra do Itaberaba Group (Ectasic). Socorro-Guaxupé terrane: 21. Peraluminous granites (ca. 0.625 Ga), 22. Hbl-Bt-bearing granitoids (ca. 0.63 Ga), 23. Sil-Grt-bearing migmatites of Piracaia Complex.

The São Roque Group (Fig. 4-3) is dominated by three major volcanic and depositional sequences (Bergmann, 1988). The first one comprises metavolcanic basic rocks (including tholeiitic basaltic flow with pillow-lavas structures) on a shallow water environment associated with carbonate rocks and stromatolitic bioherm (rising to 800 m thick). They were followed by cyclic, millimetric to metric alternations between metarkose and quartzite (few metaconglomerates) with metapelite (at least 1,000 m thick), having wave ripples and climbing from weak slope bottom surface of a shelf environment. Metacalcareous lenses and thicker quartzitic rock package may occur as a southward facies. The upper unit (up to 1,600 m thick) is dominated by a metarkose with cross-stratification and flaser bedding structures. It contains two intercalations of metabasic rocks, the former with pillow-lavas and the latter with vesicular volcanic flows. A well-sorted quartzite from offshore bars compose the upper beds. Although still uncertain, the latest U-Pb data point at a Neoproterozoic III (0.61 Ga) age for the submarine basaltic flow (Hackspacher et al., 1999). As a whole, their volcanic and sedimentary process could be related to a back-arc basin evolution.

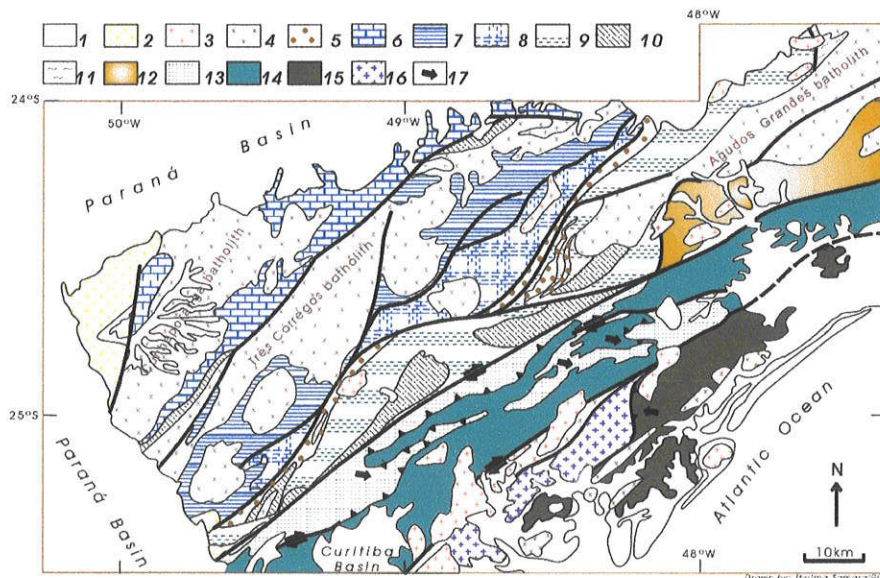


Figure 4-4: Major tectonic units from Açungui Supergroup

1. Phanerozoic covers, 2. Foreland basin (ca. 0.54 Ga), 3. A-type granitoids (ca. 0.59 Ga), 4. Hbl-Bt-bearing porphyritic syn-to-late-orogenic granitoids (ca. 0.615-0.605 Ga). **Apiáí terrane:** 5. Flysch-type deposits (Iporanga Formation), 6. Carbonatic platform (Itaiacóca Group), 7. Distal carbonatic platform (Água Clara Formation), 8. Shelf-break carbonatic ramp (Lageado SubGroup), 9. Deep-water turbidites (Votuverava Formation), 10. Rift-like volcanosedimentary sequence (Ectasic Perú Formation, and the northern Abapá Formation), 11. Schist and gneiss from unknown environment. **Juiz de Fora terrane:** 12. Schist and gneiss from Embu Complex. **Curitiba terrane:** 13. Carbonatic-psammitic passive continental margin deposits (Cryogenian?, Capirú and Setuba formations), 14. Upper Rhyacian basic-intermediate gneisses. **Luis Alves terrane:** 15. Metasediments from Tijucas belt, 16. Santa Catarina granulite complex (Archaean-Paleoproterozoic). 17. Ca. 0.60 Ga tectonic transport.

The Açuñui Supergroup (Campanha and Sadowski, 1999) apparently represents preserved paleogeographic zones of a passive continental margin environment (Fig. 4-4). The main metavolcanosedimentary sequences, which occur as windows below the basal stratigraphic level of the Açuñui Supergroup, also have an Ectasian age both on U-Pb zircon and Rb-Sr whole rock isochron (E.Dantas, personal communication and Daitx, 1996).

The northwestern belt has metasedimentary assemblage from “tropical” shallow shelf environment (up to 5,000 m thick). A pelite-carbonate marine transgression started the depositional sequences (Souza, 1990), interrupted by regression represented by restrict deposits of shelf sands. An upper transgression was related to sub-tidal carbonate platform containing bioherms of cone-shaped stromatolites (*Conophyton* cf. *C. gorganicum*, Fairchild, 1977). These units, from a drift-type episode, overlap ca. 2,000 m thick rift-type deposits. Deposits that are mainly composed of metarkoses, feldspathic metawackes and metafanglomerates, and contain within-plate, ultrapotassic, alkaline metavolcanic and metavolcanoclastic layers, and flood basalts. The Sm-Nd T_{DM} of these rocks falls in the upper Archaean (ca. 2.5 Ga, Reis Neto, 1994). Southeastward the platform gave rise to the settlement of a deep-water shelf (impure carbonates, banded calcsilicate rocks and metapelites) containing tholeiitic volcanism which grades to shoshonitic metabasalts (Frascá et al., 1990). This paleogeographic zone tops, by southeastward thrust, an uppermost regressive depositional cycle (rising 2,500m thick) of a psamitic-carbonatic epeiric platform that grades to carbonates from ramp-distally steepened setting reached by storm waves (Campos Neto, 1983, Pires, 1991). Stratigraphically bellow the transgressive depositional cycle (ca. 1,150 m thick of metasandstones with lenses of oligomicitic metaconglomerates up to thinner metarhythmites) is depicted by eastern turbidites from channel-lobe transition that grade to western proximal depositional systems. A wide deep-water basin plain dominated southeastward where large amounts of pelites (slates and phyllites) with thin, fine-grained, metasandstones rhythm enhancing distal turbidity currents.

The stratigraphic floor of the continental rise represents a shallow-water rift-basin environment (quartzite and metalimestones). It grades to a deep-water settlement (graphitic metapelites and metacherts) with remnants of oceanic crust (metabasalts from tholeiitic, sub-alkaline, T-MORB type), and iron-formation associated to high-K quartz-sericitic rocks from volcanic provenance. Isotope chemostratigraphy on Sr, C and O from calcite and baryte minerals, yield Mesoproterozoic marine source (Daitx, 1996).

A narrow belt of metarudites occurs at the boundary between the shelf-ramp carbonates and the deep-water basin. They comprise lenses of polymictic metabreccias and metaconglomerates immersed on metarhythmites (Iporanga Formation). Characteristically these metarudites have angular fragments and rounded pebbles of surrounding host rocks and already deformed phyllites, quartzites and some igneous rocks; they are devoid of limestone pebbles. This means that the Iporanga Formation could represent orogenic controlled deposits as a flysch. The metabasalts, which occur within this formation, have calc-alkaline affinity in agreement with compressive tectonic regimes.

Although the major structural framework had been built during the Neoproterozoic orogeny, the remaining metamorphic mineral assemblage locally showing kyanite ghosts (Juliani, 1993) was almost destroyed by a lower-pressure main foliation, and it was crosscut by the intrusion of the Neoproterozoic synorogenic granitoid batholiths. Among the

majority of such rift-to-drift basins some of volcanic layers depicted the transition to the plate convergent tectonic setting. The calc-alkaline volcanism marks the whole stratigraphic pile, also into the uppermost compressive driven fulfilling basin. Unfortunately the age of this orogenic process remains uncertain. On the other hand the Sm-Nd whole rock isochron for a metadolerite and Pb-Pb isotopic data for carbonate rocks from shallow and deep-water platform settings of the Açuñui Supergroup strongly suggest the Stenian-Tonian transition (ca.1.0 Ga) for the first metamorphic recrystallisation (Reis Neto, 1994, Poidevin et al., 1997). Thus a Grenvillian Stenian age should have been a coherent time span for the closure of an Ectasian oceanic crust.

4-4. The São Francisco plate margins: paleotectonic approach

The beginning of the Neoproterozoic is recorded in the São Francisco, Congo and Amazonas plates by a broad extensional tectonic regime related to the Tonian taphrogeny that led to the Rodinia break-up. The paleomagnetic reconstruction of Rodinia (Weil et al., 1998) left a Panthalassan-size ocean in the remaining Earth's surface. The large Arabian-Nubian Ocean (Stern, 1994) in the west of Congo plate and the probable South Pole connection with Pharusian Ocean (Caby, 1994) in the western portion of West Africa plate were some pieces of this jigsaw. The Goianides Ocean resulted from this former Tonian break-up, rifting apart the Amazonas plate from Congo-São Francisco plate (Fig. 4-5), as well as the Rio de la Plata plate from their African counterpart and Laurentia.

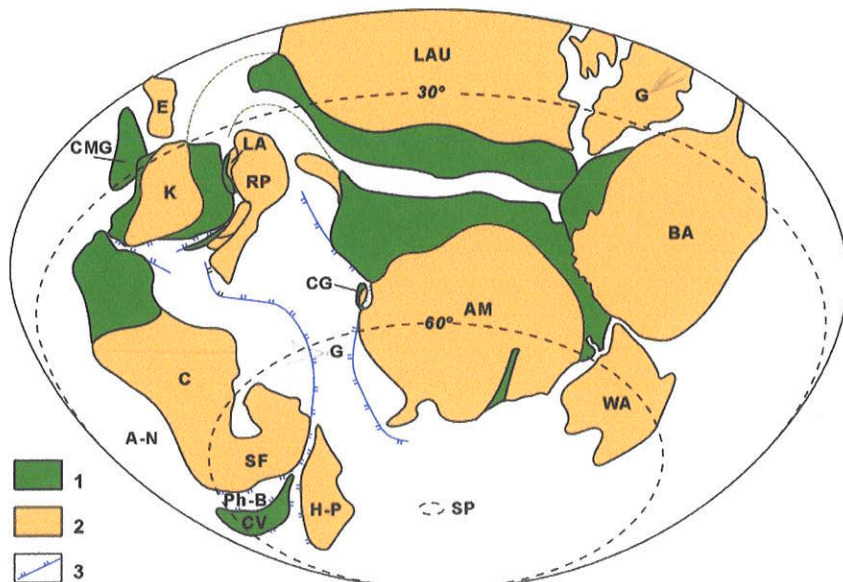


Figure 4-5: A modified view for the Rodinia reconstruction (from Weil et al, 1998).

The shape of Amazonas, São Francisco, Rio de la Plata and Western Africa continental segments of plates is modified. Speculative position of the postulate Hoggar-Potiguar plate and Cariris Velhos terrane. 1. Grenvillian orogens; 2. Continental plate segments; 3. Tonian rift lines. AM - Amazonas, BA - Baltica, C - Congo, CV - Cariris Velhos, CMG - Coates Land-Maudheim-Grune-Hogna Province, E - Ellsworth-Withmore Mountain block, G - Greenland, H-P - Hoggar-Potiguar, K - Kalahari, LAU - Laurentia, RP - Rio de la Plata, WA - Western Africa. AN - Arabian-Nubian Ocean, CG - Central Goiás terrane, CV - Cariris Velhos terrane, G - Goianides Ocean, LA - Luis Alves terrane, PhB - Pharusian-Borborema Ocean, SP - South Pole.

Extensional regimes (1.1-0.97 Ga) immediately followed the vanishing of the Grenville orogeny in the Amazonas plate, as well as in the Cariris Velhos terrane (Brito Neves et al., 1995) farther to the north of the São Francisco plate. Southeast of the Amazonas plate the records of this taphrogenic episode are the Santa Clara rapakivi granitic suite and the subalkaline and alkaline suites of the Younger Granites of Rondonia. They are coeval with the eruption of alkaline basaltic flows and the deposition of intracontinental rift sedimentary sequence. These anorogenic rock assemblages yield a zircon age between ca. 0.11 and 0.98 Ga (Bettencourt et al., 1999). At this time, the northern portion of the Congo plate was also subjected to dramatic extension episode leading to the opening of the Zambezi Ocean (Wilson et al., 1993). The Rio de la Plata continent may have been rifted apart from the western Kalahari taking part in a northeastward drift. The small fragment of the Central Goiás terrane containing Mesoproterozoic rocks over an Archaean-Paleoproterozoic framework could have been separated from Amazonas plate.

In the São Francisco plate interior taphrogeny-related magmatism occurs as within-plate microgabbro dyke swarms of tholeiitic and subalkaline affinities (Dossin et al., 1993), yielding a zircon age of ca. 905 Ma (Machado et al., 1989). Although geochronological data are not available, the rift-drift psamitic-dominated megasequence was established at the western (the Paranoá and Canastra Groups) and southwestern (Carrancas Group) extensional margins of the São Francisco plate. They seem to be related to this Tonian taphrogeny. The Paranoá Group is a ca. 1,600m thick megasequence limited by major unconformities. Its basal rudaceous layers locally overlies the Statherian Araí Group, whereas its uppermost erosive boundary is overlain either by the Sturtian-age diamictites (Jequitá Formation) or by post-Sturtian (Upper Cryogenian) carbonates of the Bambuí Group. The depositional megacycles of the Paranoá Group (Faria, 1995), represent a marine succession of an internal N.NW-elongated rift valley domain separated from the western shelf-break by paleogeographic ridges like a marginal plateau. Carbonatic rock interlayers, at least ca. 200m thick, occur at the upper transgressive unit, and grades outward to thick bioherm buildings. The bioherms occur on the ridges at the NW and SW edges of the basin, as reef lines containing weakly branching, cylindrical and large columnar stromatolites (up to 2.5 m of vertical column) of Conophyton-type (Cloud and Dardenne, 1973) developed in a subtidal environment. These carbonatic-dominated sequences, which build a local barrier up to 2,000m thick (south of Vazante Formation, Dardenne, 1981) may be related to strong subsidence due to rift-drift transition. Westward the uppermost lithostratigraphical units of the quartzitic nappe of Canastra Group is made up by pelitic-psamitic rhythmic and graphytic-bearing pelites (Campos Neto, 1984). They were intensively engraved by paraconglomerate channel deposits followed by thin sequences of pelitic-psamitic meta-rhythmites and carbonate-bearing phyllites (Ibiá Formation, Barbosa et al., 1970), like a turbiditic depositional system. Moreover this upper terrigenous sequence show a bimodal sedimentary source, either from the shelf deposits or the internal nappes, as well as bimodal Sm-Nd signature (Fischel et al., 1999, Pimentel et al., 1999). It may be placed on an inherited upper continental rise settlement, representing flysch-type deposits related to the arrival of the orogen (accretionary thrust wedge). Discret diamictite deposits correlated with the Sturtian glaciation (Middle Cryogenian, Hoffman et al., 1998) overlie the passive continental margin sequence and were covered by an extensive carbonatic cap under a shelf platform environment (the Bambuí Group) throughout the São Francisco plate interior.

On the whole (Fig. 4-6) this assemblage represented a large “lower-plate”-type passive continental margin.

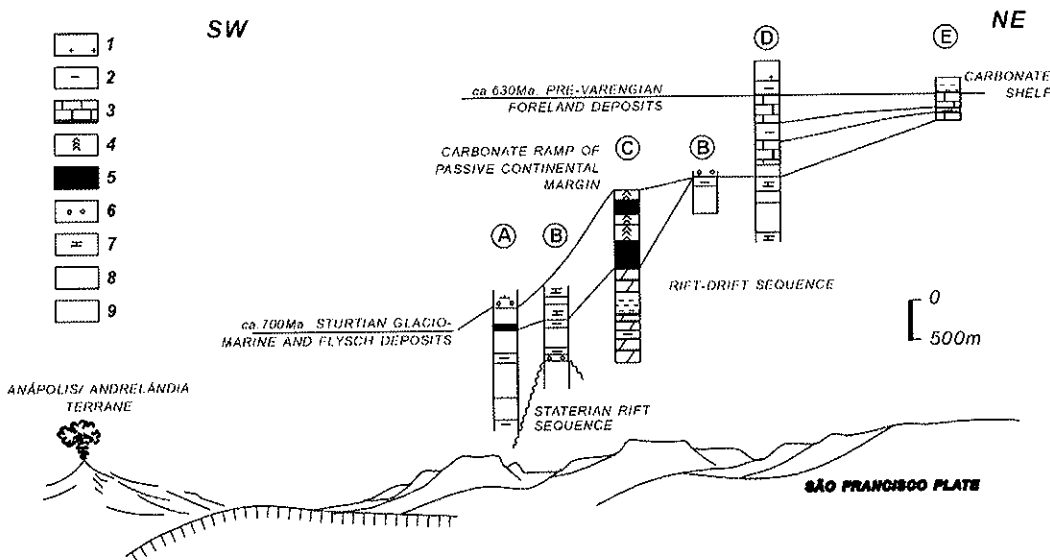


Figure 4-6: Stratigraphic and paleogeographic section through the western passive continental margin of the São Francisco plate.

1. Immature psammite and pelite, 2. Pelite, 3. Carbonates, 4. Stromatolite bioherms, 5. Graphite-rich layers, 6. Rudite, 7. Pelite and carbonate, 8. Psammite and pelites, 9. Psammite. A. Canastra Gr (Campos Neto, 1984), B. Paranoá Gr (Faria, 1995), C. Vazante Fm (Dardenne, 1981), D. Paranoá and Bambuí Grs (Dardenne, 1981), E. Bambuí Gr (Dardenne, 1981).

The pelitic micaschists and quartzites from the western upper nappes (Fig. 4-2) were intruded by small serpentinite bodies associated with podiform chromites and amphibolites, which were described as tectonically dismembered fragments of an oceanic crust, the Abadiânia-type ophiolite mélange (Strieder and Nilson 1992). Other small belts of metavolcanics have typical signatures of ocean floor basalts (Brod et al., 1991, Seer 1999), and display a Tonian Sm-Nd whole rock isochronic age with $\epsilon_{\text{Nd}}=+5.3$ (Fischel et al., 1999). Overall they form ca. 200km-long occurrences of remnants of depleted mantle-derived oceanic crust.

Opposite to that, at the northeastern margin of the São Francisco plate the Sturtian age glacial deposits recorded the beginning of the passive continental margin. Up to 100m thick of massive diamictites (with some remains of tillites on striated pavements, Rocha-Campos and Hasui, 1981) from glacio-marine origin (Jequitá Formation) grades eastward toward the basin. The basinal deposits represent up to 10km-thick glacial rocks reworked by subaqueous debris flows and turbidity currents (Macaúbas Group) that reach the deep-sea continental rise (Marshak and Alkmim, 1981, Uhlein et al., 1998). The eastern assemblage is the witness of the continental break-up. It corresponds to metamorphosed volcanic-exhalative sediments with related amphibolites, which are derived from oceanic floor basalts yielding a Middle Cryogenian age (Pedrosa-Soares et al., 1992). The shallow-water carbonates and shales of the Bambuí Group, are the thin (up to 400m thick) platform units that recovered the Jequitá diamictites (Fig. 4-2).

An “upper-plate”-type margin seems to dominate the eastern São Francisco plate. It was characterised by a narrow continental shelf, partially represented by N-S transpression sliver of metapsammitic and metapelitic rocks (Dom Silvério Group), and by broad

occurrences of metabasic and metavolcanosedimentary sequences. The tectonic provenance of this metamorphosed basic and volcanic assemblage is still unknown, but it seems that they record a Neoproterozoic extensive episode constrained by Sm-Nd data (Pimentel et al., 1998). They were tectonically imbricated with the grey gneisses of the Paleoproterozoic Mantiqueira Complex (Figueiredo and Teixeira, 1996).

Then the occidental and oriental passive continental margins of the São Francisco plate edges were developed diachronically and display asymmetrical shape (Fig. 4-7). The basal sedimentary layer of the narrow oriental margin (the Sturtian diamictites) correlates with the uppermost stratigraphic level of the wide occidental passive continental margin.

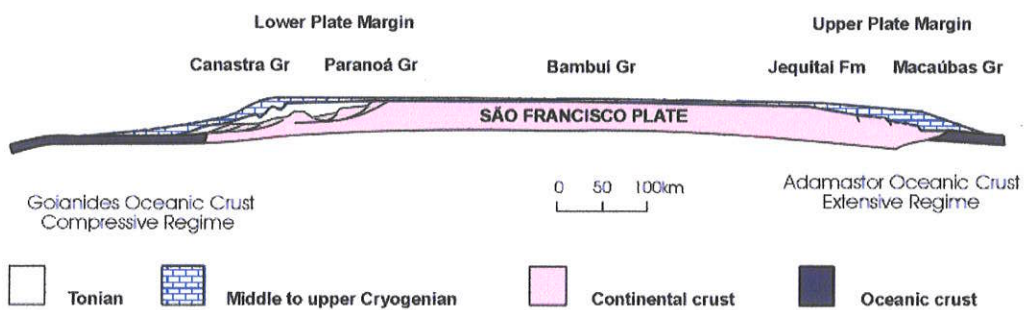


Figure 4-7: Scketche of E-W paleogeographic section through the western to eastern passive continental margins of the São Francisco Plate at ca. 700 Ma.

4-5. The Tocantins orogenic system

4-5.1. Orogenes' outline

The Tocantins orogenic system is related to the closure of the Goianides Ocean. It is a long-lived (270 Ma) plate convergence motion presupposing a large oceanic basin. The plate convergence process led to magmatic arc accretion and dockage from the Upper Tonian up to the beginning of the Neoproterozoic III when the main collision of the Central Goiás terrane and Rio de la Plata plate against the western São Francisco plate took place.

The Goianides Ocean encompasses many terranes. The ancient Central Goiás terrane is a drift fragment related to the Tonian taphrogeny. The other ones are mainly orogenic terranes related to a set of subduction zones (Fig. 4-8). The main compression kinematics of oceanic plate is related to west-dipping subduction zones. This kinematics framework is constrained by geologic and geophysic records. The first one is related either to the anatomy of a “lower plate”-type passive continental margin, or the collision-related east-driven extrusion of the high-pressure nappes. The geophysic records ascribe a west-dipping gravimetric model for the linear negative anomaly related to the suture zone (Marangoni, 1994), and the direct record of seismic P-wave and S-wave velocity perturbation models (Vandecar et al., 1995). This one displays large west-dipping low-velocity anomalies (for the P-wave) extending at least to 500-600 km depth. It is interpreted as inherited thermal and chemical remnant of the original mantle-plume formed during the main metamorphic-collisional event, by coupling of the whole upper mantle and the lithospheric plate (Fig. 4-9). Fossil S-wave mantle anisotropy with the fast-polarisation directions trend WNW-ESSE could be correlated to the ancient, Neoproterozoic, plate motion (James and Assumpção, 1996).

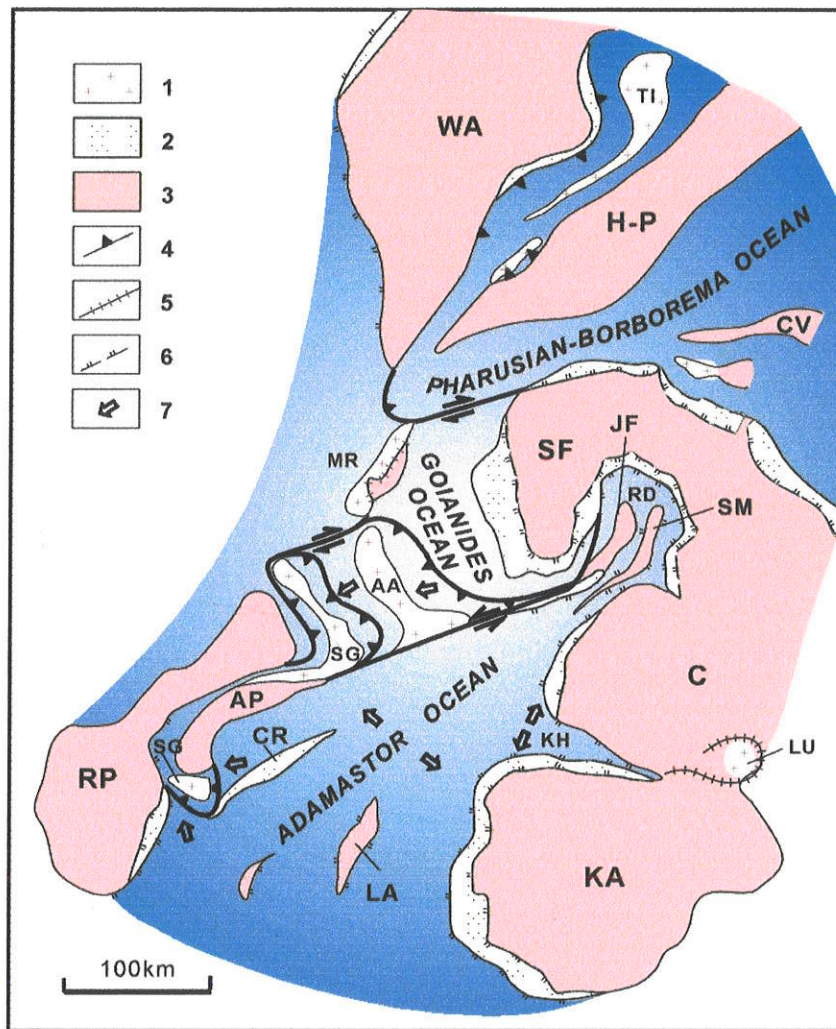


Figure 4-8: Attempt view of the lost oceans: ca. 750-700 Ma paleogeographic outline.

1. Tonian/Cryogenian magmatic arcs, 2. Passive continental margin deposits and thinner continental crust domains, 3. Mesoproterozoic belts, 4. Continental plates segments, 5. Subduction zone with sense of dip, 6. Cryogenian sutures, 7. Ancient rift lines. AA - Anápolis-Andrelândia, AP - Apiaí, C - Congo, CG - Central Goiás, CR - Curitiba, CV - Cariris Velhos, H-P - Hoggar-Potiguar, JF - Juiz de Fora, KA - Kalahari, KH - Khomas gulf, LA - Luiz Alves, LU - Lufilian, MR - Mara Rosa, RD - Rio Doce gulf, RP - Rio de la Plata, SG - Socorro-Guaxupé, SF - São Francisco, SG - São Gabriel, SM - Serra do Mar, TI - Tilemsi, WA - Western Africa.

The Upper Tonian Orogeny (0.90-0.85 Ga). It was the first subduction-related orogen recorded by the accretion of the intraoceanic Mara Rosa island arc. They are juvenile calc-alkaline volcanic belts and mantle derived metatonalites from the Arenópolis and Mara Rosa regions (Pimentel et al., 1992, 1997). Although have not supported, Pimentel et al. (1999) proposed an east-dipping subduction zone for the generation of this arc. The Lufilian arc elsewhere, in the Zambezi domain, was slightly coeval (Porada, 1989).

The Lower to Middle Cryogenian Orogeny. Two kinds of orogens seem to be related to this orogenic time. The first one is related to the dockage of the Mara Rosa arc whereas the other is related to a wide arc generation.

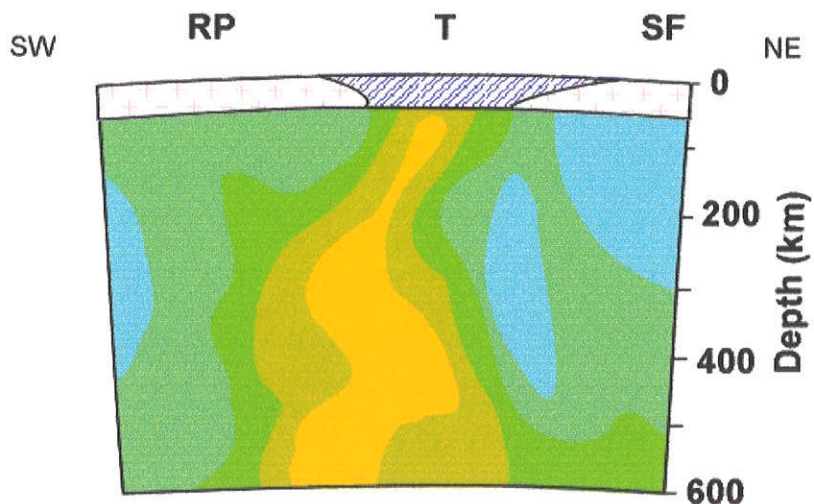


Figure 4-9: Cross-section through the P-wave velocity perturbation models. Modified from Vandecar et al (1995) with continental crust interpretation.

The low-velocity anomalies (clear grey tonalities) grade to the high-velocity anomalies (dark grey tonalities).

RP: Rio de la Plata plate, T: Tocantins orogenic system, SF: São Francisco plate.

An asymmetric subduction controlled non-continental-override-type collisional orogen could explain the dockage of the Mara Rosa island-arc on the non-destructive western edge of the Central Goiás fragment. A collection of U-Pb, Sm-Nd and Re-Os isotopic data obtained for the Central Goiás and in the Mara Rosa metasediments (Ferreira-Filho et al., 1994, Correia et al., 1996, Suita et al., 1996, Pimentel et al., 1998) support an age of 770-800 Ma for the metamorphic process. These values are not recorded in the metamorphic rocks from the passive continental margin setting. This metamorphism is mainly described as of low to medium pressure, high temperature type, interpretatively related to the lateral dockage of the hot arc crust. In spite of the poorly constrained data about the kinematics that controlled the main metamorphic structure, a dextral lateral motion is proposed based on near N-S trending mineral and stretching lineations and shear-sense indicators (Fonseca, 1996).

Two sets of arc-derived rocks dominant further south of the Mara Rosa Arc are separated by the remnants of oceanic crust in a discontinuous NW-oriented belt for at least 140-km long at Hidrolina-Morrinhos area (Fig. 4-2 and Fig. 4-8).

The western arc assemblage comprises the calc-alkaline plutonic-volcanic rocks of the Iporá-Jaupaci area (Pimentel et al., 1992), correlated by means of a NW-oriented belt (partially recovered by the Paraná Basin units) with the southernmost Socorro-Guaxupé terrane (Campos Neto and Figueiredo, 1995). The Iporá-Jaupaci area is mainly composed of tonalitic-granitic suite associated with metarhyolites both from a juvenile source (ϵ_{Nd} (T) positive). They are younger (0.76 Ga) and chemically more mature rocks ($K_2O/Na_2O > 1.0$) than the Mara Rosa Arc (Pimentel et al., 1992, Rodrigues et al., 1998) indicating a partial intraoceanic setting and the proximity of an older and thin continental crust. The continental arc basement became isotopically recorded further to the south, in the Socorro-Guaxupé terrane (Janasi, 1999).

The eastern arc environment is depicted by the calc-alkaline volcanoclastic and volcanosedimentary derived metagreywackes (see below). Metaluminous to slightly peraluminous granitoids (0.70 to 0.78 Ga) having juvenile magmatic component have been

described in this area (Pimentel et al., 1999a). However a crustal-derived magmatism predominates westward into pelitic and pelitic-carbonaceous schists and quartzites. They are peraluminous granites and sub-volcanic felsites (0.79 Ga) having an older Sm-Nd signature (Pimentel et al., 1992b, 1999a). These contrasted magmatic environments are separated by the tectonic high of the Neoproterozoic III lower crust fragment related to the Anápolis-Itauçu granulite-granite-migmatitic complex. Characteristically the rocks of this arc domain (the Anápolis-Andrelândia terrane) display bimodal peak of Sm-Nd model ages, within the 1.16 up to 1.95 Ga edges (Pimentel et al., 1999b, Janasi, 1999, Campos Neto and Caby, 1999b). It suggests a magmatic component from a juvenile source, and low crustal residence for the immature fan deposits, as well as the local presence of an older crust as magma contaminant or as sedimentary source. The metasedimentary assemblage of the Araxá nappe (Seer et al., 1998) belongs to this tectonic setting. Nevertheless the metapelites, quartzites and few carbonate lenses from Pirinópolis area (Goiás), separated from the Anápolis-Andrelândia terrane by a metamorphic jump and by a line of oceanic crust remnants would be related to the passive continental margin deposits, rather than to the Araxá Group. On the other hand the western peraluminous granites and felsites might have derived from deep crustal fusion related to a strong back-arc stretching (Fig. 4-10-A), prior to the collision episode, as previously proposed (Pimentel et al., 1999a).

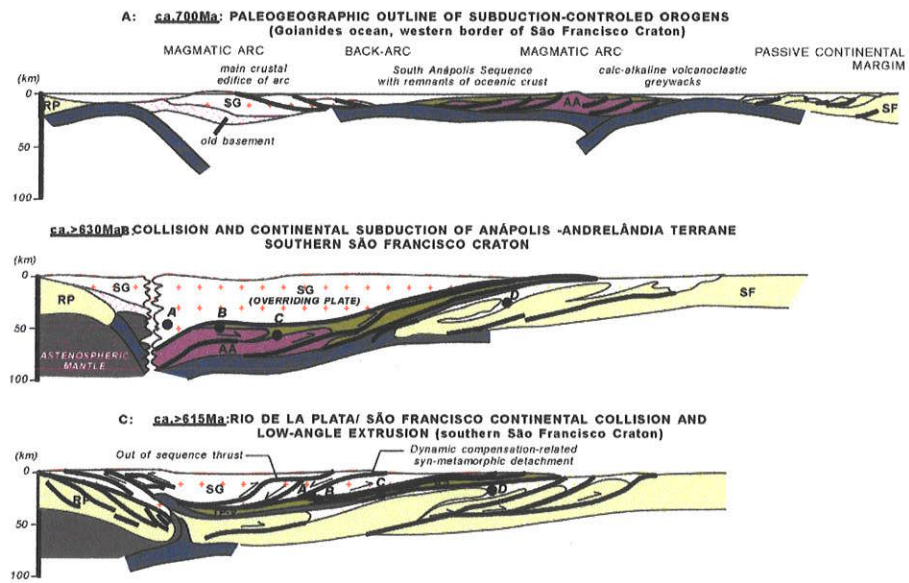


Figure 4-10: Sketches of plate kinematics evolution of the Southern Tocantins orogenic system

The Neoproterozoic III Orogeny. The roughly northeastward motion of the Rio de la Plata plate, as well as the amalgamated Mara Rosa Arc and Central Goiás terrane, led these continental plate segments to collide against the western passive continental margin of the São Francisco plate. This continental override-type collisional orogen is characterized by strong near-horizontal displacement of nappes transported over the outer domains of the parautochthonous passive continental margin, up to the autochthonous Bambuí platformal setting. The arc-related upper nappes underwent high-temperature metamorphic conditions override the subducted slabs subjected to high-pressure metamorphism. The shape of the lower-plate type passive continental margin favors the underthrust or continental

subduction of the continental plate subjecting the lower nappes to a medium-pressure metamorphic conditions. Except for the upper nappes, the metamorphism is typically reverse into each allochthon (Simões, 1995, Campos Neto and Caby, 1999a). The collisional arcuate shape of the terranes, convex toward the passive continental margin (Fig. 4-2), may be explained by an edentate action related to the original shape of the western São Francisco plate (Fig. 4-8). This edentate process may have controlled the oblique, sinistral convergence in the generation of the spoon-like flat geometry of E-SE-displaced Araxá and Passos nappes (Fig. 4-2) associated with internal a-type, NE-verging, reverse folding (Seer et al., 1998, Valeriano et al., 1998). Collision-related peripheral foreland basin adjoins the stable edge of the continental subducted margin (the Três Marias Formation).

The internal terranes of the Tocantins orogenic system yield robust U-Pb or Sm-Nd ages at ca. 625 ± 5 Ma related to the main metamorphic recrystallization and related to the emplacement of the synorogenic subduction-related porphyritic granitoids batholiths (Töpfner, 1996, Pimentel et al., 1999a, Campos Neto and Caby, 1999a, Fischel et al., 1999, Tassinari et al., 1999). The outward propagation of the orogen wedge and the out-of-sequence thrust sheets rise to 610 Ma (Janasi, 1999) up to their flat and ruptile emplacement over the autochthonous platform units at ca. 600 Ma (Valeriano, 1992).

4-5.2. The Southern Tocantins orogenic system

The southernmost portion of the Tocantins Orogenic system (Fig. 4-11) comprises a flat-lying package of east-northeastward-displaced nappes. They represent a diachronic thick-skinned and frontal growing nappe system that underwent a minimum of 300 km of magnitude of aggregate displacement, accounting for deeper crustal levels progressively exposed in the western allochthons. The uppermost tectonic unit derived from the magmatic arc (Socorro-Guaxupé terrane) displays high-pressure and high-temperature basal granulites. High-pressure terranes are underlain: the Ky-granulite from the Três Pontas-Varginha nappe, and the metapelite-metagreywacke with few eclogite relicts that form the Carmo da Cachoeira and Aiuruoca-Andrelândia nappes. The lower allochthonous units are made of medium-pressure metamorphic sequence associated with polymetamorphic orthogneisses (Luminárias-Carrancas and Lima Duarte nappes) which grade, in trailing imbricate fan-type thrusts, to the paraautochthonous units (Campos Neto and Caby, 1999a) both from the passive continental margin.

4-5.2.1 The upper high-temperature Socorro-Guaxupé nappe

The Socorro-Guaxupé terrane is a giant allochthon (at least 10 km thick) showing a right way up crustal section of hot and partially melted layered crust. It comprises (Fig. 4-11 and Fig. 4-12) basal banded enderbite (the Basal Granulitic Unit) partially derived from a Neoproterozoic near-juvenile immature magmatic arc setting (Sm-Nd T_{DM} of ca. 1.3 Ga). These granulites grades upward into a predominant grey to pink, metaluminous migmatites (the Middle Diatexitic Unit) indenting at their top with pelitic to semi-pelitic migmatites (the Upper Migmatitic Unit). From these migmatites longitudinal dextral strike-slip shear zones control a major metamorphic span to greenschist metamorphic facies southwestward (Campos Neto and Caby, 1999b). Various syn-orogenic deformed plutonic rocks show chemical and isotopic signatures compatible with the evolved subduction-related

magmatism onto continental setting. They are porphyritic rocks from the charnockitic suite that gives way upward to batholiths of porphyritic granitoids.

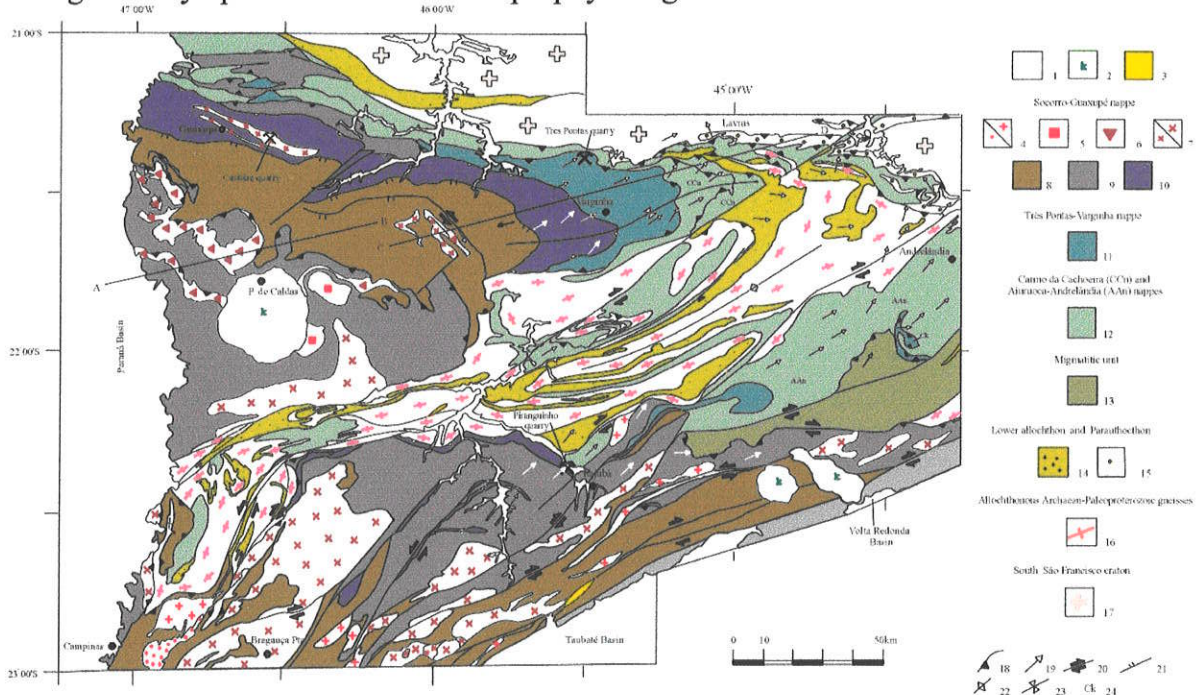


Figure 4-11: Geological map of the nappe system south of the São Francisco craton.

1. Phanerozoic deposits and basins, 2. Cretaceous alkaline plutons, 3. Pull-apart basins, 4. (small crosses) K-granites, diorites and gabbros (ca. 580 Ma) and (crosses) shear zone related granites (ca. 600-580 Ma), 5. Syenitic plutons (ca. 612 Ma); 6. Mangeritic-Granitic suite (ca. 625 Ma), 7. (x) K calc-alkaline porphyritic granitoids (ca. 630 Ma) and (small x) Charnockitic suites (ca. 640 Ma), 8. Upper Migmatitic unit and the southern schist belt, 9. Middle Diatexitic unit, 10. Basal Granulitic unit, 11. Ky-Grt granulites, 12. Metapelites and metagreywackes, 13. Migmatites and tourmaline-bearing granites, 14. Allochthonous quartzite-schist assemblage, 15 Parautochthonous quartzite-schist assemblage, 16. Allochthonous Archaean-Paleoproterozoic gneisses; 17. South margin of São Francisco Craton; 18. Major thrusts; 19. Displacement vectors; 20. Strike-slip shear-zone; 21. Detachment zone, 22. Antiformal axis, 23. Synformal axis, 24. Carvalhos klippen.

Janasi (1999) shows that the Nd T_{DM} record into the Socorro-Guaxupé nappe define coherent domains in which an old residual migmatitic granulites can be found ($Nd\ T_{DM} > 1.8$ Ga), whereas in other domains no sign of basement may be ascribed ($Nd\ T_{DM}$ of ca. 1.5 Ga). Similar bimodal distribution (Fig. 4-13) accounts for Neoproterozoic magmatic arc-derived “primitive” metagreywackes ($Nd\ T_{DM}$ around 1.2 Ga) and for an old basement-derived metapelites and “evolved” metagreywackes ($Nd\ T_{DM}$ between 1.8 and 2.2 Ga).

High-temperature throughout the crust section is the main characteristic of the Socorro-Guaxupé nappe (Fig. 4-14 A). The garnet-ortopyroxene-bearing granulites from the base of the nappe underwent $T=750-870^{\circ}\text{C}$ and $P=11.5-14.0$ kbar metamorphic conditions and yield near isobaric heating evolution toward $860-920^{\circ}\text{C}$ (Del Lama, 1994, Campos Neto and Caby, 1999b). These metamorphic data are consistent with dry melting of residual granulites in deeper levels of the crust generating anhydrous mangeritic magmas (Janasi, 1997, Campos Neto et al., 1988). The stratified behaviour of the Socorro-Guaxupé nappe is related to the higher thermal flow and controlled by the crustal level in which the widespread anatexis took place (Janasi, 1999). Thus, the pink anactetic biotite-bearing granites that belong to the Middle Diatexitic Unit were derived from metaluminous or higher Rb/Sr sources. They were generated by biotite dehydration melting at intermediate levels of the crust under ca. 850°C . On the other hand the supracrustal rocks from the

Upper Migmatitic Unit ($T=800^{\circ}\text{C}$ and $P=4.5$ kbar, Vasconcellos et al., 1991) are related to the shallowest muscovite dehydration melting as a magma source for the garnet-biotite parautochthonous granites. Sm-Nd and U-Pb results point that the age of this metamorphism is in the 630-625 Ma range. The former age is related to the syn-orogenic granitoids and basal garnet granulite. The latter is well constrained for the uppermost garnet-biotite granite and the intermediate crustal level anactetic pink granites and mangeritic gneiss (Basei, 1995, Janasi, 1999). The synorogenic (ca. 0.63 Ga) batholiths comprise an extensive suite of hornblende-biotite bearing porphyritic granitoids from high-K calc-alkaline suites (Janasi and Ulbrich, 1991). They were found intrusive into the Serra do Itaberaba Group (northern of the Apiaí terrane). There they comprise porphyritic to equigranular tonalitic-granitic gneisses.

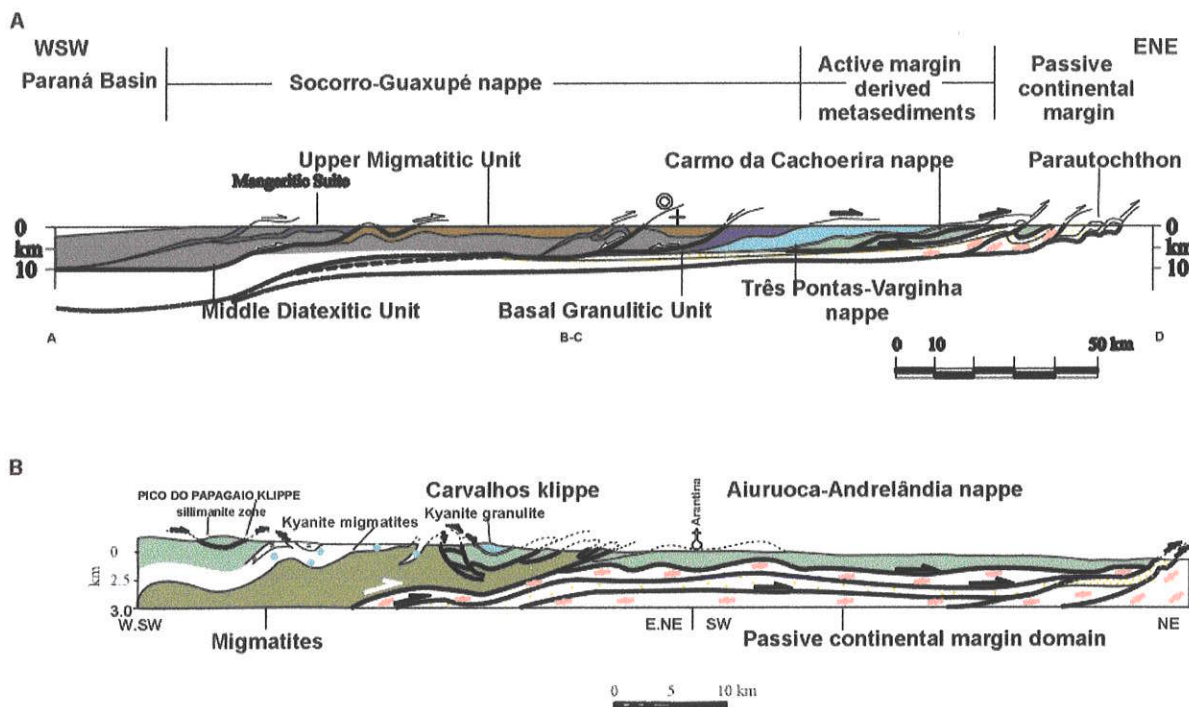


Figure 4-12: A- Cross-section across Socorro-Guaxupé, Três Pontas-Varginha, Carmo da Cachoeira and Luminárias nappes. B- Cross-section across the Aiuruoca-Andrelândia nappe. Profile A located on figure 11.

The basal thrust of the Socorro-Guaxupé nappe comprises a thick domain (up to 3 km thick) with flat-lying syn-metamorphic foliation as a strong plane-linear fabric bearing top-to-east-northeast shear sense indicators. A sole thrust overlaps the high-pressure nappes as well as the lower allochthon related to the passive continental margin units, resulting in at least 150-km of displacement. A syn-metamorphic detachment, locally accommodated by a NW-oriented oblique sinistral strike-slip fault, accounts for the direct contact of the uppermost migmatitic unit above the basal granulites where at least 5 km of the Middle Diatectic Unit were omitted. Late metamorphic NE-displaced out-of-sequence thrusts are younger than the ca. 625 Ma old mangerites. These structures drove the stretched magmatic arc terrane toward its shallowest dept at 610 Ma, testified by the upper level intrusion of the post-kinematics potassic syenites (Janasi et al., 1993).

4-5.2.2. The high-pressure nappes

The Três Pontas-Varginha nappe is a thick sheet that crops out for 170 km parallel to its E.NE displacement direction. The nappe package comprises mainly coarse-grained rutile-kyanite-garnet granulites, lesser impure quartzites, and few calc-silicate rocks, gondites, lenses of metabasic rocks and rare sills of mafic-ultramafic rocks. Upward the Ky assemblage gives way to Sil-bearing granulites up to migmatites. The underlying Aiuruoca-Andrelândia and Carmo da Cachoeira nappes are chiefly made up of a layered sequence of peraluminous rutile-kyanite-garnet-muscovite schists and dark-grey, massive garnet-biotite-plagioclase gneisses and schists. Small lenses of metabasic rocks rise to eclogitic metamorphic assemblage. As the metasedimentary sequence of the Socorro-Guaxupé nappe, the chemical and isotopic characteristics of these rocks (Campos Neto et al., 1990, Janasi, 1999), either under granulitic or amphibolitic metamorphic facies conditions, is characteristically bimodal (Fig. 4-13). The rocks from pelitic source have Sm/Nd T_{DM} and U-Pb ages on detrital zircon at 1.9 Ga (Söllner and Trouw, 1997). The metagreywacke record Nd T_{DM} between 1.16 and 1.55 Ga, becoming to unravel their Neoproterozoic juvenile volcanic arc source.

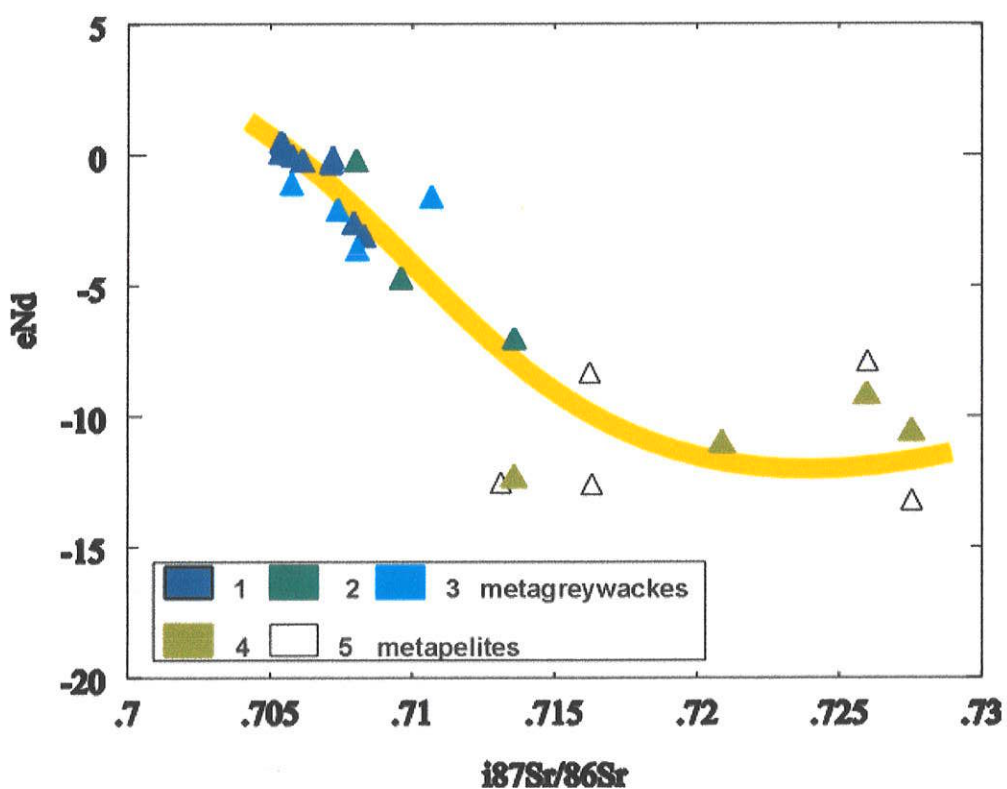


Figure 4-13: $\epsilon_{Nd}(625) \times i^{87}Sr/^{86}Sr$ diagram for metasedimentary rocks (modified from Janasi, 1999). Metagreywackes: 1. Grt-Bt-Pl gneisses from Aiuruoca-Andrelândia nappe, 2. (Crd)-Sil-Grt-Bt- gneisses from Middle Diatexitic Unit of Socorro-Guaxupé nappe, 3. Ky-Grt-Pl granulites from Três Pontas-Varginha nappe. Metapelites: 4. Sil-Ky-Gr-Kf granulites from Três Pontas-Varginha nappe, 5. Grt-Bt gneisses from Upper Migmatitic Unit of Socorro-Guaxupé nappe.

A coherent inverted metamorphic pattern is supported by these nappes (Fig. 4-14). Lower temperatures (650°C) were attained under high-pressure (12-14 kbar) related to the decompression stage of eclogite conditions (660°C-17.5 kbar). Upward the temperature

increase to 700°C ($P=15$ kbar) on Ky-granulites to get 830-950°C in a near-isobaric heating path. The syn-kinematics decompression related to the outer propagation of the out-of-sequence thrusting varies from 600-690°C and 9-11 kbar (Campos Neto and Caby, 1999b). The syn-kinematic cooling of the high-pressure pelitic granulites depicted by the closure temperature of monazite in U-Pb system done at 612 Ma (Janasi, 1999). It could be related to the outward propagation of the out-of-sequence thrust system.

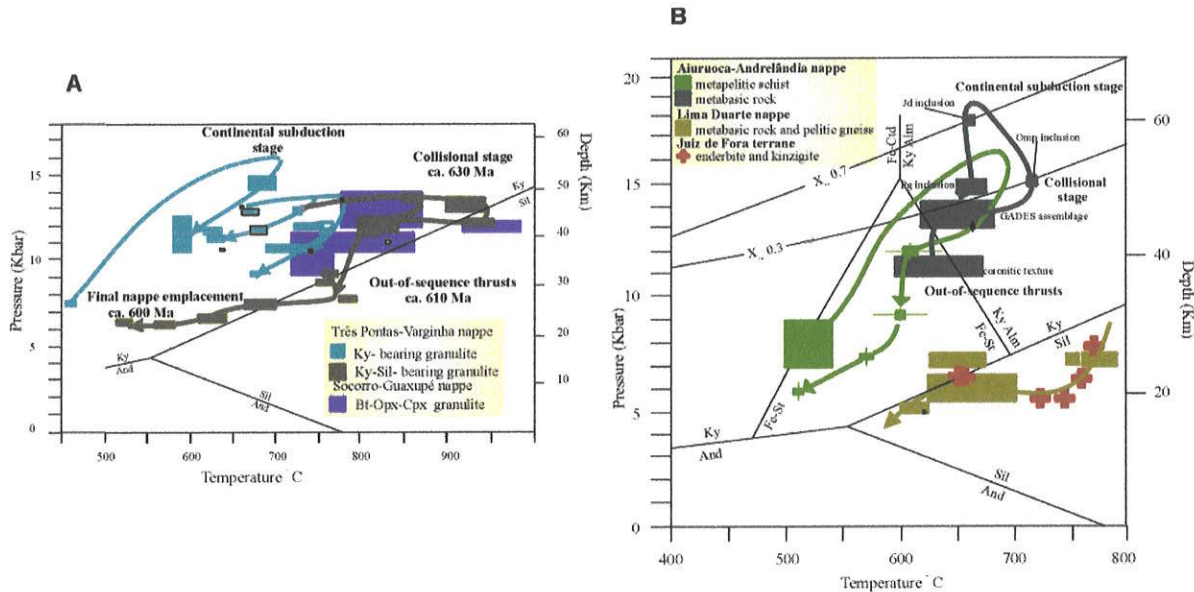


Figure 4-14: Metamorphic paths: A- Três Pontas-Varginha nappe; B- Aiuruoca-Andrelândia nappe and Lima Duarte nappe.

4-5.2.3. The medium-pressure lower nappes and foreland orogen propagation

The psamitic rock associations that are related to the passive continental margin deposits occur as the lower allochthon and parautochthonous units (Fig. 4-11). The flat-lying sheet of Luminárias-Carrancas nappe shows an eastward minimum transport of ca.140-km, and it is composed mainly of white and green mica quartzites grading upward into well bedded to laminated quartzite interlayered with graphitic and aluminous metapelites (Ribeiro et al., 1995, Paciullo, 1997). Polymetamorphic orthogneisses and migmatites also belong to the nappe package, and a barrovian-type mineral succession was described (Trouw et al., 1986).

In the parautochthonous units the ramp and flat thrust pattern prevail, involving basement orthogneisses and interbedded quartzites and grey phyllites. Locally the metapelite displays a metamorphic assemblage which accounts for medium to high-pressure conditions ($P=7$ kbar and $T=500$ °C) that may control the appearance of Zn-staurolite and kyanite in the absence of garnet and biotite (Campos Neto and Caby, 1999a).

Eastward, the main psamitic rock package with sillimanite-bearing metapelites is organised in a large, basement involved allochthon: the Lima Duarte nappe (Fig. 4-15). This is also subjected to medium-pressure metamorphism reaching granulite facies and late anatexis. Garnet-clinopyroxene bearing amphibolites (with IBC-type coronitic textures) and sillimanite-bearing gneiss show the metamorphic peak under $T_{max}=700$ °C and $P_{max}=7$

kbar. Nevertheless the syn-metamorphic structures account for north-displaced unrooted thrust system exibing monazite U-Pb age of 570 Ma (Machado et al., 1996). A thin-skinned duplex displaying the same northward displacement overprints the Lima Duarte nappe. Thus, the Lima Duarte nappe seems to be related to the foreland propagation of transpressive deep structures related to a collisional orogen of the newer Mantiqueira orogenic system. It represents the Ribeira/Brasilia belts interaction of Trouw et al. (1998).

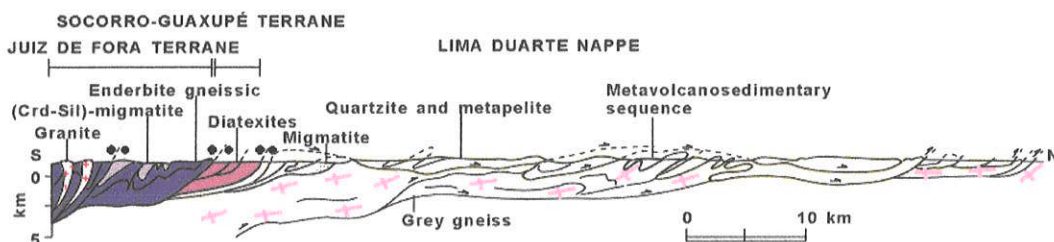


Figure 4-15: Cross-section through Lima Duarte nappe

4-5.3. Tectonic evolution of the Southern Tocantins orogenic system

The Southern Tocantins orogenic system results from the agglutination of three major geodynamic environments during the Neoproterozoic III Orogeny. The western and uppermost tectonic setting is related to the Socorro-Guaxupé Magmatic Arc terrane, which may represent deep crustal level of the Iporá-Jaupaci Arc developed during the Middle Cryogenian Orogeny. The high-pressure metasedimentary terranes (Três Pontas-Varginha, Carmo da Cachoeira and Aiuruoca-Andrelândia nappes) are the records of an active margin setting as the source area for wacke deposits, probably upon a forearc-thinned crust belonging to the Anápolis-Andrelândia terrane. The Tonian-Lower Cryogenian metasedimentary sequence from the southwestern passive continental margin environment of the São Francisco plate comprises the metapsammitic-dominated, medium-pressure lower nappes and parautochthon.

The high-pressure metamorphic conditions recorded by the kyanite-bearing granulites and eclogites from Três Pontas-Varginha nappe and Aiuruoca-Andrelândia nappe imply a low thermal gradient (ca. 11°C/km), which can only be achieved in an ocean closure (Spear, 1995) through a west-dipping subduction scenario. The microplate segment conformed by these nappes was subducted to a minimum depth of 60 ± 5 km. It is assumed that great amounts of oceanic crust and continental crust material from southern Anápolis-Andrelândia terrane were lost by subduction. Only a small portion of the subducted slabs is preserved within the high-pressure nappes. Modern analogues could be seen in the Alpine Tertiary subduction of great portion of the paleo-European margin bellow the Apulian plate (Schmid et al., 1996).

An inverted metamorphic field gradient is brought about from the perturbed paleogeotherm to an upper steady state thermal gradient (20°C/km) of the upper sillimanite-bearing granulites toward the base of the high-temperature Socorro-Guaxupé nappe (Campos Neto and Caby, 1999b). This thermal pattern related to diachronic equilibration at different temperatures throughout the metamorphic prism, as evidenced in the Indian Greater Himalayan zone (Vannay and Grasemann), requires the rapid emplacement of the

upper hot allochthon onto the Três Ponta-Varginha nappe. It resulted from the subduction driven arrival of the Socorro-Guaxupé terrane displaying, at their base, similar dT/dP gradient (Fig. 4-10-B).

At the shallow levels of the Socorro-Guaxupé terrane ($T=820^{\circ}\text{C}$ and $P=4.5$ kbar) the metamorphic high-thermal flow argue for a compressed paleogeotherm pattern (ca. 50°C/km). This steeper thermal gradient could be related to a lithospheric extension resulting from astenospheric mantle upwelling with considerable amounts of basic magma underplating. Those processes were in the origin of the widespread crustal magmatism into the Socorro-Guaxupé terrane, and occurred in a short-lived metamorphic peak robustly confined at 625 ± 5 Ma. Though nearly contemporaneous the “cold”-subduction scenario depicted by the kyanite granulite beneath the Socorro-Guaxupé terrane attests for initial different tectonic environment for both terranes. A roughly east-dipping subduction of an oceanic segment of the Rio de la Plata plate might be envisaged (Fig. 4-10-B). This subduction could be in agreement with the northwestward-displaced syn-metamorphic structures in the western area of the Socorro-Guaxupé nappe, as well as to the steepen pattern of isotherms.

The collisional outward propagation of the nappe pile (Fig. 4-10-C) submitted significant thinning was accompanied by temperature-decrease at each thrusted rock-package. The preservation of an inverted metamorphic gradient equilibrated in the kyanite-field requires rapid exhumation. This short-lived tectonic scenario began around 630 Ma and ended shortly before 612 Ma. Thus, part of the lower crust was exhumed from subduction prism and driven horizontally and thinned above the passive continental margin domain resulting a mean cooling rate of about 15°C/Ma . These subducted crustal slabs moved back up to the surface at a critical stage of the subduction while continuing underthrusting of the denser lithosphere (Chemenda et al., 1995, Matte et al., 1997). The hinterland-driven syn-metamorphic detachment may result from internal extension by dynamic compensation (Hodges et al., 1996) in reponse to the possible building of mountain range of Himalayan size.

The post-orogenic history started early in the inner terranes at 610 Ma extending thoughout 580 Ma up to 550 Ma (Pimentel, et al., 1996, Töpfner, 1996, Wernick, 1998). It was pictured by a dramatic change in the character of the plutonic magmatism. A K-rich granitoid association was recognized conforming roughly with a N.NE-oriented belt (the Itú belt, Vlach et al., 1990). They are mostly undeformed high-K calc-alkalic hornblende and biotite-bearing porphyritic monzogranites, syenogranites locally with wiborgitic texture, pink inequigranular monzogranite, muscovite and fluorine-bearing granites. Basic and intermediate rocks occur as enclaves and syn-plutonic dykes, and also as some plutons of K-rich diorites and K-syenites. Beyond the large amount of magma contribution from crustal materials, an important contribution is allowed from two fundamentally different mantle-derived magmas. A strongly oxidised magma, poor in basaltic component in the origin of the K-syenites, and the K-dioritic magmas with shoshonitic affinities (Janasi et al., 1993). This post-orogenic episode seems to represent the reactivation and melt of the subcontinental lithospheric mantle involved in extension regime on the inner orogens.

4-6. Paleotectonic approach for the Mantiqueira orogenic system

That above-mentioned phases of convergence are related to the global break-up of Rodinia and dispersion of their descendants, that commenced at ca. 0.75 Ga, including the

separation of East Gondwana from the western margin of Laurentia (Park, 1994). Accordingly (and differently from the orogenic conditions of the Goianides oceanic realm), in the São Francisco-Congo plate taphrogenic processes predominated during the mid-Cryogenian. The Sturtian glacial deposits were widespread and they were related to the main rifting stage in the Congo and Kalahari plates, as well as in the São Francisco plate. Normally they were succeeded by passive continental margin settings and the post-glacial marine cap dolomites have covered the São Francisco plate.

At the African side the first stage of Damaran extensional basin was recorded by the rift-related continental sediments of Nosib Group associated with alkaline bimodal volcanic rocks that are older than 0.75 Ga. At the western of Kalahari craton eruption of felsic volcanic have been dated at ca. 745 Ma. The supercontinental break-up and opening of the Adamastor Ocean was constrained by the major marine transgression recorded by the deposition of Octavi Group which contains basal volcanic interlayers yielding U-Pb zircon ages between 745-758 Ma. Iron-rich diamictites (Chuos Formation) have been regarded as Sturtian, once they overlie a shelf ramp facies of the base of the Octavi Group. Farther to the south this oceanic opening process was diachronically younger. At the Gariep belt the Sturtian diamictites (Kaigas Formation, ca. 720 Ma) precedes the passive continental margin succession (Hilda Subgroup) and the oceanic assemblage. Later still, the opening of the intracontinental branch of the Khomas Sea took place following the uppermost glacio-marine diamictites (Ghaub Formation) considered as Varangian (ca. 600 Ma) in age (Stanistreet et al., 1991, Frimmel et al., 1998, Hoffman et al., 1998, Kennedy et al., 1998).

As it was seen before, at the eastern portion of the São Francisco plate (South American side) the beginning of the passive continental margin was recorded by the Sturtian-related glacial deposits (Macaúbas Group) and turbidities fans (Salinas Formation) up to oceanic remnants (Ribeirão da Folha Formation) placed in the Neoproterozoic at the Middle Cryogenian (Pedrosa-Soares et al., 1998). Nevertheless an early oceanic basin (the Charrua Ocean, Fragoso-Cesar et al., 1997) seems to precede the main opening of the Adamastor Ocean, and it was recorded locally at the east of Rio de la Plata plate during the Early Cryogenian.

Several narrow and elongated (Fig. 4-8) small plate fragments (descendants of Rodinia) played an important role in the history of this orogenic system (Fig. 4-2).

The Apiaí terrane comprising the Mesoproterozoic Ectasian series is overlain by carbonatic shelf and terrigenous deep-sea turbidity fan from ramp and rise of a passive continental margin (the Açuungui Super Group described above). These rocks and the orogenic granitic batholiths record a Paleoproterozoic (ca. 1.9 Ga) Nd (T_{DM}) signature (Sato, 1998). It is possible that the Apiaí terrane had been connected with the northeastern Rio de la Plata plate after the Grenvillian orogenies.

The Luis Alves terrane conforming an Archaean-Paleoproterozoic lower-crust fragment (the Santa Catarina granulite complex) southeastern facing by a terrigenous and narrow shelf-type passive continental margin deposits of the Brusque Group and Porongos Group (Basei et al., 1998). Mesoproterozoic Calymmian/Ectasian Sm-Nd isochronal ages are suggested for the basal volcano-sedimentary sequences (Basei, 1985). Farther to the south the metasedimentary belt override Paleoproterozoic aged gneiss and the continuity of the Santa Catarina granulite complex was tectonically omitted. In spite of the northern Archaean foreland domain, these sequences, and also the later intrusive granites, display a Paleoproterozoic (2.0 Ga) Nd (T_{DM}) signature (Basei et al., 1997).

The Pelotas terrane comprising a fragment of Paleoproterozoic crust, which was mainly recognized through the evolved arc-related granitoids by the Sm-Nd studies (Basei et al., 1997, Silva et al. 1999).

Besides all that, there is a small anonymous fragment/terrane composed of migmatites with a Kibaran age of metamorphism that has preliminarily been identified in southeast Uruguay, east of the Pelotas terrane (Precciosi et al. 1999).

The Curitiba and the Juiz de Fora terranes forming a narrow and elongated crustal fragment with a general framework of juvenile Paleoproterozoic calc-alkaline intermediate plutonic rocks partially as a granulitic belt, which became more evolved further to the south (Sollner et al., 1991, Sato, 1998, Basei et al., 1997, Heilbron et al., 1998). It seems that these terranes might be derived both from the rifting and break-up of the eastern São Francisco plate. Somehow the Juiz de Fora terrane is regarded as belonging to the Paleoproterozoic juvenile within-oceanic to active margin accretion (Duarte et al., 1997, Valladares et al., 1997), which could be related to the Mineiro mobile belt, southern of São Francisco craton (Figueiredo and Teixeira, 1996, Alkimim and Marshak, 1998). Thus the Middle Cryogenian break-up of the eastern São Francisco plate may followed the weakness line related to an ancient Rhyacian suture zone.

Beyond the wide granite occurrences, high-temperature metamorphic rocks from sedimentary provenance prevail north of the Juiz de Fora terrane, associated with a few stratiform bodies of mafic-ultramafic rocks. To the south, the Paleoproterozoic Rhyacian partially melted gneisses (Machado et al., 1996), derived from plutonic rocks of calc-alkaline affinities, are tectonically associated with a metasedimentary assemblage (the Paraíba do Sul Complex) made chiefly by immature quartzite, sillimanite-garnet bearing gneiss and migmatite, and marble. An admixture of Paleoproterozoic Rhyacian and Statherian sources for these metasediments could be admitted based on ^{207}Pb - ^{206}Pb age and Nd (T_{DM}), whereas some interbedded metabasic rocks display Neoproterozoic magma provenance (Valladares et al., 1997). Further to the south (Fig. 4-3). The metasediments (the Embu Complex) prevail over a narrow and thinned strip of an Archaean tonalitic-granodioritic gneisses (Tassinari and Campos Neto, 1988). They comprise three major units showing metamorphic spans from green-schist facies to higher anfibolite metamorphic facies across steep and lateral displaced shear zones. They are (Fig. 4-3) shelf-related quartzites, a distal rhythmic succession of pelitic schists and quartzites, and metavolcanic-volcanosedimentary rocks (amphiboles, calc-silicate gneiss, metagreywackes) with restricted marbles and immature quartzites (Fernandes et al., 1990). Although isotopic and geochemical data are not available, these sequences are supposed to have derived from a Neoproterozoic tectonically active environment.

The Curitiba terrane is mainly composed of basic/intermediate banded gneiss and migmatites, and subordinately charnockitic gneiss, related to the Paleoproterozoic Atuba complex (Basei et al., 1992, Siga Jr. et al., 1993). The metasedimentary cover consists of a marine regressive sequence of shallow water carbonates (Capiru Formation) associated with quartzite-schist assemblage (Setuba Formation) grading eastward to rhythmic deep-sea type terrigenous sequence. They have characteristics of an extensional basin related to a narrow and asymmetric rift reaching a passive continental margin (Yamato, 1999).

The Serra do Mar terrane is on the whole mainly composed of migmatites and elongated and diffuse bodies of (garnet)-biotite-bearing granites with nebulitic and schlieren structures with variable strain rate. Sometimes they contain enclaves and/or resisters of quartzites, calc-silicate marbles and amphibolites. North of Rio de Janeiro

State, preserved from the wide and deep strike-slip shear belt, three distinct crustal segments can be recognized (Sluitner and Weber-Diefenbach, 1989, Campos Neto and Figueiredo, 1995, Wiedemann et al., 1997). They are: the westernmost and basal supracrustal unit, the overlying gneiss-migmatite unit, and the eastern and upper granulite-granite-migmatite unit, displaying an inverted structural pile related to a westward nappe displacement. Immature quartzite, garnet-sillimanite-bearing quartzite and quartz-schists, marbles and calc-silicate rocks, and gneiss from wacke provenance constitute the majority of the supracrustal unit. Slices of metabasic and meta-intermediate rocks display protoliths chemically identified with high-Ti and low-Mg tholeiitic basalts and alkaline basalts associated with an arc-type calc-alkaline andesites (Sad and Dutra, 1988). These assemblages come together with an active continental margin environment. The gneiss-migmatitic unit is made up of (cordierite-sillimanite)-garnet-biotite stromatic migmatite having a wacke-pelitic provenance, whereas the upper granulite-granite-migmatite terrane is mostly composed of sin to late-kinematics peraluminous (cordierite-sillimanite-garnet-bearing kinzigitites) and metaluminous diatexites, normally associated with enderbite series.

The contrasted Sm/Nd isotopic signature (data from Sato, 1998) between Serra do Mar and Juiz de Fora terranes being prominent projecting the low $^{143}\text{Nd}/^{144}\text{Nd}$ and $^{147}\text{Sm}/^{144}\text{Nd}$ ratio for the Serra do Mar rocks than those from the Juiz de Fora terrane (Fig. 4-16). On the other hand, the Mesoproterozoic T_{DM} age that dominates all over the Serra do Mar terrane concurs to an African rifting-apart.

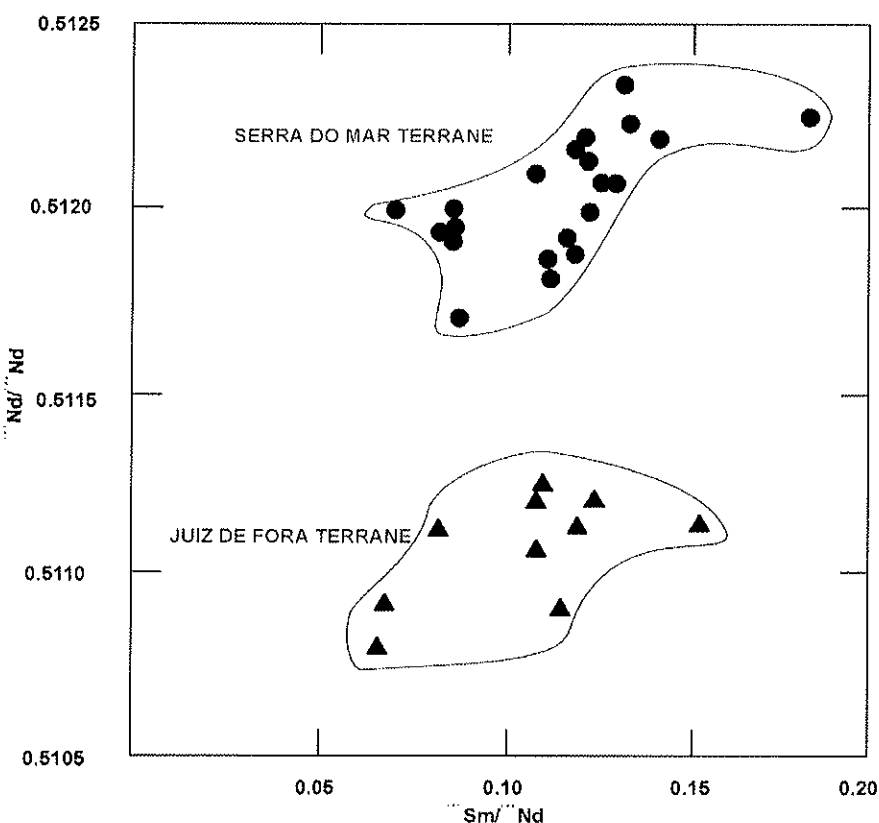


Figure 4-16: $^{143}\text{Nd}/^{144}\text{Nd} \times ^{147}\text{Sm}/^{144}\text{Nd}$ relationships between Serra do Mar and Juiz de Fora terranes.

The *Cabo Frio terrane* comprises orthogneiss from diorite-tonalite-granite series associated with orthoamphibolite slices of Paleoproterozoic age (Zimbres et al., 1990, Schmitt et al., 1998). The orthogneissic complex overrides a metasedimentary sequence mainly composed of paragneiss and quartzite, with subordinated lenses of calc-silicate rock and amphibolite (Heilbron et al., 1982). These metasediments have a Mesoproterozoic Nd (T_{DM}) signature suggesting a Neoproterozoic aged deposition.

4-7. The Mantiqueira orogenic system

The geological scenario of the south-southeastern Atlantic coastal area of Brazil and Uruguay (up to the Mantiqueira Range on the continent interior) is a NE-trending orogenic system, mostly controlled by steep, strike-slip shear zones. It comprises a series of terranes that have diachronically collided against the just-assembled (0.63-0.62 Ga) São Francisco-Rio de La Plata plates, so forming the orogenic system related to the closure history of the Adamastor Ocean.

4-7.1. Regional view on plate convergence in the Southern Mantiqueira orogenic system

The plate convergence started with the closure of the small (?) Charrua oceanic basin. It was recorded by the metavolcanic and metaplutonic rocks from calc-alkaline affinities (the Vila Nova belt, Silva Filho and Soliani, 1987) yielding U-Pb on zircon age of 705 Ma and a $\varepsilon_{Nd}(t)$ rising to +7.8 (Babinsky et al., 1996). It was the first well-constrained plate interaction record for an Upper Cryogenian intraoceanic subduction-controlled orogen (the São Gabriel Orogeny) in the southern of Mantiqueira Orogenic system.

Sedimentary and volcanic belts from Brusque and Porongos Groups which underwent medium to low-pressure metamorphism are associated with W-NW verging collision-related structures. Although scarce and imprecise geochronological data the metamorphic peak must have been reached around 630 Ma (Silva et al., 1999) slightly before the late-kinematics granite batholiths (Basei, 1985). Many pieces of the plate interactions for this collision-controlled orogen seem to have been disguised by or concealed under the ca. 460km-long Phanerozoic Paraná Basin (Fig. 4-2).

The Neoproterozoic III subduction-controlled Pelotas magmatic arc orogen (0.61 to 0.60 Ga) took place facing the southeastern edge of the Brusque and Porongos orogen. This arc comprises a series of calc-alkaline plutonic rocks and high-K porphyritic granites mingled with coeval migmatites, all of them displaying flat-lying foliation related to W-NW tectonic transport (Basei, 1985, Tommasi et al., 1994, Fernandes et al., 1995). Based on the extrusion vector of the collision structures and the eastward zonation toward the post-collision pink granites (ca. 595 Ma), an southeastward-dipping subduction could be admitted.

The main collisional orogenic interaction ca. 0.6 Ga was responsible for the juxtaposition of Pelotas magmatic arc, Luis Alves terrane, and the southeastern boundary of Rio de La Plata plate. The major strike-slip shear zones define the main collision boundary: a northern, dextral and a southern, sinistral shear zones that contained and controlled the emplacement of peraluminous and metaluminous granites. Impactogenic processes were related to the origin of the undeformed volcano-sedimentary basins that were associated

with alkaline-peralkaline granitic intrusion. This process took place mostly in the Luís Alves and Curitiba terranes at ca. 0.6-0.57 Ga (Siga Jr. et al., 1997).

The development of the collision-related foreland basins at the southern of Luis Alves terrane and the eastern of Rio de la Plata plate are recorded by remnants of continental environments up to deep marine deposits. Unconformity and volcanic episode separated these sedimentary environments. They are the Itajaí, Camaquã and Arroyo del Soldado Groups, which were pierced by intrusive granites and volcanic felsites (0.56 Ga), and which contain several Vendian species of palynomorphs. Their stratigraphic history was broken at 0.53 Ga, related to the age of the thin-skinned deformation (Basei et al., 1997, Gaucher et al., 1998, Rostirolla et al., 1999).

4-7.2. The Central and Northern Segments of the Mantiqueira orogenic system

The tectonic evolution of the Central and Northern segments of the Mantiqueira orogenic system is related to the diachronous kinematics of oceanic plates convergence generating widespread magmatism. Collisions and dockage processes leading to the closure of the oceanic spaces between the major terranes controlled the geometry of this tectonic scenario. Thus the knowledge of the petrology and plutonic stratigraphy for the magmatic rocks (Söllner et al., 1987, Söllner et al., 1988, Offman and Weber-Diefenbach, 1989, Soares et al., 1990, Söllner et al., 1991, Janasi and Ulbrich, 1991, Figueiredo and Campos Neto, 1993, Wiedmann, 1993, Gimenez Filho et al., 1995, Machado et al., 1996, Wiedmann et al., 1997), and the knowledge about the structural framework (Heilbron et al., 1982, Campos Neto and Figueiredo, 1990, Machado and Demange, 1990, Pedrosa-Soares et al., 1992, Campos Neto and Figueiredo, 1995, Heilbron et al., 1998, Ebert and Hasui, 1998) were taken as the principal tools to unravel the tectonic history.

The Rio Negro subduction-controlled orogeny (ca. 0.63 Ga) was the first record of the Central Mantiqueira Orogenic system of an orogen related to a plutonic magmatic arc. It was accreted on the Serra do Mar terrane (Oriental Terrane for Tupinambá et al., 1998) as a batholithic complex of gabbro-diorite-tonalite from high-Ca and low-K calc-alkaline magma provenance, yielding a (ϵ_{Nd})_{0.6 Ga} of -0.9 (Tupinambá et al., 1998, Tupinambá, 1999). These rocks display a horizontal to NW gently dipping foliation related to a low-pressure, amphibolite facies metamorphism. The blockage of the subduction and docking of the Rio Negro orogen against the southeast portion of the Juiz de Fora terrane was admitted herein. The dockage process was laterally-controlled developing variable steep to low-angle dipping mylonitic foliation with NE-trending stretching and mineral lineation related to a main dextral displacement, leading to a local override of the Juiz de Fora terrane upon the magmatic arc (Heilbron et al., 1998, Tupinambá, 1999). This main tectonic edge ("the central tectonic boundary") was developed coeval with the generation of the post-arc metaluminous to peraluminous leucogranites (ca. 0.60 Ga). The oblique juxtaposition of the arc and the Juiz de Fora terrane released, further to the north, remnant of oceanic basin (see Fig. 4-18 below).

The Paranapiacaba orogen is related to a complex subduction and extensional tectonic setting that took place farther to the south attaining the domains of Apiaí and Curitiba terranes (Fig. 4-17). It was coeval or slightly younger than the Pelotas orogen. This orogenic scenario is pictured by huge and elongated batholiths corresponding to syn-orogenic intermediate to felsic metaluminous, high-K calc-alkaline granitic series. Hornblende-biotite porphyritic quartz monzonite and monzogranite prevails upon the fine-

to medium-grained, grey colored, biotite-bearing monzogranites. Tonalitic rocks are subordinated. They correspond to an evolved magmatism that reworked Paleoproterozoic lithospheric crust (Reis Neto, 1994, Harara et al., 1997). The Rio Pien Magmatic Arc southeastern facing the Curitiba terrane yields an age of about 0.615 Ga (Harara et al., 1997). It slightly preceded the 0.61 Ga age of the Agudos Grandes high-K calc-alkaline batholiths facing the southeast of Apiaí terrane. Inequi to equigranular muscovite-biotite granites with porphyritic facies normally wrap up the terminations of the calc-alkaline batholiths. They are 0.60-0.605 Ga and are followed by the younger, post-kinematic (0.565 Ga), porphyritic biotite syenogranite with an "A-type" chemical signature (Janasi et al., submitted). Farther to the interior of the Apiaí terrane the westernmost Três Córregos and Cunhaporanga batholiths (Fig. 4-4) are associated with high-temperature and low-pressure amphibolite facies metamorphism of the country rocks and detachment structures could be recognized. At this domain U-Pb zircon ages are still poorly constrained and the preliminary data display strong variable values suggesting roughly a westward age decreasing from 0.61 Ga up to 0.57 Ga for the calc-alkaline granites (Prazeres, personal communication). The metasedimentary sequences of São Roque Group that occur at the northwestern edge of the Apiaí terrane (Fig. 4-3) contain at their base bodies of metabasalts derived from sub-alkaline tholeiitic volcanism, locally displaying pillow-lava structures. The zircon U-Pb age for this submarine volcanic flow has the same value (0.61 Ga) of the magmatic arcs suggesting a narrow back-arc basin setting (Hackspacher et al., 1999). The collisions between the Luis Alves and the Curitiba terranes and between the Curitiba and the Apiaí terranes led to the closure of the São Roque back-arc basin amalgamating the continental fragments at the southeastern portion of the Rio de la Plata plate segment. At the Curitiba terrane the collision led to strong shortening by low-angle, east-southeastward transported ductile shear upon overall crust. It is associated with ca. 0.6 Ga (Siga Jr. et al., 1995) metamorphic slices that underwent greenschist to high-grade amphibolite, up to granulite metamorphic facies. Double vergence and contrasted tectonic regimes are admitted for the Apiaí terrane. A steep dextral strike-slip shear zone controlled the major geometry of the structures normally disguising an early flat-lying foliation. At their southeastern boundary the flat-lying foliation is roughly related to an eastward thrusting transport. Toward the hinterland the low-grade metamorphic shallow-dipping foliation is related to a northwest-direct transport (Campos Neto and Basei, 1983, Juliani, 1993). The central magmatic arc seems to be related to many hinterland and foreland driven detachments, the major ones bordering the batholiths and displaying a strong strike-slip component. An alternative tectonic scenario is also considered: a high-angle, west-dipping subduction zone under the Curitiba terrane gave way to an active continental margin setting (the Rio Pien Magmatic Arc). Toward the hinterland strong lithospheric extension might be related to the generation of the huge batholithic zone comprising the wide calc-alkaline plutons nearly coeval with peraluminous magma, both intrusive in older units from a passive continental margin setting. This lithospheric extension rises, on the plate interior, to rifting and break-up of the São Roque back-arc basin. For both tectonic scenarios the main collision-controlled orogen took place at 0.60 Ga and was followed by post-orogenic lithospheric extensional regimes around 570 Ma.

The main 0.60 Ga collision episode related to the Paranapiacaba and Rio Negro orogens were described elsewhere in the main magmatic arcs. It has been recorded in peraluminous monzogranites and migmatites from the southern Juiz de Fora (Embu Complex) and the southernmost termination of Serra do Mar terranes.

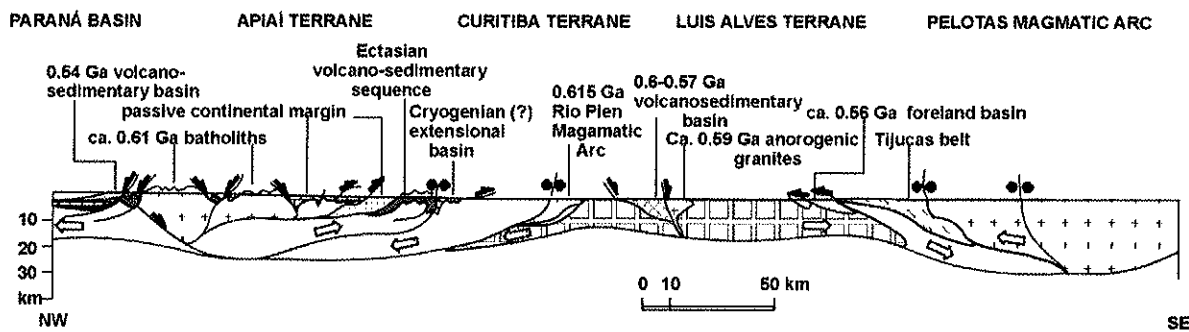


Figure 4-17: Profile through Apiaí and Curitiba Terranes.

To the north, this collisional amalgamation released an oceanic branch between the eastern São Francisco passive continental margin and the Juiz de Fora terrane (Fig. 4-18), which is by this time closed. The beginning of the *Araçuaí Orogeny* took place with the growing of the Galiléia Magmatic Arc in an active margin setting west-facing the Juiz de Fora terrane through east-dipping oceanic lithosphere subduction. The granitoids from Galiléia Batholiths (Nalini Jr. et al., 1998) show a relatively extensive compositional trend (tonalite-granodiorite-granite), containing amphibole and biotite as major mafic mineral phase, and grossular-rich garnet characterizing a deep crust (up to 10 kbar) magma crystallization. They have a zircon U-Pb age at 595 Ma (Nalini et al., 1998) and they were followed by semi-circular plutons of the peraluminous Urucum Suite comprising monazite, tourmaline, garnet and/or two micas granite types. The Urucum granites are thought to be a collision-type suite yielding an age of about 580 Ma (Nalini et al., 1998). The collisional development of the Araçuaí orogen (Pedrosa-Soares et al., 1998, Ulhein et al., 1998) is pictured by foreland-driven nappes depicting relatively high-pressure metamorphic rocks at the suture zone (kyanite-garnet-bearing schist). The cratonic edge was reached by the westward thrusting of the Espinhaço Range up to the thin-skinned behavior of the platform cover. Southward the Abre Campo discontinuity (Fischel et al., 1998) represented the suture boundary between the active margin of Juiz de Fora terrane and the western Archaean-derived thinned continental crust from passive margin domain (the Mantiqueira Gneiss). A ductile and oblique, dextral strike-slip shear zone delineates it.

The *Rio Doce Orogeny* developed early in the Serra do Mar terrane, renewed as a microplate after the complete consumption of the oceanic lithospheric plate segment at the eastern São Francisco passive continental margin domain. It resulted from the final convergence episodes leading to the closure of the Adamastor Ocean. Thus its record may be pursued, with variable intensity, overall in the Mantiqueira orogenic system. As a variance of Campos Neto and Figueiredo's (1995) tectonic scenario, a V-shape oceanic branch must have been released northwest of Serra do Mar terrane and the first record of its lithosphere resorption was the Rio Doce Magmatic Arc (Figueiredo and Campos Neto, 1993). This assumption could be let by the west-direct low-angle extrusion of the roots of the magmatic arc (Fig. 4-19A). Elsewhere, in the African side, the structural patterns of the West-Congolian belt (Trompette, 1994), and farther to the south, the oceanic nappe of the Marmora terrane (Frimmel et al., 1998), both displaying east-displacement toward the cratonic areas, are the converging diagnose for a west-dipping oceanic lithosphere subduction. This process has been constrained at 575 Ma in the Gariep and Damara belts (Frimmel et al., 1998). Based upon the chemical and compositional zonation of the main

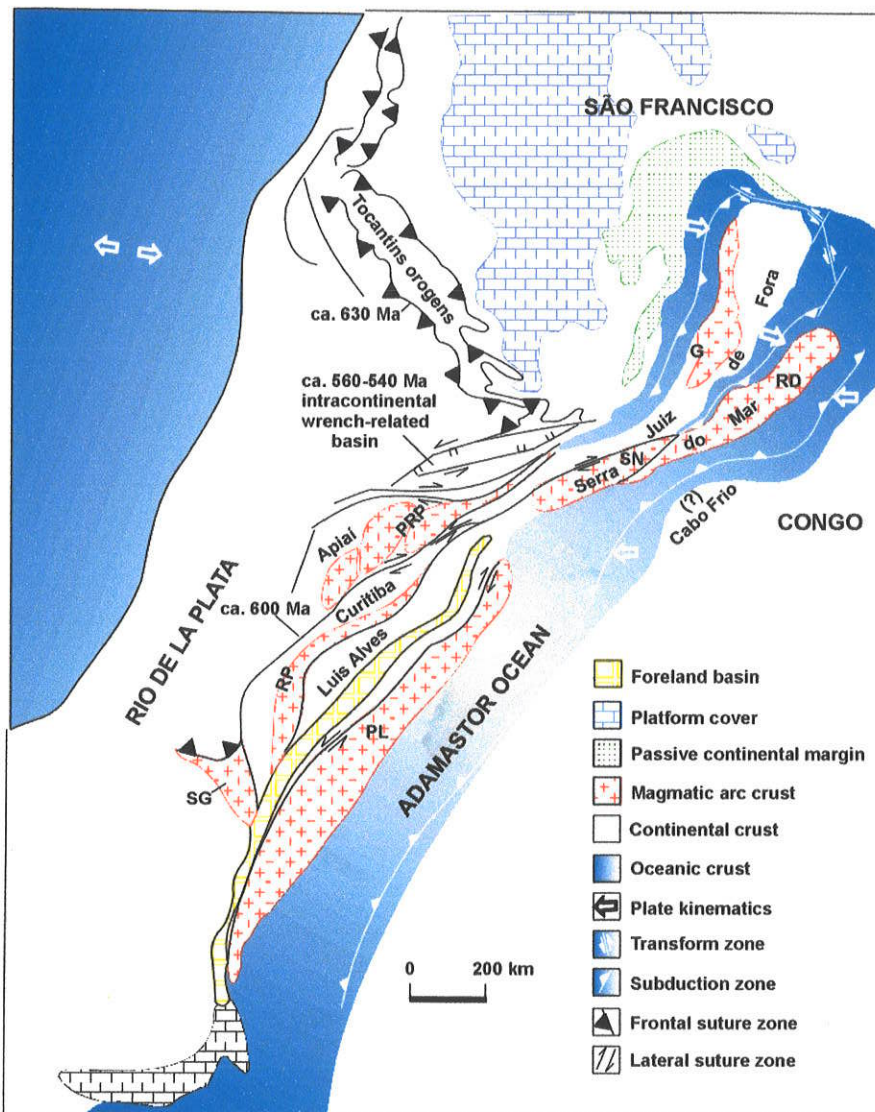


Figure 4-18: Vestiges of the lost Adamastor Ocean at ca. 590 Ma: paleogeographic sketch of oceanic plate interactions

plutonic rock types of the Rio Doce Magmatic Arc, Figueiredo and Campos Neto (1993) also admitted a west-dipping subduction-controlled regime. The steeping of the paleo-isotherms depicted by the close relations between the plutonic calc-alkaline rocks and peraluminous garnet, sillimanite and/or cordierite-bearing diatexites (Wiedemann et al., 1986, Rego, 1989, Campos Neto and Figueiredo, 1990, Fritzer, 1991, Campos Neto and Figueiredo, 1995) might be related to the asthenosphere upwelling below the arc ascribed by subduction at both sides of the northern Serra do Mar terrane. The calc-alkaline plutonic rocks of the arc comprise expanded suites of norite-enderbite-charnoenderbite and gabbro-diorite-tonalite-granodiorite forming elongated batholiths. They are mostly a low-K, high-Al calc-alkaline series, for both the western and the easternmost suites. More evolved K-rich tonalite and enderbite also occurs within a NE-oriented trend (Sluitner and Weber-Dienbach, 1989, Rego, 1989, Figueiredo and Campos Neto, 1993, Wiedemann et al., 1997). These gneissic batholiths have intrusive contacts into metasedimentary and

migmatitic sequences. At the deeper granulitic units they generally show diffuse boundaries with the country rocks, although containing xenoliths of peraluminous migmatites. The life span of this subduction-related plutono-metamorphic orogen is robustly constrained between 580-565 Ma (Söllner et al., 1987, Söllner et al., 1989, Söllner et al., 1991). To the south, the Rio Negro Magmatic Arc was being renewed by the tonalite-granodiorite-granite suite from Serra dos Órgãos batholith (Machado and Demange, 1994). It is a thick stratiform-shaped and high-Ca calc-alkaline massif displaying mostly magmatic flow foliation, and having an age of 560 Ma (Tupinambá, 1999).

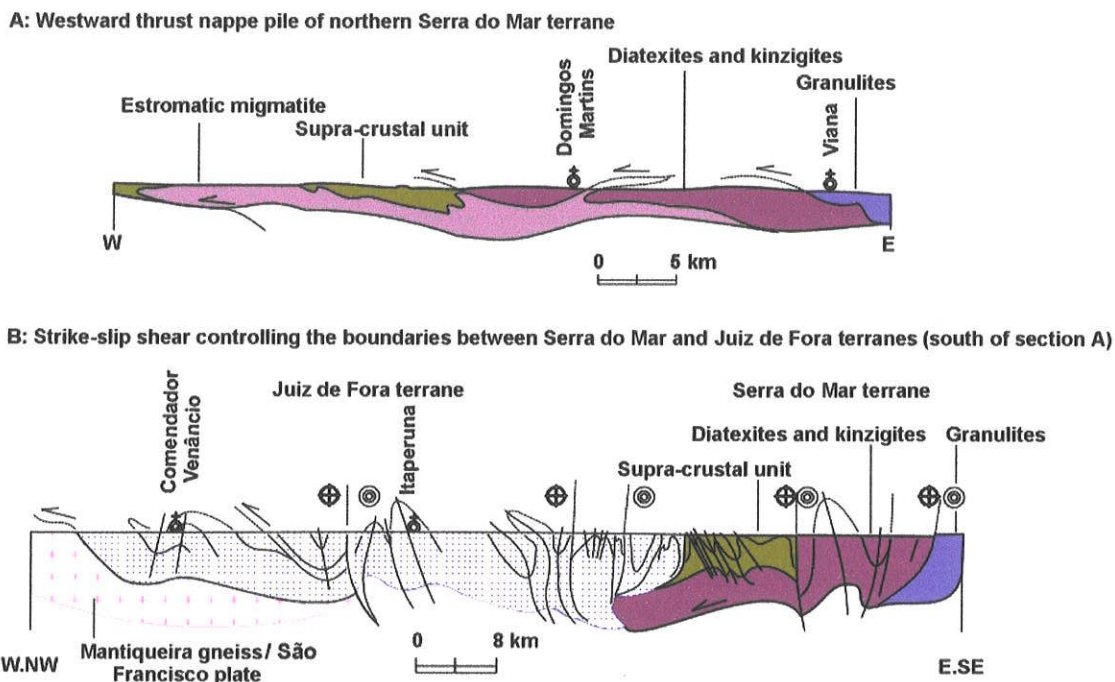


Figure 4-19: Cross-sections across Serra do Mar and Juiz de Fora terranes.

A widespread series of syn-kinematic peraluminous diatexites, and I-type granite and mangerite suites occur in the Serra do Mar terrane. They are related to the collision closure of the oceanic remnants. The apparently conflicting low-angle direction of displacement is found in the main rock package of the Serra do Mar terrane. To the north, a westward high-temperature ductile shearing was followed by thrusting and the building of an inverted crustal pile. Further to the south, east-verging structures are in agreement with the east-verging, near-isoclinal recumbent folds (Heilbron et al., 1982) and eastward-displaced low-angle ductile shear zones and thrusting at the Cabo Frio terrane (Machado and Demange, 1990). The Cabo Frio terrane resembles a small fragment of passive margin related to a southwestern promontory of the Congo plate.

However these structures record diachronic collision episodes.

The voluminous ultra-high metamorphic, crustal magma generation and its upper related migmatitic fingers took place coeval with the western overriding of the Serra do Mar terrane, mostly at its northern extension. They were related to the closure of the V-shaped oceanic remnant between Serra do Mar and Juiz de Fora landmasses. This collision episode is recorded in the Neoproterozoic III-Cambrian boundary (ca. 550-540 Ma) by

zircon and monazite U-Pb geochronology (Delhal et al., 1969, Söllner et al., 1989, Söllner et al., 1991). At the African counterpart the widespread foreland deposits of the Nama Group and the unconformable uppermost cover of the Fish River Group were the cratonic record of a collision tectonics at the same time (Frimmel et al., 1998).

Nevertheless the final closure of the Adamastor Ocean was later in the Cambrian times. The high-pressure metamorphic conditions depicted by the kyanite-bearing assemblages in high-temperature metasediments from Cabo Frio terrane are incompatible with the low-pressure, high-temperature rocks at its neighbor Rio Negro and Serra dos Órgãos superposed batholiths. These different metamorphic belts are related to an eastern displacement and apparently ascribing a northwestward continental subduction of the western promontory of the Congo plate under the Serra do Mar terrane. This collision-related metamorphism is recorded by monazite and zircon U-Pb geochronology at 520 Ma. (Schmitt et al., 1999).

Pb/Pb isotopic studies carried out on undeformed carbonate rocks from the Bambuí Group in the cratonic area evidenced an incorporation of Pb-fluid phase promoting isotopic resetting and severe remagnetization at about 530-500 Ma (Babinsky et al., 1999, Agrella Filho et al., 1999). These data ascribe the continent-scale record for the last Mantiqueira collision, although most of the suture lines must have been hidden by the Atlantic drift.

Thus, the estimated life span of the Adamastor Ocean is at least of ca. 230 Ma from the Middle Cryogenian to the Middle Cambrian (750-520 Ma). Their complex plates and microplates interaction make it compatible with the Cordilleran-type evolution.

4-7.2.1. Late-orogenic basins

A series of pull-apart basins occur at the northwestern suture boundary of the Mantiqueira Orogenic system, reaching the Tocantins orogens up to the northern edge of the extrusion-related strike-slip shear zones. The development of these basins evidence several pulses of shear zones displacements. After the high-temperature dextral motion (ca.575 Ma, Machado et al., 1996) of the shear zones, and the exhumation of the metamorphic belt, a main sinistral displacement took place developing the pull-apart basins at their releasing bends. The sedimentation was storm-dominated with alluvial fans reaching the asymmetrical basin border and grading to alluvial plain deposits up to distal lacustrine environment though seaward conection (Juliani et al., 1990, Teixeira, 1995). They were weakly deformed by dextral transpression and metamorphosed under very low grades during the Mid-Cambrian last collision.

4-7.2.2. Post-orogenic transition from compressive to extensional collapse

Mixing-mingling of mantle and crustal derived magmas strongly characterized the post-orogenic plutonic rocks accreted mainly in the Serra do Mar terrane. They are coeval to circular zoned plutons of monzogabbro-norites and diorites partially wrapped by granites that characteristically display a wide and discontinuous central commingling and mixing zone. More mature magmatic phases comprise diorite-tonalite and granodiorites surrounded by granites (Wiedmann et al., 1993). Allanite granite from the zoned Angelica pluton displays a zircon age at the Upper Cambrian (ca. 513 Ma, Söllner et al., 1987). This magmatic event could be connected with the maintenance of the high-thermal gradient inducing metamorphism up to Lower Ordovician times (Siga Jr., 1986, Wiedmann et al.,

1993, Schmitt et al., 1999, Machado et al., 1996) that followed the final ca. 520 Ma collision episode.

4-7.3. General framework: the Ribeira Belt

The Ribeira Belt describes the main geometric features produced by the complex and diachronic kinematics plates interaction at the northern Mantiqueira orogenic system (Fig. 4-20).

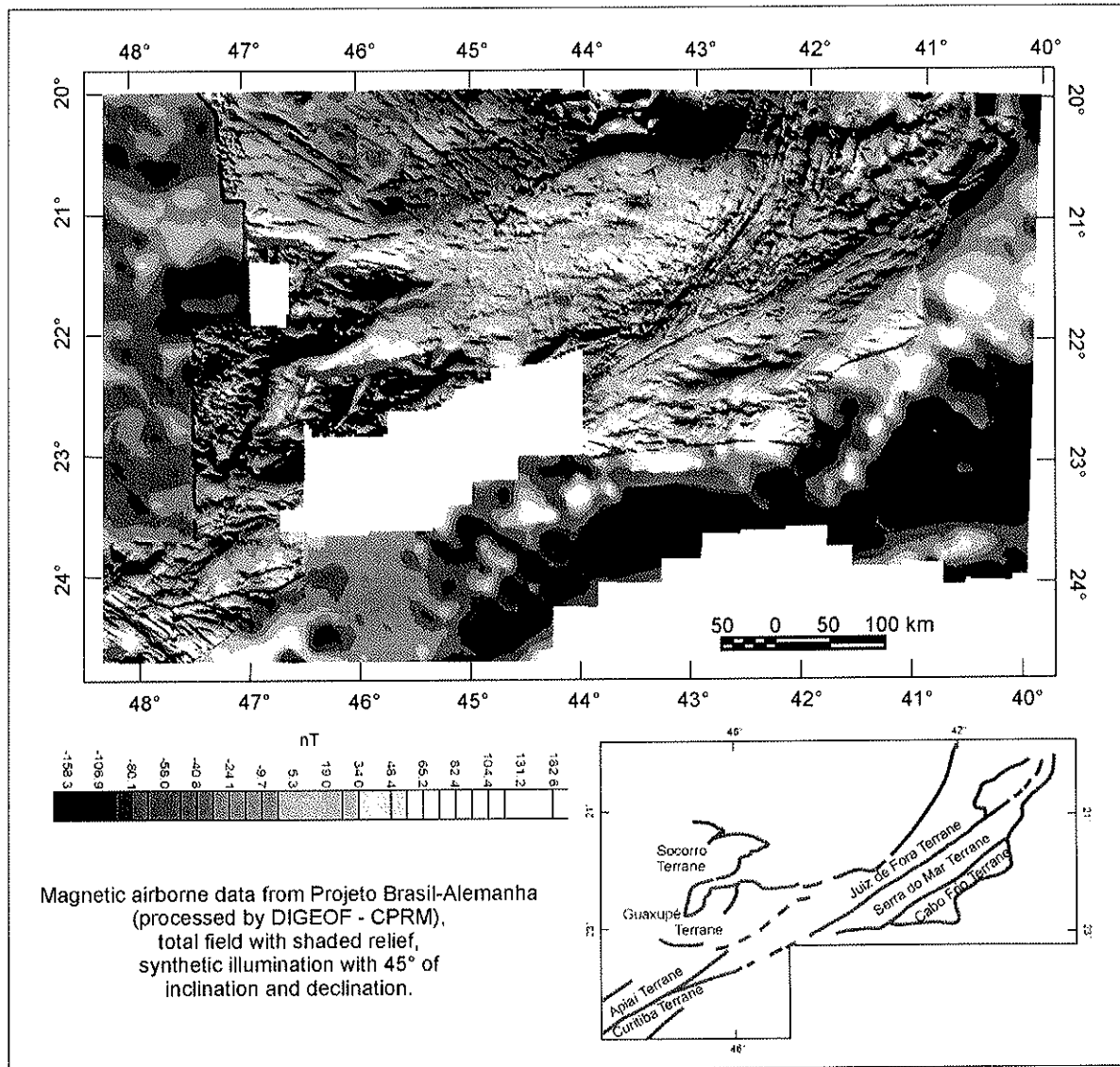


Figure 4-20: Aeromagnetic map from SE-Brazil. The NE-trending anomalies correspond to major shear-zones of the Ribeira belt.

The São Paulo Shear Belt (Hasui et al., 1984), up to 100 km wide, extends for 1000 km, delineating the boundaries between the terranes and normally overprinting low-angle metamorphic slices (Campos Neto and Figueiredo, 1995, Heilbron et al., 1995). The linear

belts of strong non-coaxial strain resulted from several pulses of mostly dextral strike-slip motion. They are a crust-scale shear-strain ascribed by an early high-temperature amphibolite to granulite facies metamorphism that decreases up to low greenschist facies toward the southwest. Most of the granites (Machado and Demange, 1998) display a shear zone-controlled emplacement. They are equigranular to porphyritic biotite-bearing metaluminous granites, and deeper garnet bearing coarse-grained to porphyritic granites associated with partial melting of the country rocks. They grade to shallow muscovite-bearing granites farther to the south, into the Embú Complex. Likewise the diachronous southeastward step up of the collision episodes, the granites related to the shear zones are older (590-565 Ma) in the Juiz de Fora terrane than the other ones emplaced in the Serra do Mar terrane (535-520 Ma). There the high-thermal gradient prevailed up to Lower Ordovician at 503-492 Ma (Ebert et al., 1996, Machado et al., 1996, Schmitt et al., 1999).

Toward the south the strike-slip shear zones display relict sinistral displacement. They are related to an amphibolite facies metamorphic condition at the northwestern of Apiaí terrane (Garcia and Campos Neto, 1997) contrasting with the low-grade mylonites from Lencinha shear zone at the southeastern edge of this terrane. Both shear zones were reprinted by later dextral displacement.

It results from dramatic episodes of lateral extrusion controlled by the kinematics of plate interaction related to the closure of the Adamastor Ocean acting against an oblique plate and microplates margins (Vauchez et al., 1994). The main west-oriented compression related to the northern Adamastor Ocean plate convergence explains the dextral vector of the shear zones. On the other hand the north-northeastern oriented compression related to the precedent southern closure of the oceanic branches results in a sinistral shear zone motion. The ca. 520 Ma-old westward collision controlled the locally intense dextral strike-slip overprint.

4-8. From Rodinia to Gondwana: SE-Brazil geodynamic evolution

Extensional regimes immediately followed the Grenvillian orogens in the Amazonas plate. They were also recorded in the São Francisco plate, and related to the Tonian-age taphrogeny (1.1-0.9 Ga), leading to the former break-up of Rodinia. A NW-elongated rift-valley dominates the western border of the São Francisco plate. A wide lower plate-type passive continental margin settlement is the record of the rift-drift evolution. These basin-forming tectonic processes were related to the Tonian taphrogeny and the opening of the Goianides Ocean. The spreading life of this ocean was early and locally replaced by intra-oceanic plate convergence triggering the Tocantins Orogenic system. A set of west-dipping subduction plates occurred diachronously generating island arcs, evolved magmatic arcs, and back-arc basins. The Rio de la Plata plate and Central Goiás terrane were driven against the western margin of the São Francisco plate. The early orogenies are recorded by the Mara Rosa Island Arc accretion (0.90-0.85 Ga) further docking over the western boundary of the Central Goiás terrane (0.80-0.77 Ga), promoting local metamorphism and relief. Farther to the south a back-arc spreading basin could have been nearly coeval with the Mara Rosa docking, separating two other magmatic arc built at the Middle Cryogenian: the eastern Anápolis-Andrelândia terrane, and the western active continental margin related to the Iporá-Jaupaci/Socorro-Guaxupé terranes. The supracrustal units of these magmatic arcs were preserved at the opposite termination of both terranes. The southernmost comprises the collisional-related low-angle slices of high-pressure subducted continental slab of the

Anápolis-Andrelândia terrane, suggesting an oblique west-southwest driven plate subduction. At this time, the Upper Cryogenian diamictites correlated with the Sturtian-age glacial deposits preceded the carbonate cap toward the São Francisco plate interior and overlaying, unconformable, the western passive continental margin. The east-northeastward displacement of the southernmost high-pressure nappes seems to be controlled by the back up extrusion at a critical state of the west-dipping lithosphere subduction from the western edge of the São Francisco plate. The magmatic, metamorphic and depositional records of this main collision-controlled orogeny, juxtaposing the Rio de la Plata and the São Francisco plates and closing the Goianides Ocean, can be found everywhere in the Tocantins orogens, robustly constrained at 0.63-0.62 Ga. South of this orogenic system, the outward propagation of the high-pressure nappe system (comprising Ky-granulites and eclogites) reaching 200-km of displacement, was subjected to strong thinning, and temperature decrease at each thrusted slice. The overriding of the high-temperature root of the Socorro-Guaxupé nappe controlled an inverted metamorphism related to a near-isobaric heating throughout the upper high-pressure nappe. The external passive continental margin sequences following roughly this nappe kinematics displayed a medium-pressure metamorphic pattern. They attained the platform setting as a stretched, flat-lying, spoon-like, metamorphic nappe. The post-orogenic relaxation, at the inner nappe, took place at 612 Ma. Thus, a long life span (Fig. 4-21) of oceanic plate convergence (ca. 270 Ma) and the rapid overriding-type collision episode (ca. 18 Ma) required to preserve the high-pressure metamorphic slices are the main characteristic of the Tocantins orogenic system, having as modern analogous the India-Asia collision.

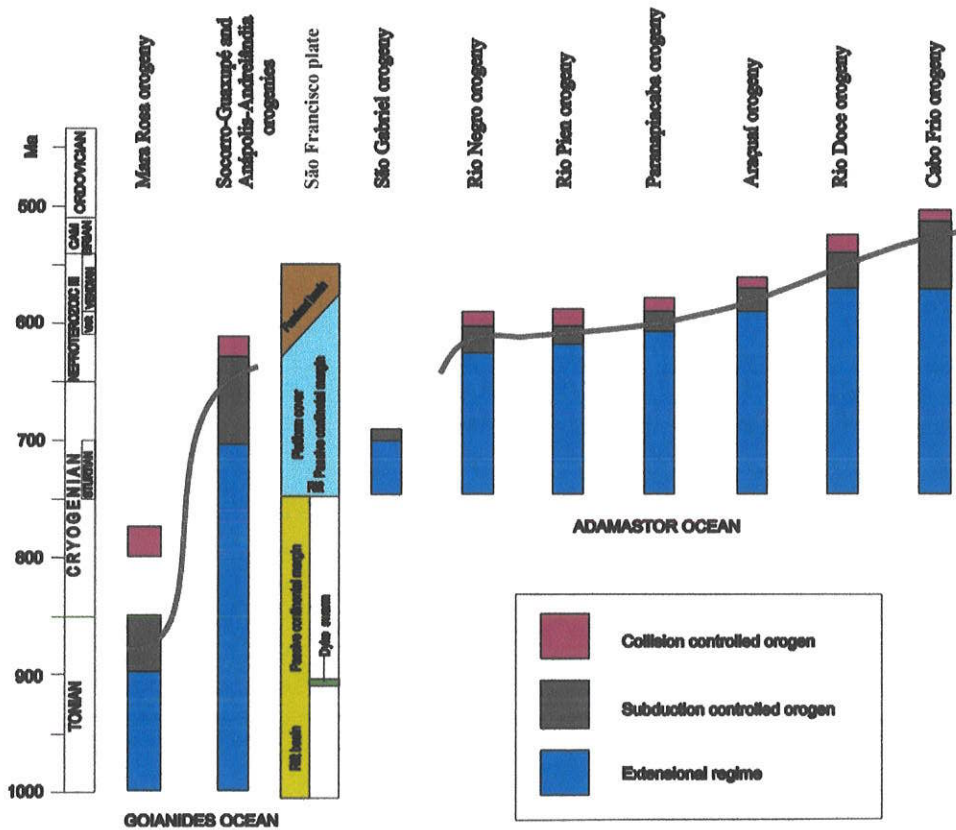


Figure 4-21: An attempt to a tectonic correlation table.

At the eastern margin of the São Francisco plate the Sturtian-age glacial deposits triggered the rift stage that evolved eastward to a deep marine basin connected with the Adamastor oceanic crusts. This extensional tectonic regime was coeval with the African counterpart rifting. Thus, the Mid-Cryogenian global break-up of Rodinia coexisted with the Tocantins orogenies. The diachronism of the succeeding orogenic processes was a key characteristic of the Mantiqueira orogenic system. It was wholly related to complex interaction between several small continental plate fragments mostly turned to microplates closing the Adamastor oceanic branches.

The first record of plate convergence occurred early and locally (?) south of the Brazilian counterpart of this oceanic context, as a juvenile island arc accretion at 0.70 Ga (the São Gabriel intra-oceanic subduction-controlled orogeny). Therefore the plate interaction kinematics with an apparent northwest motion caused the closure of the southern Adamastor Ocean. The southern Mantiqueira orogens, mainly associated with evolved magmatic arcs and high-temperature metamorphic conditions recorded Neoproterozoic III subduction-controlled orogenies decreasing in age toward the eastern Rio de la Plata boundary, up to the 0.61 Ga back-arc basin. The main collisional period that closed the southern oceanic branches between terranes and the just-amalgamated Rio de la Plata-São Francisco plate took place at 0.60 Ga. NE-oriented sinistral shearing accommodated the crustal shortening. A wide peripheral foreland basin, containing Vendian palinomorphs, reached deep sea conditions and was contemporaneous with felsite volcanic up to 0.56 Ga. Small succeeding volcanosedimentary basins associated with extensive alkaline-peralkaline plutonism occurs essentially within this time span, up to younger (0.54 Ga) elsewhere farther the plate interior.

The northern Mantiqueira orogens started with the plate convergence and docking between Juiz de Fora and Serra do Mar terranes (the Rio Negro orogen 0.63-0.61 Ga) advancing the east-dipping subduction of the eastern margin of the São Francisco plate. The Araçuaí orogen that started at 0.60 Ga was ascribed to be responsible for the inversion of this passive continental margin and the eastward continental growing related to the subduction-controlled Galiléia Magmatic Arc (northwest-facing the Juiz de Fora terrane) and their collision against the eastern São Francisco passive continental margin (0.58 Ga). The Serra do Mar terrane was overprinted by newly magmatic arc (0.58-0.565 Ga) further overriding the northeastern of the Araçuaí orogen (~0.54 Ga) ascribing, as a whole, the Rio Doce orogen in a continued continental growing. NE-oriented dextral shearing mostly accommodated the strong east-west shortening and crustal thickening. This orogeny seems to have been wide in the Mantiqueira system on account of their shortening propagation controlling the inversion of the NE-trending foreland basins. At the African counterpart the major episode of continent-continent collision and oceanic crust obduction was essentially contemporaneous. Nevertheless the final consumption of the oceanic lithosphere was related to the collision of the western promontory of the Congo plate (the Cabo Frio terrane) against the just-amalgamated eastern Brazil, at the Middle Cambrian (0.52 Ga). The post-kinematic magmatism proceeded up to the Ordovician boundary. Excluding the early São Gabriel juvenile orogenic accretion the main convergence life span of the Adamastor Ocean lasted for 100 Ma (Fig. 4-21). The continent growth by long-lived succession of orogens, related to arc-derived crust accretions and docking against an older

plate enhancing the analogies between Mantiqueira orogens and the Cordilleran-style tectonics Clowes et al. (1999).

REFERENCIAS BIBLIOGRÁFICAS

- Abalos, B., Azcarraga, J., Ibarguchi, J. I. G., Menda, M. S. and Zalduegui, J. F. S., 1996. Flow stress, strain rate and effective viscosity evaluation in a high-pressure metamorphic nappe (Cabo Ortegal, Spain). *Journal of Metamorphic Geology*, 14, 227-248.
- Agrella Filho, M.S., Trindade, R.I.F., Siqueira, R., Ponte Neto, C.F. and Pacca, I. I. G., 1998. Paleomagnetic constraints on the Rodinia Supercontinent: Implications for its Neoproterozoic break-up and the formation of Gondwana. *International Geology Review*, 40, 171-188.
- Agrella Filho, M.S., Babinski, M., Trindade, R.I.F., VanSchmus, W.R. and Ernesto, M., 1999. Simultaneous remagnetization and U-Pb isotope resetting in Neoproterozoic carbonates of the São Francisco craton, Brazil. *Precambrian Research*, in press.
- Alkmim, F.F., Brito Neves, B.B. and Alves, J.A.C., 1993. Arcabouço tectônico do Cráton do São Francisco – uma revisão. In J.M.L. Dominguez and A. Misi, eds: O CRÁTON DO SÃO FRANCISCO. SBG-Bahia/Sergipe, SGM, CNPq, 45-62.
- Alkmim, F.F. and Marshak, S., 1998. Transamazonian Orogeny in the Southern São Francisco Craton Region, Minas Gerais, Brazil: evidence for Paleoproterozoic collision and collapse in the Quadrilátero Ferrífero. *Precambrian Research*, 90, 29-58.
- Alkmim F. F. and Endo, I., 1998. An outline of the geology of the southern São Francisco craton region. In: 14th International Conference on Basement Tectonics, Post-Conference field trip, Ouro Preto, Brazil, 1-23.
- Almeida, F.F.M., Amaral, G., Cordani, U.G. and Kawashita, K., 1973. The Precambrian evolution of South American cratonic margin South of Amazonas River. In: The Oceans Basins and Margins (Nairn & Stelli, Eds.), I, Plenum: 411-446.
- Almeida, F.F.M., 1977. O cráton do São Francisco. *Revista Brasileira de Geociências*, 7: 349-364.
- Almeida, F.F.M., Hasui, Y., Brito Neves, B.B. & Fuck, R. A., 1981. Brazilian structural provinces: an introduction. *Earth Sciences Review*, 17, 1-29.
- Arenas, R., 1991. Opposite P, T, t paths of Hercynian metamorphism between the upper units of the Cabo Ortegal Complex and their substratum (northwest of the Iberian Massif). *Tectonophysics*, 191, 347-364.
- Arndt, N.T., Teixeira, N.A. and white, W.M., 1989. Bizarre geochemistry of komatiites from the Crixás greenstone belt, Brazil. *Contribution to Mineralogy and Petrology*, 101, 187-197.
- Attoh, K. 1998. High-pressure granulite facies metamorphism in the Pan-African Dahomeyide orogen, West Africa. *Journal of Geology*, 106, 236-246.
- introduction. *Earth Science Reviews*, 17: 1-29.
- Babinski, M., Chemale Jr, F., Hartmann, L.A., VanSchmus, W.R. and Silva, L.C., 1996. Juvenile accretion at 750-700 Ma in southern Brazil. *Geology*, 24, 439-442.
- Babinski, M., VanSchmus, W.R. and Chemale Jr., F., 1999. Pb-Pb dating and Pb isotope geochemistry of Neoproterozoic carbonate rocks from the São Francisco basin,

- Brazil: implications for the mobility of Pb isotopes during tectonism and metamorphism. *Chemical Geology*, 160, 175-199.
- Bahlburg, H. and Hervé, F., 1997. Geodynamic evolution and tectonostratigraphic terranes of the northwestern Argentina and northern Chile. *Geological Society of America Bulletin*, 109, 869-884.
- Barbosa, O., Braun, O.P.G., Dyer, R.C. and Cunha, C.A.B., 1970. Geologia da região do Triângulo Mineiro. DNPM-DFPM, Bul. 136, 0-140.
- Barbosa, P.A. and Jost, H., 1990. Caracterização das sequências supracrustais precambrianas a leste de Mossâmedes - GO. In: 36th Congresso Brasileiro de Geologia, 1, 1-16.
- Basei, M.A.S., 1985. O cinturão Dom Feliciano em Santa Catarina. Unpublished Thesis, Universidade de São Paulo, 190p.
- Basei, M.A.S., Siga Jr., O., Machiavelli, A., Mancini, F., Avelar, A.S. and Coelho Neto, A.L., 1992. Evolução tectônica dos terrenos entre os cinturões Ribeira e Dom Feliciano. *Revista Brasileira de Geociências*, 22, 216-221.
- Basei, M.A.S., Siga Jr., O., Sato, K. and Sproesser, W.M., 1995. A metodologia Urânia-Chumbo na USP, princípios metodológicos, aplicações e resultados obtidos. *Anais da Academia brasileira de Ciências*, 67, 221-237.
- Basei, M.A.S., Citroni, S.B.V. and Siga Jr., O., 1997. Stratigraphy and age of Fini-Proterozoic Basins of Paraná and Santa Catarina states, southern Brazil. In: A.J. Asmus, A.R. Rocha Campos and O.L. Gamundi, eds. *Sedimentary Basins of South America*, in press.
- Basei, M.A.S., Siga Jr., O., Reis Neto, J.M., Harara, O.M., Passarelli, C.R. and Machiavelli, A., 1997. Geochronological map of the Precambrian terrains of Paraná and Santa Catarina States, southern Brazil: Tectonic implications. *South-American Symposium on Isotope Geology, Extended Abstracts*, 44-46.
- Basei, M.A.S., McReath, I. and Siga Jr., O., 1998. The Santa Catarina granulite complex of southern Brazil: a review. *Gondwana Research*, 1, 383-392.
- Basei, M.A.S., Siga Jr., O., Sato, K. & Sproesser, W.M., 1995. A metodologia Uranio-Chumbo na USP. Princípios metodológicos, aplicações e resultados obtidos. *Anais da Academia brasileira de Ciências*, 67, 221-237.
- Bettencourt, J.S., Onstott, T.C., Jesus, T. and Teixeira, W., 1996. Tectonic interpretation of $^{40}\text{Ar}/^{39}\text{Ar}$ ages on country rocks from the central sector of the Rio Negro-Juruena Province, Southwest Amazonian craton. *International Geology Review*, 38, 42-56.
- Bettencourt, J.S., Tosdal, R.M., Leite, W.B. and Payolla Jr., B.L., 1999. Mesoproterozoic rapakivi granites of the Rondônia Tin Province, southwestern border of the Amazonian craton, Brazil -I. Reconnaissance U-Pb geochronology and regional implications. *Precambrian Research*, 95, 41-67.
- Bergmann, M., 1988. Caracterização estratigráfica e estrutural da sequência vulcanosedimentar do Grupo São Roque na região de Pirapora do Bom Jesus - Estado de São Paulo. Unpublished Thesis, IG-USP, 164p.
- Biino, G., 1994. The pre Late Ordovician metamorphic evolution of the Gotthard-Tavetsch massifs (Central Alps): from lawsonite to kyanite eclogites to granulite retrogression. *Schweiz. Mineral. Petrogr. Mitt.*, 74, 87-104.
- Blundy, J.D. & Holland, T.J.B., 1990. Calcic amphibole equilibria and a new amphibole-plagioclase geothermometer. *Contributions to Mineralogy and Petrology*, 104, 208-224.

- Bohlen, S.R., Wall, V.J. & Boettcher, A.L., 1983. Experimental investigations and geological applications of equilibria in the system FeO-TiO₂-Al₂O₃-SiO₂-H₂O. *American Mineralogist*, 68, 1049-1058.
- Bohlen, S.R. & Liotta, J.J., 1986. A barometer for garnet amphibolites and garnet granulites. *Journal of Petrology*, 27, 1025-1034.
- Brito Neves, B.B., Kawashita, K., Cordani, U.G. and Delhal, J., 1979. A evolução geocronológica da cordilheira do Espinhaço, dados novos e integração. *Revista Brasileira de Geociências*, 9, 71-85.
- Brito Neves, B.B. and Cordani, U.G., 1991. Tectonic evolution of South America during the Late Proterozoic. *Precambrian Research*, 53, 23-40.
- Brito Neves, B. B., Sá, J. M., Nilson, A. A. and Botelho, N. F., 1995. A tafrogênese Easteriana nos blocos paleoproterozoicos da América do Sul e processos subsequentes. *Geonomos*, 3, 1-21.
- Brito Neves, B.B., Campos Neto, M.C. and Fuck, R.A., 1999. From Rodinia to Western Gondwana: An approach to the Brasiliano-Pan African Cycle and orogenic collage. *Episodes*, 22, 155-166.
- Burchfiel, B. C., Chen, Z., Hodges, K. V., Liu, Y., Royden, L. H., Deng, C., and Xu, J.. The South Tibetan Detachment System, Himalayan orogen: Extension Contemporaneous With and Parallel to Shortening in a Collisional Mountain Belt, 41 pp., *Geol. Soc. of Am.*, Boulder, Colorado, 1992.
- Burg, J.P., Leyreloup, A., Girardeau, J. & Chen, G-M., 1987. Structure and metamorphism of a tectonically thickened continental crust: the Yalu Tsagpo suture zone-Tibet. *Phil. Trans. R. Soc. Lond.* 321, 67-86.
- Caby R., Pecher, A., and Lefort, P., 1983. Le grand chevauchement central himalayen: nouvelles données sur le métamorphisme inverse à la base de la Dalle du Tibet. *Rev. Géol. dyn. Géogr. Phys.*, 24, 89-100.
- Caby R., 1989. Precambrian terranes of Benin-Nigeria and northeast Brazil and the Late Proterozoic south Atlantic fit. *Geological Society of American Special Paper*, 230, 145-158.
- Caby, R., 1994. First record of Precambrian coesite from Northern Mali: implications for Late Proterozoic plate tectonics around the west African craton. *European Journal of Mineralogy*, 6: 235-244.
- Campanha, G.A.C. and Sadowski, G.R., 1999. Tectonics of the southern portion of the Ribeira Belt (Apiaí Domain). *Precambrian Research* (in press).
- Campos Neto, M.C., 1983. Contribuição à litoestratigrafia e estrutura do Grupo Açuengui no sudeste do Estado de São Paulo. In: 4th Simpósio Regional de Geologia, São Paulo, Atas, 103-112.
- Campos Neto, M.C. and Basei, M.A.S., 1983. Evolução estrutural brasileira do nordeste de São Paulo: dobramentos superpostos e esboço estratigráfico e tectônico. . In: 4th Simpósio Regional de Geologia, São Paulo, Atas, 61-78.
- Campos Neto, M.C., 1984a. Litoestratigrafia, relações estratigráficas e evolução paleogeográfica dos Grupos Canastra e Paranoá (região de Vazante-Lagamar, MG). *Revista Brasileira de Geociências*, 14, 81-91.
- Campos Neto, M. C., 1984b. Geometria e fases de dobramentos superpostos no oeste de Minas Gerais. *Revista Brasileira de Geociências*, 14, 60-68.

- Campos Neto, M.C., Figueiredo, M.C.H., Basei, M.A.S. & Alves, F.R., 1984. Os granitóides da região de Bragança Paulista, SP. In 33th. Congresso Brasileiro de Geologia, 6, 2854-2868.
- Campos Neto, M.C., Figueiredo, M.C.H., Janasi, V.A., Basei, M.A.S. & Fryer, B.J., 1988. The São José do Rio Pardo Mangeritic-Suite, southeastern Brazil. *Geochimica Brasiliensis*, 2, 185-199.
- Campos Neto, M.C., Perrotta, M.M., Peloggia, A.U. & Figueiredo, M.C.H., 1990. A porção ocidental da Faixa Alto Rio Grande (SP-MG). In 36th Congresso Brasileiro de Geologia, 6: 2615-2630.
- Campos Neto, M.C. & Figueiredo, M.C.H., 1995. The Rio Doce Orogeny, Southeastern Brazil. *Journal of South American Earth Sciences*, 8, 143-162.
- Campos Neto, M.C., Janasi, V.A. & Caby, R., 1996. Ocorrência de granulitos empobrecidos nas porções basais da Nappe de Empurro Socorro-Guaxupé. *Boletim do IG-USP*, 18: 11-14.
- Campos Neto, M.C. and Caby, R., 1999a. Neoproterozoic high-pressure metamorphism and tectonic constraint from the nappe system south of the São Francisco Craton, southeast Brazil. *Precambrian Research*, 97, 3-26.
- Campos Neto, M.C. and Caby, R., 1999b. Terrane accretion and upward extrusion of high-pressure granulites in the Neoproterozoic nappes of Southeast Brazil: Petrological and structural constraints. *Tectonics*
- Carswell, D. A. and O'Brien, P. J., 1993. Thermobarometry and geotectonic significance of high-pressure granulites: examples from the Moldanubian zone of the Bohemian massif in Lower Austria. *Journal of Petrology*, 34, 427-439.
- Castaing, C., Triboulet, C., Feybesse, J.L., Chèvremont, P., 1993. Tectonometamorphic evolution of Ghana, Togo and Benin in the light of the Pan-African-Brasiliano orogeny. *Tectonophysics*, 218, 323-342.
- Chemenda, A., Mattauer, M., and Bokun, A., 1995. A mechanism for syn-collisional rock exhumation and associated normal faulting: Results from physical modelling. *Earth Planet. Sci. Lett.*, 132, 225-232.
- Chemenda, A., Mattauer, M. and Bokun, A., 1996. Continental subduction and mechanism for exhumation of high-pressure rocks: new modelling and field data from Oman. *Earth Planet. Sci. Lett.*, 143, 172-182.
- Choudhuri, A., Schrank, A., Roig, H.L. & Szab, G.A.J., 1995. Negative Ce anomaly in mafic rocks of a possible Late Proterozoic ophiolite from SW Minas Gerais, Brazil. In: R. K. Srivastava & R. Chandra (eds.) *Magmatism in relation to diverse tectonic settings*. Oxford & IBH Publishing Co., 283-290.
- Cloud, P. and Dardenne, M.A., 1973. Proterozoic age of the Bambuí Group in Brazil. *Geological Society of America Bulletin*, 84, 1673-1676.
- Clowes, R., Cook, F., Hajnal, Z., Hall, J., Lewry, J., Lucas, S. and Wardle, R., 1999. Canada's LITHOPROBE Project (Collaborative, multidisciplinary geoscience research leads to new understanding of continental evolution). *Episodes*, 22, 3-20.
- Cordani, U. G., Brito Neves, B.B., Fuck, R.A., Porto, R., Thomaz Filho, A. and Cunha, F.M.B., 1984. Estudo preliminar de integração do Pré-Cambriano com os eventos tectônicos das bacias sedimentares brasileiras. *Ciência Técnica Petróleo*, 15: 10-70.
- Correia, C.T., Girardi, V.A.V., Lambert, D.D., Kinny, P.D. and Reeves, S.J., 1996. 2 Ga U-Pb (SHRIMP II) and Re-Os ages for the Niquelândia basic-ultrabasic layered

- intrusion, central Goiás, Brazil. In: 39th Congresso Brasileiro de Geologia, SBG, Extend Abstracts, 187-189.
- Correia, C.T., Jost, H., Tassinari, C.C.G., Girardi, V.A.V. and Kinny, P.D., 1999. Ectasian Mesoproterozoic U-Pb ages (SHRIMP II) for the metavolcano-sedimentary sequences of Juscelândia and Indaianópolis and for high grade metamorphosed rocks of Barro Alto stratiform igneous complex, Goiás State, Central Brazil. In: 2th South American Symposium on Isotope Geology, Extend Abstracts, 31-33.
- Daitx, E.C., 1996. Origem e evolução dos depósitos sulfetados tipo-Perau (Pb-Zn-Ag), com base nas jazidas Canoas e Perau (Vale do Ribeira, Pr). Unpublished Thesis, UNESP, 453p.
- Dalziel, I.W.D., 1997. Neoproterozoic-Paleozoic geography and tectonics: Review, hypothesis, environmental speculation. Geological Society of America Bulletin, 109, 16-42.
- Danni, J.C.M., Fuck, R.A. and Leonards, O.H., 1982. Archaean and lower Proterozoic units in Central Brazil. *Geol. Rundschau*, 71, 291-317.
- Dardenne, M.A., 1981. Os Grupos Paranoá e Bambuí na Faixa Brasília. In: Simpósio sobre o Cráton do São Francisco, Anais, 140-157.
- Debon, F. & Le Fort, P., 1983. A chemical mineralogical classification of common plutonic rocks and associations. *Trans. of the Royal Society of Edinburgh: Earth Sciences*, 73, 135-149.
- Delhal, J., Ledent, D. and Cordani, U.G., 1969. Ages Pb/U, Sr/Rb et Ar/K des formations métamorphiques et granitique du sudeste du Brésil (État de Rio de Janeiro et de Minas Gerais). *Annales de la Société Géologique Belgique*, 92, 271-283.
- Del Lama, E.A., Oliveira, M.A.F. & Zanardo, A., 1994. Geotermobarometria em rochas do Complexo Campos Gerais ao norte da zona de cisalhamento Varginha. *Revista Brasileira de Geociências*, 24: 233-239.
- Dominguez, J.M.L., 1993. As coberturas do cráton do São Francisco: uma abordagem do ponto de vista da análise de bacias. In: J.M.L. Dominguez and A. Misi editors. O CRÁTON DO SÃO FRANCISCO, SBG, SGM, CNPq, 137-159.
- Dossin, T.M., Dossin, I.A., Charvet, J., Pouclet, A. and Lapierre, H., 1993. Late Proterozoic mafic dykes swarm from the Espinhaço Range (Minas Gerais, Brazil): geochemistry and tectonic setting. In: 2th Simpósio sobre o cráton do São Francisco, Anais, 128-130.
- Duarte, B.P., Figueiredo, M.C.H., Campos Neto, M.C. and Heilbron, M., 1997. Geochemistry of granulite facies orthogneisses of the Juiz de Fora Complex, central segment of Ribeira Belt, SE Brazil. *Revista Brasileira de Geociências*, 27, 67-82.
- Ebert, H. Chemale, F. ; Babinski, M. ; Artur, A. .C.; Van Schmus, W. R. 1996. Tectonic setting and U-Pb zircon dating of the plutonic Socorro complex in the transpressive Rio Paraiba do Sul Shear Belt, SE Brazil. *Tectonics*, 15: 688-699.
- Ebert, H.D. and Hasui, Y., 1998. Transpressional tectonics and strain partitioning during oblique collision between three plates in the Precambrian of southeast Brazil. In: R.E. Holdsworth, R.E. Strachan and J.F. Dewey, eds. Continental Trasnpressional and Transtensional Tectonics. Geological Society, London, Special publications, 135, 231-252.

- Eckert, J.O., Newton, R.C. & Kleppa, O.J., 1991. The DH of reaction and recalibration of garnet-pyroxene-plagioclase-quartz geobarometers in the CMAS system by solution calorimetry. *American Mineralogist*, 76, 148-160.
- Ellis, D. J. and Green, E. H., 1979. An experimental study of the effect of Ca upon garnet-clinopyroxene Fe-Mg exchange equilibria. *Contribution to Mineralogy and Petrology*, 71, 13-22.
- Ernst, W. G., 1988. Tectonic history of subduction zones inferred from retrograde blueshist P-T paths. *Geology*, 16, 1081-1084.
- Fairchild, T.R., 1977. Conophyton and other columnar stromatolites from the Upper Precambrian Açuñgui Group near Itapeva, SP, Brazil. In: Ith Simpósio de Geologia Regional-SP, Atas, 179-198.
- Faria, A., 1995. Estratigrafia e sistemas deposicionais do Grupo Paranoá nas áreas de Cristalina, Distrito Federal e São João da Aliança-Alto Paraíso de Goiás. Unpublished Thesis, UnB, 199p.
- Fernandes, A.J., Campos Neto, M.C. and Figueiredo, M.C.H., 1990. O Complexo Embú no leste do Estado de São Paulo: limites e evolução geológica. In: 36th Congresso Brasileiro de Geologia, 6, 2755-2763.
- Fernandes, L.A.D., Menegat, R., Costa, A.F.U., Koester, E., Porcher, C.C., Tommasi, A., Kraemer, G., Ramgrab, G.E. and Camozzato, E., 1995. Evolução tectônica do cinturão Dom Feliciano no escudo Sul-Riograndense: Parte I – uma contribuição a partir do registro geológico. *Revista Brasileira de Geociências*, 25, 351-374.
- Fernandes, J.F., Iyer, S.S., Imakuma, K. & Chouhuri, A., 1987. Geochemical studies in the Proterozoic metamorphic terrane of the Guaxupé Massif, Minas Gerais, Brazil. A discussion on large ion lithophile element fractionation during high-grade metamorphism. *Precambrian Research*, 36, 65-79.
- Ferreira-Filho, C.F., Nilson, A. and Naldrett, A., 1992. The Niquelândia mafic-ultramafic complex, Goiás, Brazil: a contribution to the ophiolite X stratiform controversy based on new geological and structural data. *Precambrian Research*, 59, 125-142.
- Ferreira-Filho, C.F., Kamo, S.L., Fuck, R.A., Krogh, T.E. and Naldrett, A.J., 1994. Zircon and rutile U-Pb geochronology of the Niquelândia layered mafic and ultramafic intrusion, Brazil: constraints for the timing of magmatism and high grade metamorphism. *Precambrian Research*, 68, 241-255.
- Ferreira-Filho, C.F., Moraes, R., Fawcett, J.J. and Naldrett, A.J., 1998. Amphibolite to granulite progressive metamorphism in the Niquelândia Complex, central Brazil: regional tectonic implications. *Journal of South American Earth Science*, 11, 35-50.
- Ferry, J.M. & Spear, F.S., 1978. Experimental calibration of the partitioning of Fe and Mg between biotite and garnet. *Contributions to Mineralogy and Petrology*, 66, 113-117.
- Figueiredo, M.C.H. and Campos Neto, M.C., 1993. Geochemistry of the Rio Doce Magmatic Arc, Southeastern Brazil. *Anais da Academia brasileira de Ciências*, 63, 63-82.
- Figueiredo, M.C.H. and Teixeira, W., 1996. The Mantiqueira metamorphic complex, eastern Minas Gerais State: preliminary geochronological and geochemical results. *Anais da Academia brasileira de Ciências*, 68, 223-246.
- Fischel, D.P., Pimentel, M.M., Fuck, R.A., Costa, A.G., and Rosière, C.A., 1998. Geology and Sm-Nd isotopic data for the Mantiqueira and Juiz de Fora Complexes (Ribeira

- Belt) in the Abre Campo-manhuacú Region, Minas Gerais, Brazil. In: 14th International Conference on Basement Tectonics, Extend Abstracts, 21-23.
- Fischel, D.P., Pimentel, M.M., Fuck, R.A., 1999. Preliminary Sm-Nd isotopic study of the Anápolis-Itaçú Complex, Araxá Group and associated granite intrusions, Central Brazil: implications for the evolution of the Brasília Belt. In: 2th South American Symposium on Isotope Geology, Extend Abstracts, 302-305.
- Fonseca, M.A., 1996. Estilos estruturais e arcabouço tectônico do segmento setentrional da Faixa Brasília. Unpublished Thesis, UnB, 172p.
- Fragoso-César, A.R.S., 1980. O Cráton Rio de la Plata e o Cinturão Dom Feliciano no Escudo Uruguaio Sul-riograndense. In: 31th Congresso Brasileiro de Geologia, 5: 2879-2892.
- Fragoso-César, A.R.S., 1991. Tectônica de placas no ciclo Brasiliano: as orogenias dos cinturões Dom Feliciano e Ribeira no Rio Grande do Sul. IG-USP, unpublished Thesis: 1-367.
- Frascá, M.H.B.O., Figueiredo, M.C.H., Almeida, M.A. and Coutinho, J.M.V., 1990. Petrografia e geoquímica da Formação Água Clara - região de Araçáiba, SP. Boletim do Instituto de Geociências, USP, 21, 73-92.
- Frascá, M.H.B.O., Campanha, G.A.C., Figueiredo, M.C.H. and Sadowski, G.R., 1997. Geoquímica e ambiência tectônica de metabasitos do Alto e Médio Vale do Ribeira, São Paulo e Paraná. Revista Brasileira de Geociências, 27, 41-48.
- Frimmel, H. E., Almond, J. and Gesse, P.G., 1998. Gariep belt and Nama basin. In Excursion Guidebook, Gondwana-10, Department of Geological Sciences, University of Cape Town, 1-75.
- Fritzer, T., 1991. Das Guaçuí-linament und die orogene entwicklung des zentralen Ribeira-Belts. Münchener Geologie Hefte, 2, 1-195.
- Fuck, R.A., Brito Neves, B.B., Cordani, U.G. and Kawashita, K., 1989. Geocronologia Rb-Sr no Complexo Barro Alto, Goiás: evidência de metamorfismo de alto grau e colisão continental há 1300 Ma no Brasil central. Geochimica Brasilienses, 3, 125-140.
- Fuck, R.A., Sá, E.F.J., Pimentel, M.M., Dardenne, M.A. and Soares, A.C.P., 1993. As faixas de dobramentos marginais do cráton do São Francisco: síntese dos conhecimentos. In: J.M.L. Dominguez and A. Misi eds. O Cráton do São Francisco, SBG-Ba/Se, SGM,CNPq, 161-185.
- Fuck, R.A.; Pimentel, M.M. & Silva, L.J.H.D., 1994. Compartimentação tectônica da porção oriental da Província Tocantins. In 38th Congresso Brasileiro de Geologia, 1, 215-216.
- Fugi, M.Y., 1989. REE geochemistry and Sm-Nd geochronology of the Cana Brava Complex, Brazil. Master Thesis, Kobe University, Japan, 55pp.
- Garcia, M.G.M. and Campos Neto, M.C., 1997. Superposição destral em ampla zona de cisalhamento sinistral: cinturão de cisalhamento São Paulo, imediações de Piracaia-SP. Revista Brasileira de Geociências, 27: 339-348.
- Gaucher, C., Sprechmann, P. and Montaña, J., 1998. New advances in the geology and paleontology of the Vendian to Cambrian Arroyo del Soldado Group of the Nico Pérez terrane of Uruguay. N. Jb. Geol. Paläont. Mh., 3, in press.
- Gimenez Filho, A., Teixeira, W., Figueiredo, M.C.H. and Trevizoli Jr., L., 1995. Geologia, petrografia e litogegeoquímica do complexo granítico Três Córregos na região de

- Barra do Chapéu e Ribeirão Branco, SP. Revista Brasileira de Geociências, 25, 92-106.
- Girardi, V.A., Rivalente, G. and Sinigoi, S., 1986. The petrogenesis of the Niquelândia layered basic-ultrabasic complex, central Goiás, Brazil. Journal of Petrology, 27, 715-744.
- Graham, C.M. & Powell, R., 1984. A garnet-hornblende geothermometer: calibration, testing and application to the Pelona Schist, Southern California. Journal of Metamorphic Geology, 2, 13-31.
- Green, T. H. & Hellman, P. L., 1982. Fe-Mg partitioning between coexisting garnet and phengite at high pressure, and comments on garnet-phengite geothermometer. Lithos, 15, 253-266.
- Guillot, S., Sigoyer, J., Lardeaux, J. M. and Mascle, G., 1997. Eclogitic metasediments from the Tso Morari area (Ladakh, Himalaya): evidence for continental subduction during India-Asia convergence. Contribution to Mineralogy and Petrology, 128, 197-212.
- Hackspacher, P., Dantas, E.L., Godoy, A.M., oliveira, M.A.F., Fetter, A. and VanSchmus, W.R., 1999. Considerations about the evolution of the Ribeira Belt in the São Paulo state, Brazil, from U-Pb geochronology in metavolcanic rocks of the São Roque Group. 2th South American Symposium on Isotope Geology, Extend Abstracts, 310-313.
- Haddad, R.C., 1995. O batolito Pinhal-Ipuiuna (SP-MG): um exemplo do magmatismo calcio-alcalino-potassico neoproterozóico no sudeste brasileiro. IG-USP, 270 p, unpublished thesis.
- Hammarstron, J. M. and Zen, E., 1986. Aluminium in hornblende: an empirical igneous geobarometre. American Mineralogist, 71, 1297-1313.
- Hanmer, S. and Passchier, C., 1991. Shear-sense indicators: a review. Geological Survey of Canada, paper 90-17, 1-72.
- Harara, O.M., Basei, M.A.S. and Siga Jr., O., 1997. Geochronoloical and geochemical data on the trasition zone betwee Luis Alves and Atuba Complexes, south Brazil. In: South-American Symposium on Isotope Geology, Extended Abstracts, 134-136.
- Harley, S.L., 1984. An experimental study of the partitioning of the Fe and Mg between garnet and orthopyroxene. Contributions to Mineralogy and Petrology, 86, 359-373.
- Hartnady, C.J.H., Joubert, P. and Stowe, C.W., 1985. Proterozoic crustal evolution in southwestern Africa. Episodes, 8, 236-244.
- Hasui, Y., 1982. The Mantiqueira Province: Archaean strucutre and Proterozoic evolution. Revista Brasileira de Geociências, 12: 167-172.
- Heilbron, M., 1985. O metamorfismo da área de Itutinga-Madre de Deus de Minas - MG. In: 3 th Simpósio de Geologia de Minas Gerais, Belo Horizonte, Anais: 219-233.
- Heilbron, M., Chrispim, S.J., Alves, N.P. and Simões, L.S.A., 1982. Geologia do Cabo dos Búzios (Estado do Rio de Janeiro). Anais da Academia brasileira de Ciências, 54: 553-562.
- Heilbron, M., Valeriano, C., Valladares, C.S. and Machado, N., 1995. A orogênese brasiliiana no segmento central da Faixa Ribeira, Brasil. Revista Brasileira de Geociências, 25, 249-265.
- Heilbron, M., Tupinambá, M., Almeida, J.C.H., Valeriano, C.M., Valladares, C.S. and Duarte, B.P., 1998. New constraints on the tectonic organisation and structural

- styles related to the Brasiliano collage of the Central segment of the Ribeira Belt, SE Brazil. In: 14th International Conference on Basement Tectonics, Extend Abstracts, 15-17.
- Hodges, K.V. & Spear, F.S., 1982. Geothermometry, geobarometry and the Al₂SiO₅ triple point at Mt. Moosilauke, New Hampshire. *American Mineralogist*, 67, 1118-1134.
- Hodges, K.V., Parrish, R.R. & Searle, M.P., 1996. Tectonic evolution of central Annapurna Range, Nepalese Himalayas. *Tectonics*, 15, 1264-1291.
- Hoffman, P.F., Kaufman, A.J., Halverson, G.P. and Schrag, D.P., 1998. A Neoproterozoic Snowball Earth. *Science*, 281, 1342-1346.
- Hollister, L. S., Grissom, G. C., Peters, E. K., Stowell, H. H. and Sisson, B., 1987. Confirmation of the empirical correlation of Al in hornblende with pressure solidification of calc-alkaline plutons. *American Mineralogist*, 72, 231-239.
- Hubbard, M.S., 1989. Thermobarometric constraints on the thermal history of the Main Central Thrust Zone and Tibetan Slab, eastern Nepal, Himalaya. *Journal of Metamorphic Geology*, 7, 19-30.
- Ibarguchi, J. I. G., Mendia, M., Girardeau, J. and Peucat, J. J., 1990. Petrology of eclogites and clinopyroxenite-garnet metabasites from Cabo Ortegal Complex (northwest Spain). *Lithos*, 25, 133-162.
- Indares, A. & Martignole, J., 1985. Biotite-garnet in the granulite facies: the influence of the Ti and Al in biotite. *American Mineralogist*, 70, 272-278.
- Iyer, S.S., Choudhuri, A., Pattison, D.R.M. & De Paoli, G.R., 1996. Petrology and geochemistry of the Neoproterozoic Guaxupé granulite facies terrain, SE Brazil. *Precambrian Research*, 77: 23-40.
- James, D.E. and Assumpção, M., 1996. Tectonic implications of S-wave anisotropy beneath SE Brazil. *Geophys. J. Int.*, 126, 1-10.
- Janasi, V. A., 1997. Neoproterozoic mangerite-granite magmatism in southeastern Brazil: the São Pedro de Caldas massif. *Anais da Academia Brasileira de Ciências*, 69, 267-234.
- Janasi, V.A., 1999. Petrogênese de granitos crustais na Nappe de Empurrão Socorro-Guaxupé (SP-MG): uma contribuição da geoquímica elemental e isotópica. Unpublished Thesis, IG-USP, 1-304.
- Janasi, V.A. and Ulbrich, H.G.J., 1991. Late Proterozoic grnitoid magmatism in the state of São Paulo, southeastern Brazil. *Precambrian Research*, 51, 351-374.
- Janasi, V.A., Vlach, S.R.F. and Ulbrich, H.H.G.J., 1993. Enriched-mantle contributions to the Itú Granitoid Belt, Southeastern Brazil: evidence from K-rich diorites and syenites. *Anais da Academia brasileira de Ciências*, 65, 107-118.
- Janasi, V.A. & Vlach, S.R.F., 1997. Sr and Nd isotope systematics of the Capituva and Pedra Branca syenitic massifs (SW Minas Gerais, Brazil): petrogenesis and inference on Neoproterozoic lithospheric mantle reservoirs. In South-American Symposium on Isotopic Geology, Extend Abstracts, 143-146.
- Janasi, V.A., Haddad, R.C. & Vlach, S.R.F., 1997. Comments on the Sm-Nd isotopic systematics of calc-alkaline granitoids from the Pinhal-Ipuoca batholith (São Paulo and Minas Gerais, Brazil). In South-American Symposium on Isotope Geology, Extend Abstracts, 147-150.
- Janasi, V.A., Leite, R.J. and VanSchmus, W.R., (submitted). U-Pb ages and stratigraphy of the granitic magmatism in the Agudos Grandes Batholith (W of São Paulo, Brazil): Implications for the evolution of the Ribeira Belt.

- Jost, H., Theodoro, S.M.C.H., Figueiredo, A.M. G. and Boaventura, G.R., 1996. Propriedades geoquímicas e proveniência de rochas metassedimentares detriticas arqueanas dos greenstone belts de Crixás e Guarinos, Goiás. Revista Brasileira de Geociências, 26, 151-166.
- Juliani, C., 1993. Geologia, petrogênese e aspectos metalogenéticos dos grupos Serra do Itaberaba e São Roque na região das serras do Itaberaba e da Pedra Branca, NE da cidade de São Paulo. Unpublished thesis, IG-USP, 803p.
- Juliani, C. and Beljavskis, P., 1995. Revisão da litoestratigrafia da faixa São Roque/Serra do Itaberaba (SP). Revista do Instituto Geológico, 16, 33-58.
- Juliani, C., Pérez-Aguilar, A., Martin, M.A.B. and Beljavskis, P., 1996. Ocorrência e petrografia dos metarriólitos da Formação Nhanguçu - Grupo Serra do Itaberaba (SP). Revista Brasileira de Geociências, 26, 113-116.
- Junho, M. C. B., Dehler, N. M., Xavier, E. M. and Capuano, C. S., 1992. Geologia preliminar da região entre Aiuruoca e Alagoa, sul de MG. In: Revista da Escola de Minas de Ouro Preto, 45, 146-147.
- Kennedy, M. J., Runnegar, B., Prave, A.R., Hoffmann, K.H. and Arthur, M.A., 1998. Two or four Neoproterozoic glaciations. Geology, 26, 1059-1063.
- Kohn, M. J. and Spear, F. S., 1990. Two new barometers for garnet amphibolites with applications to southeastern Vermont. Amer. Mineral. 75, 89-96.
- Koziol, A.M. & Newton, R.C., 1988. Redetermination of the anorthite breakdown reaction and improvement of the plagioclase-garnet-Al₂SiO₅-quartz geobarometer. American Mineralogist, 73, 216-223.
- Kretz, R., 1983. Symbols for rock-forming minerals. American Mineralogist, 68, 277-279.
- Le Fort, P., Pécher, A. & Upreti, B.N., 1986. A section through the Tibetan slab in central Nepal (Kali Gandaki valley): mineral chemistry and termobarometry of the Main Central Thrust zone. Sciences de la Terre, Nancy, 47, 211-228.
- Le Fort, P., Guillot, S. and Pécher, A., 1997. HP metamorphic belt along the Indus suture zone of NW Himalaya: new discoveries and significance. Compte Rendu Academie Sciences Paris, 325, 773-778.
- Lister, G.S., Etheridge, M.A. and Symonds, P.A., 1986. Detachment faulting and the evolution of passive continental margins. Geology, 14, 246-250.
- Liu, Y. and Zhong, D., 1997. Petrology of high-pressure granulites from the eastern Himalayan syntaxis. Journal of metamorphic Geology, 15, 451-466.
- MacFarlane, A. M., 1995. An evaluation of the inverted metamorphic gradient at Langtang National Park, Central Nepal, Himalaya. Journal of metamorphic Geology, 13, 595-612.
- Machado, N., Schrank, A., Abreu, F.R. Knauer, L.G. and Abreu, P.A.A., 1989. Resultados preliminares da geocronologia U-Pb na Serra do Espinhaço Meridional. In: 5th Simpósio de Geologia de Minas Gerais, Anais, 171-174.
- Machado, N., Valladares, C. Heilbron, M. and Valeriano, C., 1996. U-Pb geochronology of the central Ribeira Belt (Brazil) and implications for the evolution of the Brazilian Orogeny. Precambrian Research, 79, 347-361.
- Machado, R. and Demange, M., 1990. Reinterpretação estrutural e tectônica da região a leste da baía da Guanabara e a definição do batolito de Araruama (RJ). In: 36th Congresso Brasileiro de Geologia, 6, 2744-2754.

- Machado, R. and Demange, M., 1994. Classificação estrutural e tectônica dos granitóides neoproterozóicos do Cinturão Paraíba do Sul no Estado do Rio de Janeiro. Boletim do Instituto de Geociências, Universidade de São Paulo, Série Científica 25, 81-96.
- Machado, R. and Demange, M., 1998. Caracterização geoquímica e tectônica dos granitóides pré-colisionais Neoproterozóicos do cinturão Paraíba do Sul no Estado do Rio de Janeiro. In: H. Conceição edt. Contribuição ao Estudo dos Granitos e Rochas Correlatas. Sociedade Brasileira de Geologia, Núcleo Bahia-Sergipe, Publicação Especial 5, 21-38.
- Mantovani, M.S.M. and Shukowsky, W., 1996. Geofísica da litosfera (GEOLIT). Instituto Astronômico e Geofísico, USP, Atividades de Pesquisa, 99-102.
- Marangoni, Y.R., 1994. Modelo crustal para o norte de Goiás a partir de dados gravimétricos. Unpublished Thesis, IAG-USP, 105 p.
- Marini, O.J., Fuck, R.A., Danni, J.C.M., Dardenne, M.A. Loguerio, S.O.C. and Ramalho, R., 1984. As faixas de dobramentos Brasília, Uruaçu e Paraguai-Araguaia e o maciço mediano de Goiás. In: C. Schobbenhaus, D.A. Campos, G.R. Derze and H.E. Asmus eds. GEOLOGIA DO BRASIL, Texto explicativo do mapa geológico do Brasil e da área oceânica adjacente incluindo depósitos minerais. Escala 1:2 500 000. MME/DNPM, 251-303.
- Marshak, S. and Alkmim, F.F., 1989. Proterozoic contraction/extension tectonics of the southern São Francisco region, Minas Gerais, Brazil. Tectonics, 8, 555-571.
- Martins-Neto, M.A., 1998. O Supergrupo Espinhaço em Minas Gerais: registro de uma bacia rifte-sag do Paleo/Mesoproterozóico. Revista Brasileira de Geociências, 28, 151-168.
- Matte, P., 1998. Continental subduction and exhumation of HP rocks in Paleozoic orogenic belts: Uralides and Variscides. G. F. F. , 120, 209-222.
- Matte, P., Mattauer, M., Olivet, J. M. and Griot, D. A., 1997. Continental subductions beneath Tibet and the Himalayan orogeny: a review. Terra Nova, 9, 264-270.
- McLennan, S.M., Taylor, S.R., McCulloch, M.T. & Maynard, J.B., 1990. Geochemical and Nd-Sr isotopic composition of deep-sea turbidites: Crustal evolution and plate tectonic associations. *Geochimica et Cosmochimica Acta*, 54, 2015-2050.
- Meyre, C., Capitani, C. and Partzsch, J. H., 1997. A ternary solid solution model for omphacite and its application to geothermobarometry of eclogites from the Middle Adula nappe (Central Alps, Switzerland). *Journal of metamorphic Geology*, 15, 687-700.
- Moraes, R. and Fuck, R.A., 1994. Deformação e metamorfismo das seqüências Juscelândia e Serra da Malacacheta, complexo Barro Alto, Goiás. Revista Brasileira de Geociências, 24, 189-197.
- Moraes, R., Fuck, R.A. and Figueiredo, A.M., 1998. Litogegeoquímica das rochas da Seqüência Jucelândia: evidência de rifte continental Mesoproterozóico em Goiás. In: 40th Congresso Brasileiro de Geologia, Anais, 35.
- Nalini Jr., H.A., Bilal, E. and Correia Neves, J.M., 1998. Mineralogical, geochemical and isotopic constraints of Neoproterozoic Granitoids (Urucum and Galiléia suites) Eastern Minas Gerais State, Brazil. In: 14th International conference on Basement Tectonics, Extend Abstracts, 44-46.

- Newton, R.C. & Haselton, H.T., 1981. Thermodynamics of the garnet-plagioclase-Al₂SiO₅-quartz geobarometer. In: Newton, R. C., Navrotsky, A. & Wood, B.J., eds. *Thermodynamics of minerals and melts*. Springer, 129-145.
- Neogi, S., Dasgupta, S. & Fukuoka, M., 1998. High P-T polymetamorphism, dehydration melting, and generation of migmatites and granites in the Higher Hymalayan Crystalline Complex, Sikkim, India. *Journal of Petrology*, 39, 61-99.
- Oberhänsli, R., Goffé, B. and Bousquet, R., 1995. Record of a HP-LT metamorphic evolution in the Valais zone: Geodynamic implications. In: B. Lombardo (Editor), *Studies on metamorphic rocks and minerals of the western Alps*. Boll. Museo Regionale Scienze Naturali, Torino, 13, 221-239.
- Offman, R.A. and Weber-Diefenbach, K., 1989. Two zoned complexes in the Icôna region, Espírito Santo, Brazil: A geochemical characterization of an intrusive series. *Zentralblatt für Geologie und Paläontologie*, I, 903-916.
- Oliveira, M.A.F. & Ruberti, E., 1979. Granada-cordierita gnaisses do Complexo Granulítico-Migmatítico de São José do Rio Pardo, Caconde, SP: indicações sobre pressão e temperatura de formação. *Boletim Mineralógico*, 6: 15-29.
- Paciullo, F.V.P., Ribeiro, A., Andreis, R.R. & Trouw, R.A.J., 1998. Sedimentary, igneous and thermo-tectonic events in the folded belts at the southern border of the São Francisco craton, Minas Gerais state, Brazil. In 14th International Conference on Basement Tectonics, Ouro Preto, Brazil, Abstracts, 66-68.
- Paciullo, F.V.P., 1997. A Sequência Depositional Andrelândia. UFRJ, 265p, unpublished thesis.
- Park, J.K., 1994. Paleomagnetic constraints on the position of Laurentia from Middle Neoproterozoic to Early Cambrian times. *Precambrian Research*, 95-112.
- Peacock, M. S., 1992. Blueschist facies metamorphism, shear heating, and P-T-t paths in subduction shear zones. *Journal Geophysical Research*, 97, 17693-17707.
- Pedrosa-Soares, A.C., Noce, C.M., Vidal, P., Monteiro, R.L.B.P. and Leonardos, O.H., 1992. Toward a new tectonic model for the late Proterozoic Araçuaí (SE Brazil)-West Congolian (SW Africa) belt. *Journal of South American Earth Sciences*, 6, 33-47.
- Pedrosa-Soares, A.C., Vidal, P., Leonardos, O.H. and Brito Neves, B.B., 1998. Neoproterozoic oceanic remnants in eastern Brazil: Further evidence and refutation of an exclusively ensialic evolution for the Araçuaí-West Congo orogen. *Geology*, 26, 519-522.
- Piekarz, G.F., 1981. Reconhecimento de unidades correlacionáveis à sequência mineralizada do Peraú, Estado do Paraná. In: 3th Simpósio Regional de Geologia, Curitiba, 1, 148-154.
- Pimentel, M.M., Heaman, L., Fuck, R.A. and Marini, O.J., 1991. U-Pb zircon geochronology of Precambrian tin-bearing continental-type acid magmatism in central Brazil. *Precambrian Research*, 52, 321-335.
- Pimentel, M.M., Herman, L. & Fuck, R.A., 1991. Zircon and sphene U-Pb geochronology of Upper Proterozoic volcanic-arc rock units from southwestern Goias, central Brazil. *Journal of South American Earth Sciences*, 4, 295-305.
- Pimentel, M.M. and Fuck, R.A., 1992a. Neoproterozoic crustal accretion in central Brazil. *Geology*, 20, 375-379.

- Pimentel, M.M., Heaman, L. and Fuck, R.A., 1992b. Idade do meta-riolito da Seqüência Maratá, Grupo Araxá, Goiás: estudo geocronológico pelos métodos U-Pb em zircão, Rb-Sr e Sm-Nd. Anais da Academia brasileira de Ciências, 64, 19-28.
- Pimentel, M.M., Fuck, R.A. and Silva, L.J.H.D.R, 1996a. Dados Rb-Sr e Sm-Nd da região de Jussara-Goiás-Mossâmedes (GO) e o limite entre os terrenos antigos do maciço de Goiás e o arco magmático de Goiás. Revista Brasileira de Geociências, 26, 61-70.
- Pimentel, M.M., Fuck, R.A. & Alvarenga, C.J.S., 1996. Post-Brasiliano (Pan-African) high-K granitic magmatism in Central Brazil: the role of late Precambrian-early Paleozoic extension. Precambrian Research, 80, 217-238.
- Pimentel, M.M., Whitehouse, M.J., Viana, M.G., Fuck, R.A. & Machado, N., 1997. The Mara Rosa Arc in the Tocantins Province: further evidence for Neoproterozoic crustal accretion in Central Brazil. Precambrian Research, 81, 299-310.
- Pimentel, M.M., Fuck, R.A. and Botelho, N.F., 1999a. Granites and the geodynamic history of the neoproterozoic Brasília belt, Central Brazil: A review. Lithos, 46, 463-483.
- Pimentel, M.M., Dardenne, M.A., Viana, M.G., Gioia, B.M.C.L., Junges, S. and Seer, H.J., 1999b. Nd isotopes and the provenance of sediments of the Neoproterozoic Brasília Belt, Central Brazil: geodynamic implications. In: 2th South American Symposium on Isotope Geology, Extend Abstracts, 426-429.
- Pin, C. and Vielzeuf, D., 1983. Granulites and related rocks in Variscan Median Europe: a dualistic interpretation. Tectonophysics, 93, 47-74.
- Pires, F.A., 1991. Faciologia e análise paleoambiental da seqüência deposicional Furnas-Lageado (Group. Açuungui), de idade proterozóica. Revista Brasileira de Geociências, 21, 355-362.
- Pognante, U. and Spencer, D. A., 1991. First report of eclogites from the Himalayan belt, Kaghan valley (northern Pakistan). European Journal of Mineralogy, 3, 613-618.
- Pognante, U., Benna, P. and Le Fort, P., 1993. High-pressure metamorphism in the High Himalayan Crystallines of the Stak valley, northeastern Nang Parbat-Haramosh syntaxis, Pakistan Himalaya. In: P. J. Treolar and M. P. Searle (eds.) Himalayan Tectonics. Geological Society Special Publication 74, 161-172.
- Poidevin, J.L., Viallet, Y. and Reis Neto, J.M., 1997. Radiometric ages (Pb-Pb) of the Ribeira belt calcareous rocks. In: 1th South-American Symposium on Isotope Geology, Extend Abstracts, 242-243.
- Powell, R., 1985. Regression diagnostics and robust regression in geothermometer/geobarometer calibration: the garnet-clinopyroxene geothermometer revisited. Journal of Metamorphic Geology, 3, 231-243.
- Powell, R. & Holland, T., 1990. Calculated mineral equilibria in the pelite system, KFMASH (K₂O-FeO-MgO-Al₂O₃-SiO₂-H₂O). American Mineralogist, 75, 367-380.
- Pownceby, M.I., Wall, V.J. and O'Neill, H. St. C., 1991. An experimental study of the effect of Ca upon garnet-ilmenite Fe-Mn exchange equilibria. American mineralogist, 76, 1580-1588.
- Preciozzi, F., Masquelin, H. and Basei, M.A.S., 1999. The Namaqua/Greenville terrane of eastern Uruguay. In: 2th South-American Symposium on Isotope Geology, Extended Abstracts, 338-340.

- Queiroz, C.L., Jost, H. and McNaughton, N.J., 1999. U-Pb - SHRIMP ages of Crixás Granite-Greenstone belt terranes: from Archaean to Neoproterozoic. In: 2th South-American Symposium on Isotope Geology, Extended Abstracts,
- Ramos, V.A. and Vujovich, G.I., 1995. New appraisal on the southwestern Gondwana terranes and their Laurentian affinities: Laurentia-Gondwanan connections before Pangea. In: IGCP Field Conference Project 376, Abstracts, 31-32.
- Rego, I.T.S.F., 1989. Petrologia e geoquímica da unidade charnockítica Bela Joana, região de São Fidélis, RJ. Unpublished Thesis, Universidade de São Paulo, SP, 348p.
- Reis Neto, J.M., 1994. Faixa Itaiacoca: registro de uma colisão entre dois blocos continentais no Neoproterozóico. Unpublished Thesis, IG-USP, 253p.
- Ribeiro, A. and Heilbron, M., 1982. Estratigrafia e metamorfismo dos Grupos Carrancas e Andrelândia, sul de Minas Gerais. In: 32th Congresso Brasileiro de Geologia, Salvador, 1: 177-186.
- Ribeiro, A., Trouw, R.A. J., Andreis, R.R., Paciullo, F.V.P & Valença, J., 1995. Evolução das bacias Proterozóicas e o termo-tectonismo Brasiliense na margem sul do Cráton do São Francisco. Revista Brasileira de Geociências, 25: 235-248.
- Rivalenti, G., Girardi, V.A.V., Coltorti, M., Correia, C.T. and Mazzucchelli, M., 1989. Geochemical models for the petrogenesis of komatiites from Hidrolina greenstone belt, central Goiás, Brazil. Journal of Petrology, 30, 175-197.
- Rivers, T., Martignole, J., Gower, C. F. and Davidson, A., 1989. New tectonic divisions of the Grenville Province, Southeast Canadian Shield. Tectonics, 8, 63-84.
- Rocha-Campos, A.C. and Hasui, Y., 1981. Tilites of the Macaúbas Group (Proterozoic) in central Minas Gerais and southern Bahia, Brazil. M.J. Hambrey and W.B. Harland, ed. Earth pre-Pleistocene glacial record. Cambridge University Press, 933-938.
- Roser, B.P. & Korsch, R.J., 1988. Provenance signatures of sandstone-mudstone suites determined using discriminant function analyses of major element data. Chemical Geology, 67, 119-139.
- Sad, J.H.G. and Dutra, C.V., 1988. Chemical composition of supracrustal rocks from Paraíba do Sul Group, Rio de Janeiro State, Brazil. Geochimica Brasiliensis, 2, 143-165.
- Sadowski, G.R. and Bettencourt, J.S., 1996. Mesoproterozoic tectonic correlations between eastern Laurentia and the western border of the Amazon Craton. Precambrian Research, 76, 213-227.
- Sato, K., 1998. Evolução crustal da plataforma Sul Americana, com base na geoquímica isotópica Sm-Nd. Unpublished Thesis, Universidade de São Paulo,
- Schmid, S.M., Pfiffner, O.A., Froitzheim, N. and Schönborn, G., 1996. Geophysical-geological transect and tectonic evolution of the Swiss-Italian Alps. Tectonics, 15, 1036-1064.
- Schmitt, R.S., Trouw, R.A.J. and VanSchmus, W.R., 1999. The characterization of a Cambrian (~520 Ma) tectonometamorphic event in the coastal domain of the Ribeira belt (SE Brazil) – using U/Pb in syntectonic veins. In: 2th South American Symposium on Isotope Geology, Extended Abstracts, 363-366.
- Seer, H.J., Dardenne, M.A. and Fonseca, M.A., 1998. Deformation and tectonic framework of the Meso/Neoproterozoic units of the southeastern Brasília fold belt. In: 14th International Conference on Basement Tectonics, 57-61.
- Sengör, A.M.C., 1990. Plate Tectonics and orogenic Research after 25 Years: A Tethyan Perspective. Earth Science Reviews, 27, 1-201.

- Siga Jr., O., 1986. A evolução geotectônica da porção nordeste de Minas Gerais, com base em interpretações geocronológicas. Unpublished Thesis, Universidade de São Paulo, SP, 140p.
- Siga Jr., O., Basei, M.A.S. and Machiavelli, A., 1993. Evolução geotectônica da porção NE de Santa Catarina e Se do Paraná, com base em interpretações geocronológicas. Revista Brasileira de Geociências, 23, 215-223.
- Siga Jr., O., Basei, M.A.S., Reis Neto, J.M., Machiavelli, A. and Harara, O.M., 1995. O Complexo Atuba: um cinturão Paleoproterozóico intensamente retrabalhado no Neoproterozóico. Boletim do Instituto de Geociências, Universidade de São Paulo, Série Científica 26, 69-98.
- Siga Jr., O., Basei, M.A.S., Reis Neto, J.M., Harara, O.M., Passarelli, C.R., Prazeres Filho, H.J., Weber, W. and Machiavelli, A., 1997. Ages and tectonic setting of alkaline-peralkaline granitoids of Paraná and Santa Catarina, States, southern Brazil. In: South-American Symposium on Isotope Geology, Extended Abstracts, 301-303.
- Sigoyer, J. de, Guillot, S., Lardeaux, J-M and Mascle G., 1997. Glaucophane-bearing eclogites in the Tso Morari dome (eastern Ladakh, NW Himalaya). European Journal of Mineralogy, 9, 1073-1083.
- Silva Filho, B.C. and Soliani Jr., E., 1987. Origem e evolução dos gnaisses Cambaí: Exemplo de estudo integrado de análise estrutural, petroquímica e geocronologia. In: 3th Simpósio Sul Brasileiro de Geologia, 1, 127-145.
- Silva, L.C., Hartmann, L.A., McNaughton, N.J. and Fletcher, I.R., 1999. SHRIMP U/Pb zircon dating of Neoproterozoic granitic magmatism and collision in the Pelotas Batholith, southernmost Brazil. International Geologic Review, 41, 531-551.
- Simões, L.S.A., 1995. Evolução tectonometamórfica da nappe de Passos, sudoeste de Minas Gerais. Unpublish Thesis, IG-USP, 1-149.
- Simões, L.S.A. and Fuck, R.A., 1984. Estratigrafia, deformação e metamorfismo do Grupo Araxá na região de Mossâmedes, Goiás. In: 33th Congresso Brasileiro de Geologia, 7, 3181-3195.
- Slüttner, Z. and Weber-Diefenbach, K., 1989. Geochemistry of charnockitic granulites and associated amphibolitic gneisses in the coastal region of Espírito Santo, Brazil. Zentralblatt für Geologie und Paläontologie, I, 917-931.
- Soares, P.C., Fiori, A.P. and Carvalho, S.G., 1990. Tectônica colisional oblíqua entre o bloco Paraná e a margem sul do cráton do São Francisco, no maciço de Guaxupé(1). In: 36th Congresso Brasileiro de Geologia, 6, 2723-2734.
- Söllner, F., Lammerer, B. and Weber-Diefenbach, K., 1987. The Brasiliano Orogenesis: Age determination (Rb-Sr and U-Pb) in the coastal mountain region of Espírito Santo, Brazil. Zentralblatt für Geologie und Paläontologie, I, 729-741.
- Söllner, F., Lammerer, B. and Weber-Diefenbach, K., 1989. Brasiliano age of a charnoenderbitic rock suite in the Complexo Costeiro (Ribeira Mobile Belt), Espírito Santo/Brazil: Evidence from U-Pb geochronologien zircons. Zentralblatt für Geologie und Paläontologie, I, 993-945.
- Söllner, F., Lammerer, B. and Weber-Diefenbach, K., 1991. Die krustenentwicklung in der küstenregion nördlich von Rio de Janeiro/Brasilien. Münchener Geologische Hefte, 4, 1-100.
- Söllner, F. and Trouw, R.A.J., 1997. The Andrelândia depositional cycle (Minas Gerais/Brazil), a post-Transamazonic sequence south of the São Francisco craton:

- evidence from U-Pb dating on zircons of a metasediment. *Journal of South American Earth Sciences*, 10, 21-28.
- Souza, A.P., 1990. Mapa geológico na escala 1:50.000 e esboço da evolução tectônica e sedimentar do Grupo Itaiacoca, nas Folhas Barra do Chapéu e Ouro Verde - SP/PR. Unpublished Thesis, IG-USP, 200p.
- Spear, F.S., 1995. Metamorphic Phase Equilibria and Pressure-Temperature-Time Paths. Mineralogical Society of America, 1-799.
- Spear, F.S. & Cheney, J.T., 1989. A petrogenetic grid for pelitic schists in the system SiO₂-Al₂O₃-FeO-MgO-K₂O-H₂O. *Contributions to Mineralogy and Petrology*, 101, 149-164.
- Stanistreet, I.G., Kukla, P.A. and Henry, G., 1991. Sedimentary basinal responses to a Late Precambrian Wilson Cycle: the Damara orogen and Nama foreland, Namibia. *Journal of African Earth Sciences*, 13, 141-156.
- Strider, A.J. and Nilson, A.A., 1992. Melange ofiolítica nos metassedimentos Araxá de Abadiânia (GO) e implicações tectônicas regionais. *Revista Brasileira de Geociências*, 22, 204-215.
- Suita, M.T.F., Kamo, S.L., Krogh, T.E., Fyfe, W.S. and Hartmann, L.A., 1996. U-Pb ages from the high-grade Barro Alto mafic-ultramafic complex (Goiás, central Brazil): Middle Proterozoic continental mafic magmatism and Upper Proterozoic continental collision. In: 8th International Conference on Geochronology, Cosmochronology, and Isotope Geology, US Geological Survey Circular 1107, Abstracts, 309p.
- Tassinari, C.C.G. and Campos Neto, M.C., 1988. Precambrian continental crust evolution of southeastern São Paulo State – Brazil: Based on isotopic evidences. *Geochimica Brasiliensis*, 2, 175-183.
- Tassinari, C.C.G., Nutman, A.P., VanSchmus, W.R., Bettencourt, J.S. and Taylor, P.N., 1996. Ceochronological systematics on basement rocks from the Rio Negro-Juruena Province (Amazonian Craton) and tectonic implications. *International Geological Review*, 38, 161-175.
- Tassinari, C.C.G., Cordani, U.G., Correia, C.T., Nutman, A., Kinny, P. and Dians Neto, 1999. Dating of granulites by SHRIMP U-Pb systematics in Brazil: constraints for the age of the metamorphism of Proterozoic orogenies. In: 2th South-American Symposium on Isotope Geology, Extended Abstracts,
- Teixeira, A.L., 1995. Ambientes geradores dos sedimentos da Bacia Eleutério. IG-USP, unpublished Thesis: 122p
- Teixeira, W., Tassinari, C.C.G., Cordani, U.G. and Kawashita, K., 1989. A review of the geochronology of the Amazonian Craton: tectonic implications. *Precambrian Research*, 42, 213-227.
- Teixeira, W., Cordani, U.G., Nutman, A.P. and Sato, K., 1998. Polyphase Archaean evolution in the Campo Belo metamorphic complex, Southern São Francisco craton, Brazil: SHRIMP U-Pb zircon evidence. *Journal of South American Earth Sciences*, 11, 279-289.
- Tommazi, A., Vauchez, A., Fernandes, L.A.D. and Porcher, C.C., 1994. Magma-assisted strain localization in an orogen-parallel transcurrent shear zone of southern Brazil. *Tectonics*, 132, 421-437.

- Tonarini, S., Villa, I. M., Oberli, F., Meier, M., Spencer, D.A., Pognante, U. and Ramsay, J. G., 1993. Eocene age of eclogite metamorphism in Pakistan Himalaya. *Terra Nova*, 5, 13-20.
- Töpfner, C., 1996. Brasiliano-granitoide in den bundesstaaten São Paulo und Minas Gerais, Brasilien-eine vergleichende studie. *Münchener Geol. Hefte*, 17, 1-258.
- Trompette, R., 1994. Geology of Western Gondwana (2000-500 Ma). Balkema, 352p.
- Trouw, R.A.J., Ribeiro, A. & Paciullo, F.V.P., 1983. Geologia estrutural dos Grupos São João del Rei, Carrancas e Andrelândia, sul de Minas Gerais. *Anais da Academia brasileira de Ciências*, 55: 71-85.
- Trouw, R.A.J., Ribeiro, A., Paciullo, F.V.P. & Heilbron, M., 1984. Os Grupos São João Del Rei, Carrancas e Andrelândia interpretados como continuação dos Grupos Canastra e Araxá. In: 33th Congresso Brasileiro de Geologia, 2: 3227-3240.
- Trouw, R. A. J., Paciullo, F. V. P., Chrispim, S. J. and Dayan, H., 1982. Análise de deformação numa área a SE de Lavras, Minas Gerais. In: 32th Congresso Brasileiro de Geologia, Salvador, 1: 187-196.
- Trouw, R.A.J., Ribeiro, A. & Paciullo, F.V.P., 1986. Contribucão geologia da Folha Barbacena-1:250.000. In 34th Congresso Brasileiro de Geologia, 2: 974-984.
- Trouw, R.A.J. & Castro, E.M. O., 1996. Significado tectónico de granulitos Brasilianos de alta pressão no sul de Minas Gerais. In: 39th Congresso Brasileiro de Geologia, 6: 145-148.
- Trouw, R.A.J., 1992. Evolução tectónica do sul do Cráton do São Francisco baseada em análise metamórfica. In 37th Congresso Brasileiro de Geologia, 327.
- Trouw, R.A. J., Paciullo, F.V.P. and Ribeiro, A., 1998. Tectonic significance of Neoproterozoic high pressure granulites in southern Minas Gerais. In: 14th International Conference on Basement Tectonics, Ouro Preto, Brazil, Abstracts, 69-71.
- Tupinambá, M., 1999. Evolução tectônica e magnmática da Faixa Ribeira na região serrana do Estado do rio de janeiro. Unpublished Thesis, Universidade de São Paulo, SP, 221p.
- Tupinambá, M., Teixeira, W., Heilbron, M. and Basei, M.A.S., 1998. The Pan-African/Brasiliano arc-related magmatism at the Costeiro Domain of the Ribeira Belt, Southeastern Brazil. In: 14th International Conference on Basement Tectonics, Extend Abstracts, 12-14.
- Turpin, L., Maruejol, P. and Cuney, M., 1988. U-Pb, Rb-Sr and Sm-Nd chronology of granitic basement, hydrothermal albítites and uranium mineralization (Lagoa Real, south Bahia, Brazil). Contribution to Mineralogy and Petrology, 98, 139-147.
- Uhlein, A., Trompette, R.R., and Egydio-Silva, M., 1998. Proterozoic rifting and closure, SE border of the São Francisco Craton, Brazil. *Journal of South American Earth Sciences*, 11, 191-203.
- Valeriano, C.M., 1992. Evolução tectônica da extremidade meridional da Faixa Brasília, região da represa de Furnas, sudoeste de Minas Gerais. Unpublished Thesis, IG-USP, 192p.
- Valeriano, C.M., Almeida, J.C.H., Simões, L.S.A., Duarte, B.P., Roig, H.L. & Heilbron, M., 1995. Evolução estrutural do domínio externo da Faixa Brasília no sudoeste de Minas Gerais: registros de uma tectónica pré-Brasiliana. *Revista Brasileira de Geociências*, 25, 221-234.

- Valeriano, C.M., Simões, L.S.A., Teixeira, W. & Heilbron, M., 1998. Southern Brasilia belt (SE Brazil): thrust-discontinuities and evolution during the Neoproterozoic Brasiliano orogeny. In: 14th International Conference on Basement Tectonics, Ouro Preto, Brazil, Abstracts, 62-65.
- Valladares, C.S., Heilbron, M., Figueiredo, M.C.H. and Teixeira, W., 1997. Geochemistry and geochronology of paleoproterozoic gneissic rocks of the Paraíba do Sul Complex (Quirino Unit), Barra Mansa region, Rio de Janeiro, Brazil. Revista Brasileira de Geociências, 27, 11-121.
- Vannay, J.C. & Hodges, K.V., 1996. Tectonometamorphic evolution of the Himalayan metamorphic core between the Annapurna and Dhaulagiri, central Nepal. Journal of Metamorphic Geology, 14, 635-656.
- Vannay, J.C. & Grasemann, B., 1998. Inverted metamorphism in the High-Himalaya of Himachal Pradesh (NW India): phase equilibria versus thermobarometry. Schweiz. Mineral. Petrogr. Mitt., 78, 107-132.
- Vandecar, J.C., James, D.E. and Assumpção, M., 1995. Seismic evidence for a fossil mantle plume beneath South America and implications for plate driving forces. Nature, 378, 25-31.
- Vasconcellos, A.C.B.C., 1988. O Grupo Andrelândia na região norte de Ouro Fino, MG. Unpublished These, IG-USP, 199pp.
- Vasconcellos, A.C.B.C., Harris, N.B.W. and Tindle, A.C., 1991. The relationships between metamorphism and tectonics: evidence from the Socorro-Guaxupé Thrust nappe, southeastern Brazil. Res. Terras. Ser., 85, 86.
- Vlach, S.R.F., Janasi, V.A. and Vasconcellos, A.C.B.C., 1990. The Itú belt: associated calc-alkalic and aluminous A-type late Brasiliano granitoids in the States of São Paulo and Paraná, southern Brazil. In: 36th Congresso Brasileiro de Geologia, 4, 1700-1711.
- Vauchez, A., Tommasi, A. & Egydio-Silva, M., 1994. Self-identification of a heterogeneous continental lithosphere. Geology, 22, 967-970.
- Weil, A.B., Van der Voo, R., Niocail, C.M. and Meert, J.G., 1998. The Proterozoic supercontinent Rodinia: paleomagnetically derived reconstructions for 1100 to 800 Ma. Earth and Planetary Science Letters, 154, 13-24.
- Wernick, E., Hormann, P., Artur, A.C. & Eulert, H., 1984. Aspectos petrológicos do Complexo Socorro (SP/MG): dados analíticos e discussão preliminar. In 33th Congresso Brasileiro de Geologia, 6, 2919-2934.
- Wernick, E., 1998. The pluriserial Ribeira Magmatic System 590, SE/S Brazil and Uruguay. Revista Brasileira de Geociências, 28, 533-542.
- Wiedmann, C., Bayer, P., Horn, H., Lammerer, B., Ludka, I.P., Schmidt-Thomé and Weber-Diefenbach, K., 1986. Maciços intrusivos do sul do Espírito Santo e seu contexto regional. Revista Brasileira de Geociências, 16, 24-37.
- Wiedmann , C , Mendes, J.C . , Moura, J .C., Nascimento, R . C . C . ; Ludka, L . P .1997. Granitoides of the Espírito santo Magmatic Arc. In: 2th International Symposium on granites and Associated Mineralizations, Excursion guide, 57-76.
- Wilson, T.J., Hanson, R.E. and Wardlaw, M.S., 1993. Late Proterozoic evolution of the Zambezi belt, Zambia: implications for regional Pan-African tectonics and shear displacements in Gondwana. In: R.H. Findlay, R. Urung, M.R. Banks and J.

- Veevers (eds), Gondwana 8-Assembly, Evolution and Dispersal. Rotterdam, Balkema, 69-82.
- Yamato, A. A., 1999. Mapeamento Geológico de parte da Folha Bocaiúva do Sul – PR (SG.22-X-D-I-2), escala 1:50.000. Unpublished Dissertation, IG-USP, 108 p.
- Xu, G., Will, T. M. and Powell, R., 1994. A calculated petrogenetic grid for the system K_2O - FeO - MgO - Al_2O_3 - SiO_2 - H_2O , with particular reference to contact-metamorphosed pelites. *Journal of metamorphic Geology*, 12, 99-119.
- Zimbres, E., Kawashita, K. and VanSchmus, W.R., 1990. Evidências de um núcleo Transamazônico na região de Cabo Frio, RJ e sua correlação com o cráton de Angola. In: 36th Congresso Brasileiro de Geologia, 6, 2735-2743.
- Zinng, A., Handy, M. R., Hunziker, J. C. and Schmid, S. M. , 1990. Tectonometamorphism history of the Ivrea Zone and its relationship to the crustal evolution of the Southern Alps. *Tectonophysics*, 182, 169-192.